University of Alberta

Study of Hydrocyclones for Separation of Light and Heavy Particles

by

Talat Mahmood 

A thesis submitted to the Faculty of Graduate Studies and Research in partial fulfillment of the requirement for the degree of Master of Science

in

Chemical Engineering

Department of Chemical & Materials Engineering

Edmonton, Alberta

Fall 2007

Your file Votre référence
ISBN: 978-0-494-33302-0
Our file Notre référence
ISBN: 978-0-494-33302-0

Abstract

Separation cells, ablation drums, large interstage tanks are typical equipment used in oilsands extraction for the separation of light and heavy particles in slurry. Exploring the potential of hydrocyclone as an efficient device for separation of light and heavy particles, the author constructed two different design of hydrocyclones, model A and model B. Hydrocyclone model A has a cone angle of 20° and model B consists of two conical sections having different cone angles of 20° and 10°, respectively. A series of experiments were conducted by varying operation conditions of these two models of hydrocyclones.

In terms of design variables, it was observed that increasing the vortex finder length, and decreasing the cylindrical length and the overflow to underflow diameter ratio, resulted in an increase in the recovery of light particles in the overflow. In the case of operating variables, the recovery of light particles in the overflow was improved by increasing the size of light particles, feed flowrate and decreasing feed solids concentration. Both hydrocyclones were efficient in rejecting greater than 95% heavy particles in the underflow stream at any underflow split ratio and 98% of light particles were recovered to overflow when the underflow split ratio was controlled below 0.15. However, the recovery and product quality were improved at higher underflow split ratio when hydrocyclone model A was replaced by hydrocyclone model B.

Acknowledgments

I would like to express my utmost gratitude to Dr. Jacob H. Masliyah and Dr. Zhenghe Xu, my supervisors for their continuous assistance and guidance throughout the entire process of this research. It was a great pleasure to work with both of them as they are constant source of inspiration and courage.

I would like to thank Mr. Artin Afacan for his valuable support and help in setting up and conducting the experiments. He provided me with highly appreciable constructive comments and criticism, which helped me in writing this research thesis.

I would like to thank Dr. Nandakumar and Dr. Jingli Luo, for providing their equipment to run the experiments.

I take great pleasure to thank Oilsand Research Group at University of Alberta, especially Mr. Jim Skwarok, who helped me in providing all the services and facilities, which I needed for these studies within no time.

I would like to thank the faculty and my fellow colleagues from Department of Chemical and Materials Engineering for creating a wonderful environment throughout my years here.

I also acknowledge the funding provided for this project by NSERC.

TABLE OF CONTENTS

LIST OF TABLES

LIST OF FIGURES

NOMENCLATURE

A	Area of inlet of cyclone (m^2)
A_c	Cross sectional area of particle (m^2)
C_D	Drag coefficient
C_v	Solids volume percent in feed (%)
C_w	Solids weight percent in feed (%)
d_{50}	Particle size relative to 50 percentile (μm)
D_c	Hydrocyclone diameter (mm)
D_i	Hydrocyclone inlet diameter (mm)
D_o	Hydrocyclone overflow vortex finder diameter (mm)
d_s	Diameter of solid particle (mm)
D_u	Hydrocyclone underflow apex diameter (mm)
$F_1 - F_4$	Empirical constants to be estimated from data (default value = 1)
F_B	Centripetal buoyancy force (N)
F_C	Centrifugal force (N)
F_D	Centripetal drag force (N)
g	Acceleration due to gravity (9.81 m/s^2)
k	Constant incorporating other factors, particularly cyclone geometry
$K_1 - K_6$	Empirical constants, Eq. 2.12
K	Empirical constant to be estimated from data, Eq. 2.13
L_{apex}	Length of hydrocyclone apex (mm)
L_c	Length of cylindrical chamber of hydrocyclone (m)
$L_{cone\,(1)}$	Length of hydrocyclone cone (1) in model (B) (mm)

$L_{cone\ (2)}$	Length of hydrocyclone cone (2) in model (B) (mm)
L_{cone}	Length of hydrocyclone cone in model (A) (mm)
$L_{cyclinder}$	Hydrocyclone cylindrical chamber length (mm)
$L_{cyclone}$	Hydrocyclone length (mm)
L_{vf}	Length of hydrocyclone vortex finder (mm)
m_f	Feed mass flowrate (kg/s)
M_f	Mass of the feed stream (kg)
M_o	Mass of the overflow stream (kg)
m_o	Overflow mass flowrate (kg/s)
M_u	Mass of the underflow stream (kg)
m_u	Underflow mass flowrate (kg/s)
P	Pressure drop, measured at cyclone inlet (kpa)
P_f	Feed pressure (kpa)
P_o	Overflow pressure (kpa)
Q_f	Feed volumetric flowrate (m^3/s)
Q_o	Overflow volumetric flowrate (m^3/s)
q_o	Quality of the overflow product
Q_o/Q_f	Ratio of the overflow to feed flowrate
Q_u	Underflow volumetric flowrate (m^3/s)
r	Radial position (mm)
R_f	Recovery of water to underflow (%)
R_{ho}	Recovery of the heavy particles in the underflow stream (%)
R_{Lo}	Recovery of the light particles in the overflow stream (%)

R_v	Volumetric recovery of feed slurry to underflow (%)
S	Split ratio of underflow to total feed, Q_u/Q_f
SG	Specific gravity
U_r	Radial velocity of the particle (m/s)
V_i	Volume of solid "light/heavy" particles = $\frac{\pi d^3}{6}$
V_o	Tangential component of the fluid (m/s)
V_p	Volume of the particle (m^3)
V_r	Radial velocity of the fluid at a point in cyclone (m/s)
υ_o	Relative radial velocity between the liquid and the particles (m/s)
υ_z	Absolute axial velocity between the liquid and the particles (m/s)

Greek Letters

ω	Angular velocity of the particle (s^{-1})
λ	Hindered settling velocity correction factor = $10^{1.82C_v}/(8.05(1.C_v)^2)$
θ	Hydrocyclone model (A) cone angle (degree)
μ	Viscosity of fluid (Pa.s)
θ_1	Hydrocyclone model (B) cone (1) angle (degree)
θ_2	Hydrocyclone model (B) cone (2) angle (degree)
ρ_f	Density of feed slurry (kg/m^3)
ρ_{heavy}	Density of heavy particles (kg/m^3)
α_{hf}	Mass fraction of the heavy particles in the feed stream
α_{ho}	Mass fraction of the heavy particles in the overflow stream

α_{hu}	Mass fraction of the heavy particles in the underflow stream
α_{if}	Mass fraction of the light or heavy particles in the feed stream
α_{io}	Mass fraction of the light or heavy particles in the overflow stream
α_{iu}	Mass fraction of the light or heavy particles in the underflow stream
ρ_l	Density of liquid (kg/m^3)
α_{lf}	Mass fraction of the light particles in the feed stream
ρ_{light}	Density of light particles (kg/m^3)
α_{lo}	Mass fraction of the light particles in the overflow stream
ρ_m	Density of continuous medium (kg/m^3)
ρ_s	Density of solids (kg/m^3)
ρ_w	Density of water (kg/m^3)

Chapter 1

INTRODUCTION

A hydrocyclone is a static mechanical device, which separates different species in a continuous medium by centrifugal forces. The multiphase system could be solid particles, immiscible liquids and/or gas bubbles. In the case of the continuous medium, it is mostly water but it can be gas and other organic solvents as well. Hydrocyclones are widely used in different chemical and mineral processing industries for specific applications such as liquid clarification, degassing of liquids, solids washing, particulate slurry thickening, and classification of solids according to size, shape and density. Cyclones are also used to protect the down stream equipment from erosion by removal of fine solids from the main product.

Hydrocyclone has been intensively studied for many decades. Researchers developed empirical models (Kelsall, 1952; Bradley, 1965; Bohnet, 1969; Lynch and Rao, 1975; Plitt, 1976; Svarovsky, 1984) to understand and explain the hydrocyclone performance. Until 1980, most of the literature is available for the dense media separation such as solids from liquids and solids from solids. Very little work was done on liquid-liquid separations (Simkin and Olney, 1956; Hitchon, 1959; and Kimber and Thew, 1975).

After 1980's, Colman and Thew (1980, 1981, 1984), Smyth and Thew (1987) and Young et al. (1994) developed cylindrical hydrocyclone models for separation of light dispersed oil droplets from the continuous medium, "water'. The main objective of these studies were to increase the concentration of the light dispersed phase (oil) in the overflow

stream and to improve separation efficiency of the hydrocyclone. This type of hydrocyclone was mainly used for off-shore platform oil production.

Most recently, Bednarski (1987), Dale and Charles (1994), Changirwa and Rockwell (1994, 1997, 1999) and Hashmi et al. (1992, 2004) designed and tested the models of three phase separation hydrocyclones for separation of oil, sands and water. These hydrocyclones were developed for the continuous separation of oil-solids-water from the ship ballast and bilge waters, for treatment of oily waste water from the oil tankers washing and slop oil obtained from the processing of crude oil.

The rapid development in the oil drilling, oil sand extraction and processing reveals that the solid liquid separation technology should be a unique tool for separation of light and heavy particles in a dispersed suspension.

For offshore platform applications, the solids and water are separated from the oil produced to minimize the contamination of the sea water. For this goal, the hydrocyclone is convenient because of its high throughput and short residence time, which are the main criteria for the selection of solid liquid separator for offshore platform applications (Dale and Charles, 1994).

Manufacturer of ship oil separators are also building hydrocyclones for separation of oil-solid-water from the ship ballast and bilge waters. The main objective of this application

is to remove the unemulsified oil droplets and solid particles such as "clays, silica, mud, corrosion products, asphaltenes and heavy metals" from the continuous phase.

Oily wastewater from the oil tanker washing and slop oil are conventionally conditioned by heating and chemical addition followed by utilization of skim tanks, centrifuges and filtration units. But the retention time in the skim tank is very long and a large space is required for all the units installation. The recovery of oil and solid in the respective units is also low. Under such circumstances a hydrocyclone is best choice for providing high throughput and recovery of phases in the respective streams at low operation and maintenance costs (Hashmi et al., 2004).

In a similar manner, the oil sand industry deals with the separation of light "bitumen" droplets from heavy "sand" particles in water suspensions. To achieve this milestone, oilsand ore undergoes a series of unit operations and processes such as mining, crushing, slurry conditioning, bitumen extraction and froth treatment.

Different technologies have been tested for the primary separation of light "bitumen" from heavy "sands" dispersed in water. These technologies are based on the principles (Svarovsky, 1984) such as,

- Gravitational Sedimentation
- Centrifugal Sedimentation
- Thermal Sedimentation

All the current technologies used are efficient, (According to AEUB, "Alberta Energy and Utilities Board" recovery requirement) but they have different drawbacks in terms of maintenance, initial capital cost and environment. Syncrude, Suncor and Albian Sands Limited are using Primary Separation Vessel/Cell, which is a gravity settler, for the primary separation of light "bitumen" particles from water and heavy "solids" (Masliyah, 2000). By this technique the recoveries achieved are above 90%, which fulfill AEUB (Alberta Energy and Utilities Board) requirement. But the existing extraction plants are geographically fixed. Oilsand slurry, is transported by pipelines to the extraction plant for bitumen recovery and the tailings sand is pipelined for disposal at tailing areas. With the passage of time, the transport distance between the mining and new tailing areas increases, which eventually reflects future ongoing investment with increased maintenance and energy costs. Coarser tailings produced are to be dumped into huge tailings ponds, which incur a significant initial capital cost. This process also involves a variety of environmental impacts, such as global warming and greenhouse gas emission, disturbance of mined land; and impacts on wildlife and air /water quality due to excessive chemicals usages.

Mechanical settlers (Agitating tanks) are another option for light and heavy particles separation. In such applications three or four large tanks in series are required . These tanks are equipped with a mechanical moving agitator, which provide shearing force to ablate the bitumen layer from the oilsand ore. Accompanying this ablation, the fraction of fines is also increased, which decreases the quality of the product.

When oil sand extraction is not economical by surface mining then in-situ recovery methods such as SAGD (Steam Assisted Gravity Drainage) is used. The main idea behind this technology is the heat transfer from the pressurized steam to the ore deposits to increase the flow of the bitumen by reducing its viscosity. For SAGD operations, enormous amounts of energy are required to generate steam. Large consumption of energy to produce steam contributes significantly to greenhouse gas emission (Masliyah, 2000).

Hydrocyclone has the advantage over the above mentioned separation equipment because of its simple structure, low cost, large capacity, easy maintenance and requires less space for installation. Unlike other gravitational settlers, the separation rate in a hydrocyclone is higher because the centrifugal force is 1000 times more than the earth's gravity. Most important feature of the hydrocyclone is that it can be built in mobile units, which reduces the operating and capital cost by avoiding building large tailing ponds and by dumping the sand on the mining site.

Initially, hydrocyclone was designed for the separation of high specific gravity minerals from ores. But with the passage of time its application widened. The design and operation variables were modified to suit separation of low specific gravity material and coarse from fines.

1.1 Objective and Scope of Study

The oilsand industry is one of the major driving forces in the rapid growth of the Canadian economy. Statistics show that Alberta is on the top in the economic growth race compared to the rest of the provinces because of its trillion barrels of oil sand reserves. So far four major companies (Syncrude, Suncor, Albian Sands and Canadian Natural Resources Limited) are operating oilsand extraction and processing plants. All these companies have started billion dollars worth of new projects in their capacity. At the moment they are spending a large fraction of their budget on research and development of oil sand extraction. The main objective is to find new cost effective technologies and equipment designs for light and heavy phase separations, which meet the AEUB minimum recovery target with improved environmental management and increased economic returns. At the moment, the above mentioned technologies are in operation, but much research work is in progress on hydrocyclone design.

According to its importance, a research project investigating the potential of hydrocyclone for the separation of light and heavy particles in a slurry was initiated. In this research project the objective was to study the effect of design and operation variables of hydrocyclones on the recovery and quality of light and heavy particles in product streams.

The hydrocyclone design is based on application requirements. The author constructed two model hydrocyclones for the separation of light "buoyant" particles from heavy "sinking" particles in a slurry. The light and heavy particles are selected according to the

physical properties of the oilsand ore composition. The results represent a simulation of separating aerated bitumen from solids in an oilsand ore slurry. Effects of operation variables (solid concentration, feed flow rate, underflow split ratio, light particles size and density) and design variables (length of cylindrical chamber, length of vortex finder, length of cyclone and overflow to underflow diameter ratio) are examined using both physical model hydrocyclones.

1.2 Structure of Study

This research thesis examines the performance of two physical model hydrocyclones for the separation of light and heavy particles in slurry. The raw material used was light particles "polyethylene and hollow cenospheres" and heavy particles " sand". Hydrocyclones were designed by the standard thumb rule for the separation of two phases as presented by Kellsel (1952) and Bradly (1965) in their studies.

A good deal of work is done in the development of hydrocyclone models. Much early research work is based on the experimental and empirical models for the single phase, density or shape separation by using cyclone. In practice, minerals are mixtures of different components having different physical characteristics. Regarding to that fact, in 1980 a new era of cyclone development started and is outlined in Chapter one.

A hydrocyclone is a fluid flow device. It has wide applications in various fields of technology, such as oil and gas cleaning, burning, spraying, powder classification etc. The separation phenomenon of a hydrocyclone is based on the effect of different forces

acting on the phases to be separated. These forces act in the radial and axial direction. The magnitude of these forces is dependent on the design and operation variables of hydrocyclone as described in Chapter two.

The third chapter expands in detail the scope of work. It provides information about material, equipment and procedure used to conduct the experiments and sampling technique.

The fourth chapter provides the experimental results of the operation and design variables effects on recovery and quality of the light and heavy particles in the product streams.

The conclusions are provided in the fifth chapter and finally some recommendations for future work are given, so the best hydrocyclone model can be commercialized for the separation of light and heavy particles in slurry.

Chapter 2

THEORY

A hydrocyclone has advantages over other gravity/centrifugal force based separation equipment because of its simple structure, low cost, large capacity, easy maintenance and less space for installation.

On the basis of design and operation principles, a hydrocyclone is classified as (Statie et al., 2002):

Forward flow hydrocyclone;

Reverse flow hydrocyclone;

or Through flow hydrocyclone;

In the forward flow hydrocyclone, the high specific gravity rejects are collected from the underflow (apex/spigot) and the low specific gravity accepts are collected from the overflow. The reverse or through flow hydrocyclones are, on the other hand, for the separation of low specific gravity material from the top as rejects and heavy from the bottom of the hydrocyclone as accepts as shown in the Figure 2.1.

The hydrocyclone consists of a Cono-Cylinderical structure. The feed is introduced in the upper vertical cylindrical chamber, by means of a circular feed entry. This orifice allows a smooth fluid flow pattern at the feed point. Two feed entry configurations (involuted and tangential) are normally used. The involuted feed entry causes the swirling motion of the feed all along the body of the hydrocyclone, which increases the conversion efficiency of kinetic energy to centrifugal force and reduces the eddies and turbulence formation. This configuration hinders the separation of fine particles and increases the

wear rate of the inner body of the cyclone. The top of the structure is enclosed by a cover, through which a tube is protruding at some distance down to the center. This tube is called vortex finder, through which overflow stream flows. It must be kept in mind that a vortex finder should extend below the feed inlet to reduce the chances of short-circuiting of the feed and above the cylindrical and conical section joint to avoid the turbulence. The section where the underflow stream flows through is called apex or spigot (Bradley, 1965 and Svarovsky, 1984).

When the feed is introduced tangentially at the top, the driving force for the separation arises from fluid pressure energy and is converted to dynamic kinetic energy. As shown in Figure 2.1, the centrifugal force pushes the particles/fluid having higher settling velocity towards the walls of the cyclone while particles/fluid having low settling velocity are pushed towards the central axis by the centripetal and radial drag forces. Both streams are open to the atmosphere, so a pressure differential is created inside the cyclone body. In the cylindrical chamber near the walls is the high-pressure zone of high settling velocity, while in the center is the low-pressure zone of low settling velocity. As a result of these different pressure zones two helical vortices are developed, outer vortex of high pressure is called the free vortex, and the inner vortex of low pressure is called the forced vortex. The fluid flows in a spiral rotation shape (helical) from the top to the bottom, and after reaching the upper tip of the apex, reverses its flow towards the vortex finder due to pressure differential as a result limited fluid flow through the spigot. The inner vortex looks like a tube and is called air core. The axial direction of flow in both helical vortexes is in the opposite direction.

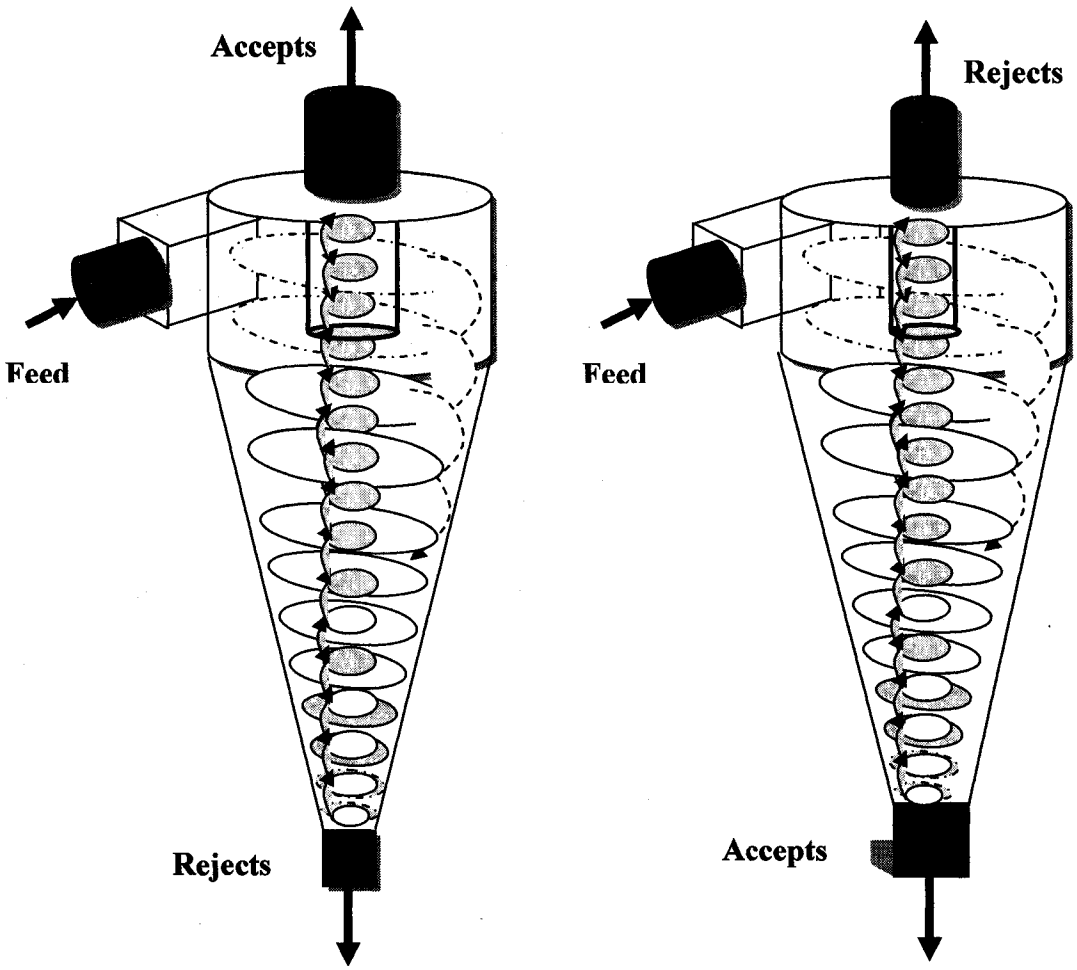

Figure 2.1: Schematic spiral flow in forward and reverse flow hydrocyclone (Redrawn as per Svarovasky, 1984)

When a more dense material is dispersed in the continuous phase, the free vortex pushes the dense material radially outward toward the walls of the hydrocyclone, forcing dispersion depleted continuous phase migrating towards the central axis and entering the overflow "vortex finder". The throughput of the continuous phase is higher in the overflow and only a small fraction of it passes to the underflow along with the dense material. When a less dense material is dispersed in the continuous phase, the light material migrated towards the centre and the continuous phase "water" towards the walls of the hydrocyclone. They are then removed from the overflow and underflow, respectively. In this case the overflow is concentrated with the dispersed phase and underflow is diluted, by forcing majority of the continuous phase to the underflow streams.

2.1 Forces Acting on Particles in Hydrocyclone

Current hydrocyclone design is based on the physical properties of the phases to be separated, such as size and density. Based on the above separation mechanism, the light particles migrate to the central axis and heavy particles towards the walls of the cyclone. They are discharged through the overflow and underflow, respectively. The separation of these phases depends on the forces acting on the particles in the radial and axial directions. The motion of the feed flow, position of the cyclone and the physical properties of the phases generate these forces.

In the radial direction three forces acting on a particle are (Changirwa, 1994, 1997);

Centrifugal force due to the tangential motion

$$F_C = \frac{\pi d_s^3 \rho_s \omega^2 r}{6} \quad 2.1$$

Centripetal buoyancy force due to the radial pressure gradient

$$F_B = \frac{\pi d_s^3 \rho_m \omega^2 r}{6} \quad 2.2$$

Centripetal drag force due to the viscosity of the liquid

$$F_D = \frac{C_D \pi d_s^2 \rho_w v_r^2}{8} \quad 2.3$$

According to Svarovasky (1984), C_D is the radial drag coefficient, given by $(24\mu/\rho_w v_o d_s)$ for low Re. The relative radial velocity between light and heavy particles is the cause for the separation in the hydrocyclone; it can be derived by considering the equilibrium between the centripetal and centrifugal forces as follows.

$$F_C = F_B + F_D \quad 2.4$$

$$v_o = \left[\frac{d_s^2 (\rho_s - \rho_m) \omega^2 r}{18.\mu} \right] \quad 2.5$$

When $F_C > F_B + F_D$, the particles will migrate towards the wall of the hydrocyclone and are trickled downward by the apex opening. When $F_C < F_B + F_D$, on the other hand, the particles will migrate towards the central axis of the hydrocyclone and are trickled upward through the vortex finder opening.

Similarly in the axial direction, the particles experience three forces in a stagnant fluid, which are

Downward gravitational force

$$F_g = \frac{\pi d_s^3 \rho_s g}{6} \qquad 2.6$$

Buoyant force in the upward direction

$$F_b = \frac{\pi d_s^3 \rho_m g}{6} \qquad 2.7$$

Vertical drag force

$$F_d = \frac{C_D \pi d_s^2 \rho_w v_z^2}{8} \qquad 2.8$$

The axial relative velocity between the particles and liquid can be obtained by considering equilibrium between upward and downward forces acting as follows.

$$F_g = F_b + F_d \qquad 2.9$$

$$V_z = \frac{d_s^2 (\rho_s - \rho_m)}{18.\mu} g \qquad 2.10$$

The magnitude of radial and axial velocity of the particles, guides their mobility toward the overflow and underflow streams in the hydrocyclone body.

According to Chu et al. (2002), increasing the positional radius, density or size of the solid particles decreases the absolute radial velocity of the solid particles because radial velocity of liquid decreases and the relative radial velocity between liquid and solids increase. The transition of axial distribution of radial velocity of solid particles from outer helical flow to inner helical flow takes place in the middle section not the upper and the

lower sections of the hydrocyclone. As a result solids radial velocity is largest in the middle.

The axial velocity of solid particles in the outer helical flow is in the downward direction, while in the inner helical flow it is in the upward direction. In the middle part of the hydrocyclone, particle axial velocity in the inner helical flow is larger than the outer helical flow. The opposite holds in the lower section.

The axial velocity of particles in the inner helical flow increases with increasing flowrate of the overflow. In the lower section, the axial velocity of particles in the outer helical flow increases with increasing the flowrate of the underflow. Chu et al. (2002) verified that increasing the inlet pressure or underflow diameter increases the particle radial velocity. When the particle density, size or feed particle concentration increases, the particle radial velocity decreases.

2.2 Hydrocyclone Models

A great deal of work is done in the development of empirical and experimental models of cyclone (Bradley, 1965; Devulpalli and Rajamanai, 1996). Much earlier research had been devoted to developing a cut size model for hydrocyclone. Bradley (1965) developed such a model:

$$d_{50} = k\left[\frac{D_c^3 \mu}{Q_f(\rho_s - \rho_l)}\right]^n \qquad (n= 0.5 - 0.6) \qquad 2.11$$

This approach is also known as the equilibrium orbit hypothesis.

Lynch and Rao model (1975) was structured to reflect correlations between performance criteria such as d_{50} and cyclone design and operating parameters. The general equation is:

$$\log_{10} d_{50} = K_1.D_o - K_2 D_u + K_3 D_i + K_4 C_w - K_5 Q_f + K_6 \qquad 2.12$$

where

$$Q_f = K.D_o^{0.73} D_i^{0.86} P^{0.42} \qquad 2.13$$

Plitt developed a semi-empirical model (1976) based on the experimental database. According to his model the equations for three performance criteria cut size, Pressure drop and split ratio are:

$$d_{50c} = \frac{F_1.39.7 D_c^{0.46} D_i^{0.6} D_o^{1.21} \mu^{0.5} \exp(0.063 C_v)}{D_u^{0.71} (h)^{0.38} Q_f^{0.45} \left[\frac{\rho_s - 1}{1.6}\right]^k} \qquad 2.14$$

$$P = \frac{F_3 \ 1.88 \ Q_f^{1.8} \ \exp(0.0055 C_v)}{D_c^{0.37} \ D_i^{0.94} \ (h)^{0.28} \ (D_u^2 + D_o^2)^{0.87}} \qquad 2.15$$

$$S = \frac{F_4 18.62 \rho_p^{0.24} (D_u / D_o)^{3.31} (h)^{0.54} (D_u^2 + D_o^2)^{0.36} \exp(0.0054 C_v)}{D_c^{1.11} P^{0.24}} \qquad 2.16$$

where

d_{50c} is corrected cut size of particle

h is distance between apex and end of vortex finder (cm)

Nageswararao model (1978) comprises empirical equations of cut size, feed volumetric flowrate, recovery of water to underflow and volumetric recovery of feed slurry to underflow. The general form of the equations is given below:

Cut size:

$$d_{50c} = K_{D1}.D_c\left[\frac{D_o}{D_c}\right]^{0.52}\left[\frac{D_u}{D_c}\right]^{-0.47}\lambda^{0.93}\left[\frac{P}{\rho_p g D_c}\right]^{-0.22}\left[\frac{D_i}{D_c}\right]^{-0.5}\left[\frac{L_c}{D_c}\right]^{0.2}\theta^{0.15} \quad 2.17$$

Feed volumetric flowrate:

$$Q_f = K_{Q1}D_c^2\left[\frac{D_o}{D_c}\right]^{0.682}\left[\frac{D_u}{D_c}\right]^{-0.473}\left[\frac{P}{\rho_p}\right]^{0.5}\left[\frac{D_i}{D_c}\right]^{0.45}\left[\frac{L_c}{D_c}\right]^{0.2}\theta^{-0.1} \quad 2.18$$

Recovery of water to underflow:

$$R_f = K_{w1}\left[\frac{D_o}{D_c}\right]^{-1.19}\left[\frac{D_u}{D_c}\right]^{2.40}\lambda^{0.27}\left[\frac{P}{\rho_p g D_c}\right]^{-0.53}\left[\frac{D_i}{D_c}\right]^{-0.5}\left[\frac{L_c}{D_c}\right]^{0.22}\theta^{-0.24} \quad 2.19$$

Volumetric recovery of feed slurry to underflow:

$$R_v = K_{v1}\left[\frac{D_o}{D_c}\right]^{-0.94}\left[\frac{D_u}{D_c}\right]^{1.83}\left[\frac{P}{\rho_p g D_c}\right]^{-0.31}\left[\frac{D_i}{D_c}\right]^{-0.25}\left[\frac{L_c}{D_c}\right]^{0.22}\theta^{-0.24} \quad 2.20$$

where

K_{w1} and K_{v1} are empirical constants.

2.3 Qualitative Analysis of Operation and Design Parameters

The qualitative analysis of major operation and design parameters which affect the separation process in a hydrocyclone are presented as follows.

2.3.1 Underflow Split Ratio

When the underflow split ratio, Q_u/Q_f is decreased or overflow split ratio, Q_o/Q_f is increased the recovery of light particles in the overflow stream is increased. This effect is same in both smaller and larger diameter particles but recovery is higher in larger size light particles (Dale and Charles, 1994). For the separation of a light phase from a heavy phase, back pressure must be applied at the hydrocyclone underflow to force the light

phase to the overflow; otherwise, all the light phase would come out the underflow (Young et al., 1994).

2.3.2 Feed Flowrate

Feed flowrate is a variable that can be controlled by using a variable frequency drive motor for the pump and by opening or closing the feed valve. According to Chaston (1958);

$$Q_f = K.AP^{0.5} \tag{2.21}$$

Increasing the feed inlet pressure, the slurry flowrate to cyclone can be increased. An increase in the slurry flowrate results an increase in the slurry velocity. The separation of light and heavy particles in the swirl chamber of the hydrocyclone depends on the forces acting on the particles in the spinning fluid and the residence time in the chamber (Young et al., 1994). Lower flowrate means longer residence time, lower acceleration forces and greater drag forces. Conversely higher flowrate results in higher acceleration forces, lower drag forces and smaller residence time as per the equations (King, 2000 and Mukherjee et al., 2003) below

$$Drag\ Force = 0.5C_D(V_r - U_r)^2 \rho_f A_c \tag{2.22}$$

$$Centrifugal\ Force = \frac{V_o^2}{rV_p(\rho_s - \rho_f)} \tag{2.23}$$

An increase in the feed flowrate increases the air-core diameter by increasing the centrifugal force on fluid elements, which in turn increases the tangential velocity component, thereby lowering the pressure at the hydrocyclone axis near the apex, so it is easier for the air to be sucked in through the apex, (Narasimha et al., 2006).

2.3.3 Feed Solids Concentration

The feed or inlet slurry concentration affects the hydrocyclone performance as predicted by the hindered settling velocity. Low concentrations of particles (<1% by volume) do not greatly interact with each other during the separation process. Increasing the solid concentration increases interaction between the solid particles. According to Changirwa (1997) if the solid particles are not uniformly distributed, the overall effect may be a net increase in the settling velocity because the return flow due to volume displacement will predominate in the particle-sparse regions. This is known as cluster formation and the effect is only significant in mono-dispersed suspensions. In poly-dispersed suspensions clusters do not survive for long enough to affect the settling behaviour and the settling rate declines with increasing concentration due to the return flow being more uniformly distributed. This is known as hindered settling behaviour.

According to Young et al. (1994), increasing the concentration of light particles in the feed results in an increase in the overflow light particles recovery. Increasing the feed solids concentration decreases the air-core diameter (Balaji, 1997).

2.3.4 Light Particles Size

Hydrocyclone performance can be predicted by using the fundamental equation for separation, Stokes law,

$$\left(V_{settling} = \frac{\Delta\rho.g.d_s^2}{18\mu} \right) \qquad 2.24$$

Separation efficiency directly depends on the settling velocity of the particles. From the above equation it is clear that four parameters act on the settling velocity.

The first parameter is the density difference. For the particles to be separated there must be a finite density difference between them because buoyancy occurs in centrifugal fields. If no density difference existed, the buoyancy would equal the centrifugal force and there would be no separation. As the particle density increases, relative to the carrier fluid density, the particles mobility will increase when subjected to centrifugal force. Radial velocity of greater density differential particles is higher than for the smaller density differential particles so their mobility in the respective zone of separation also increases. The second parameter is the particle diameter. Smaller diameter particles will take longer to separate from the continuous medium "water" than larger diameter particles, due to smaller radial velocity (Changirwa et al., 1999). This affects the settling velocity and separation efficiency. The third parameter is the acceleration field which is generated by the inlet feed velocity and is always high in hydrocyclone and leads to a better separation efficiency. The last parameter is the viscosity of the continuous phase. It is temperature dependent. Lower separation efficiency occur for high viscosity fluids.

2.3.5 Vortex Finder Diameter

The vortex finder prevents the short-circuiting of fluid inlet to the overflow. The diameter of the vortex finder is typically 30 to 40% of the hydrocyclone diameter, and it has a directly proportional relationship with the cut size, as it will affect residence time (Svarovsky, 1984). Increasing D_o/D_u ratio by increasing the vortex finder diameter results in a decrease in the air core diameter from top to bottom, the upward axial velocity

increases and the radial velocity decreases (Narasimha et al., 2006; Balaji, 1997; Chu et al., 2002). It also results in increased water recovery in the overflow stream and a denser underflow stream (Brooks et al., 1984). Increasing the vortex finder diameter reduces the pressure drop inside the hydrocyclone; hence the axial velocity acting on the light particles will be less than the previous case when the vortex finder diameter is smaller, thereby leading to less recovery of light particles in the overflow (Mukherjee et al., 2003).

The ratio of the overflow and underflow diameters D_o/D_u classifies the hydrocyclone into forward flow and reverse flow hydrocyclone. When the objective of using the hydrocyclone is to obtain high capacity of the product in a dilute form from the overflow stream then the overflow diameter of the hydrocyclone should be greater than the underflow diameter $D_o>D_u$,. To improve the quality of the overflow product, the overflow diameter is reduced but this also results in decreased overflow recovery. When the objective of using the hydrocyclone is to separate finely divided particles or to decrease the cut size, $D_o<D_u$ ratio is used which increases the residence time of the fluid and decreases the cut size of separation.

2.3.6 Vortex Finder Length

The hydrocyclone separation performance is determined by the fluid flow characteristics inside the hydrocyclone. During operation, inside the hydrocyclone there exists outer (free) and inner (forced) helical flows, a circulation flow, a short circuit flow and an air core. Svarovsky (1984) reported that the hydrocyclone efficiency could be improved by reducing the forced vortex. This can be done by increasing the vortex finder length.

Increasing the vortex finder length increases the cut size. Holland-Batt, Trawinski and Plitt used free vortex length (h) in their correlations instead of vortex finder length as given in equations 2.14 – 2.16. Plitt also defined residence time equation as;

$$\text{Re}\,sidence\ Time = \left[\frac{D_c^2 L_{cyclone}}{Q_f}\right]^{0.15} \qquad 2.25$$

According to him larger the residence time of a particle in a hydrocyclone, greater the probability of that particle reporting to the correct flow stream (Slechta et al., 1984).

2.3.7 Cylindrical Chamber Length

The cylindrical section is located between the inlet area and the conical section of the hydrocyclone. Its length is typically equal to the diameter of the hydrocyclone. Increasing the cylindrical length increases the residence time, reduces the tangential velocity and angular momentum by dragging against the wall of the cylindrical section (Young et al., 1994; Chu et al., 2002), therefore it has an inversely proportional relationship to cut size and separation efficiency. Capacity of hydrocyclone, recovery of water and recovery of feed slurry in the underflow are increased by increasing the cylindrical section length as presented by Nageswararao in his model equations 2.17 – 2.20.

2.3.8 Conical Section

Larger hydrocyclone has a cone angle of 20° and small hydrocyclones have cone angle of $6\text{-}12^{\circ}$ The smaller angle increases residence time and lengthens the acceleration zone, thereby cone angle is inversely related to cut size. Cone angles of 6° and greater provide a rapid spin up to speed with minimum loss of angular momentum (Young et al., 1994).

The tangential velocity in the conical part of the hydrocyclone increases with a decrease in the radius of the flow rotation (Zhao and Xia, 2006; Narasimha et al., 2006). Zhao and Xia (2006) also found that increasing the overflow diameter results in increased pressure drop in the conical section of the hydrocyclone. The radial velocity increases from the wall to the centre of the hydrocyclone, and reaches a maximum near the air core (air-water interface), and then decreases. The radial velocity gradient in the inner helical flow is larger than that in the outer helical flow (Dai et al., 1999).

Chapter 3

EXPERIMENTAL WORK

3.1 Experimental Setup

A schematic diagram of the closed loop used for the current studies is shown in Figure 3.1. The slurry was prepared in a 250-liter capacity holding tank equipped with a mechanical stirrer. The slurry tank had a standpipe in the centre to prevent the solid accumulation in the pipe suction line. The slurry was circulated and flow rate was controlled using a 2.24 kW (3HP) progressive cavity (Moyno) pump with a variable speed drive. A magnetic flowmeter (Rosemount) was used to measure slurry flow rates up to 30L/min. A coriolis flowmeter (Khrone MFM 4085K Corimas, type 300G+) was used to measure flow rates up to 100 L/min, the slurry density and the flow temperature. A diaphragm valve located on overflow line controlled the overflow to underflow split ratio manually. The inlet and overflow pressures were measured using a pressure gauge (Wika) having a range of 0-30 psig.

The two hydrocyclone models used for the current studies are shown schematically in Figure 3.2 with the entire dimension. Both hydrocyclones are made of transparent Plexiglas to visualize the flow field and vortex formation inside the body. Hydrocyclone **(A)** consists of two sections i.e., cylindrical chamber and conical section, which are interchangeable. It has an involute feed entry, which begins as a circular opening but becomes a slit entry into the upper swirl chamber. This swirl chamber is called cylindrical section and is connected to the conical section. Additional cylindrical lengths can be connected to the swirl chamber. In the swirl chamber a tube protrudes axially from

the top of the hydrocyclone body down to the lower edge of the feed entry. This tube is called the vortex finder. Its length is adjusted by moving it up and down inside the cap. The overflow vortex finder diameter is greater than the underflow spigot diameter. Such type of hydrocyclone is called Forward Flow Hydrocyclone. This type of hydrocyclone has the characteristic of separating the higher specific gravity reject material from the underflow of the hydrocyclone, and the overflow is in the diluted form

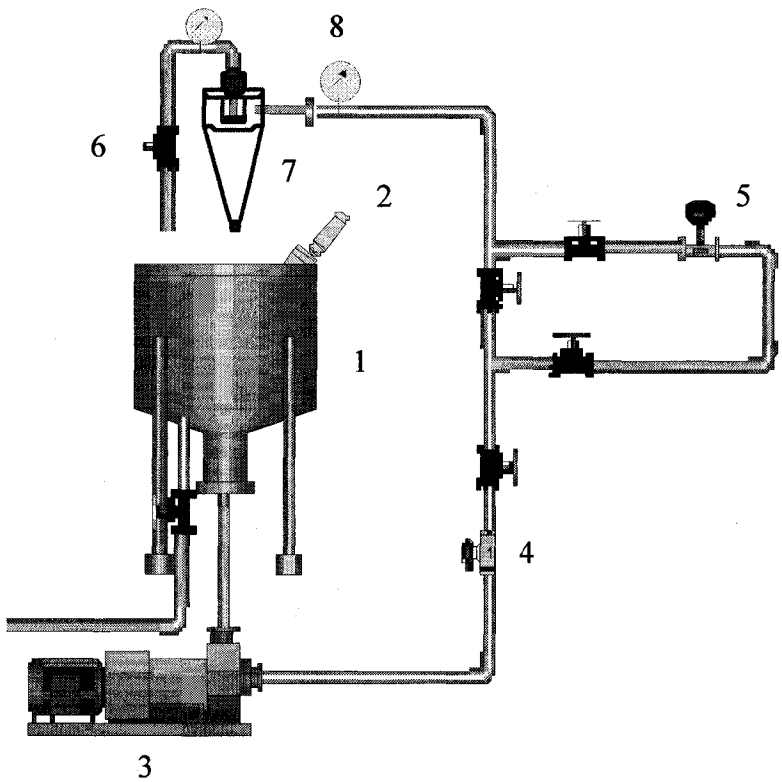

1- Slurry Holding Tank 2-Mixer 3- Monyo Pump

4- Magnetic Flowmeter 5- Coriolis Meter 6- Overflow Control Valve

7- Hydrocyclone 8- Pressure Gauge

Figure 3.1: Schematic diagram of experimental Setup

of the valuable product. This is convenient when the objective is to separate the valuables in the overflow, which can be concentrated in the next step by using another hydrocyclone for the overflow stream or by using a flotation column.

Hydrocyclone model **(B)** was developed by Changirwa (1994, 1997) for the separation of three phase material "oil, solids, water" having different densities and the author, after conducting some modifications used it for light and heavy particles separation. This design was selected after performing experiments with model (A) and the results were remarkable in terms of separation of light and heavy particles but the quality of overflow product was not significantly improved. All the dimensions of model (B) are shown in Figure 3.2. It differs from model (A) in that it consists of two conical sections having different cone angles 20° and 10°, respectively and structured coaxially with the hydrocyclone axis. It has a long underflow aperture. The overflow diameter is less than the underflow, such type of hydrocyclones are used for the separation of fine particles and the cut point is low as compared to model (A). Such types of hydrocyclones are called Reverse Flow Hydrocyclones.

3.2 Light and Heavy Particles Used in this Study

This project is focused on the separation of light from heavy particles in a slurry using two types of hydrocyclones. The light and heavy particles are used to simulate bitumen and solid (coarse and fine) particles as in the oilsand extraction plants. The particles were selected on the basis of density and size distribution of the oilsand ore components.

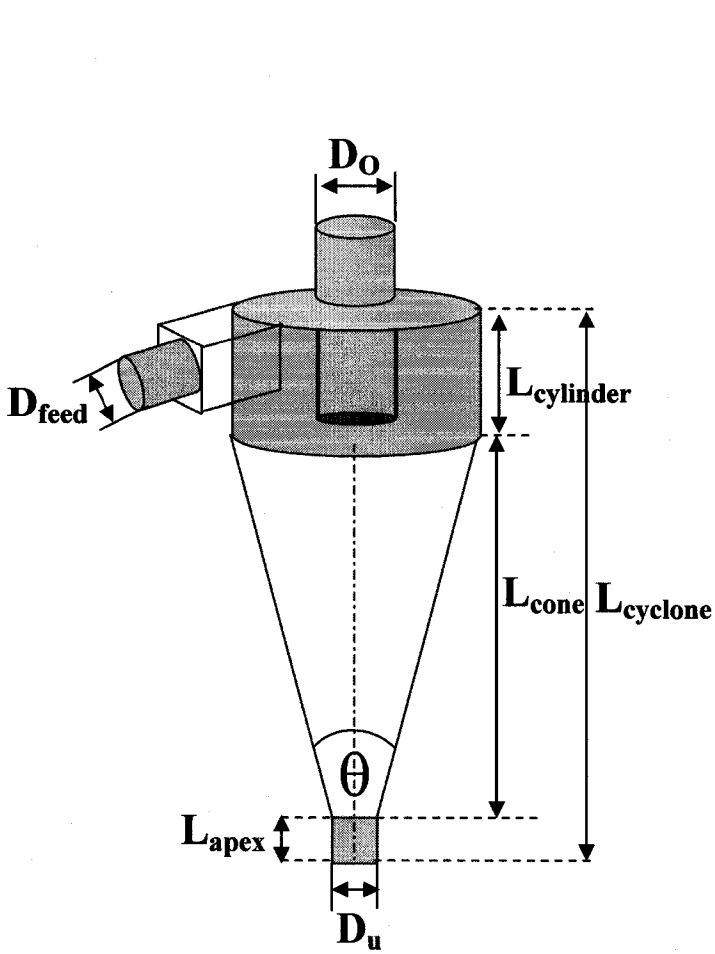

Hydrocyclone (A)

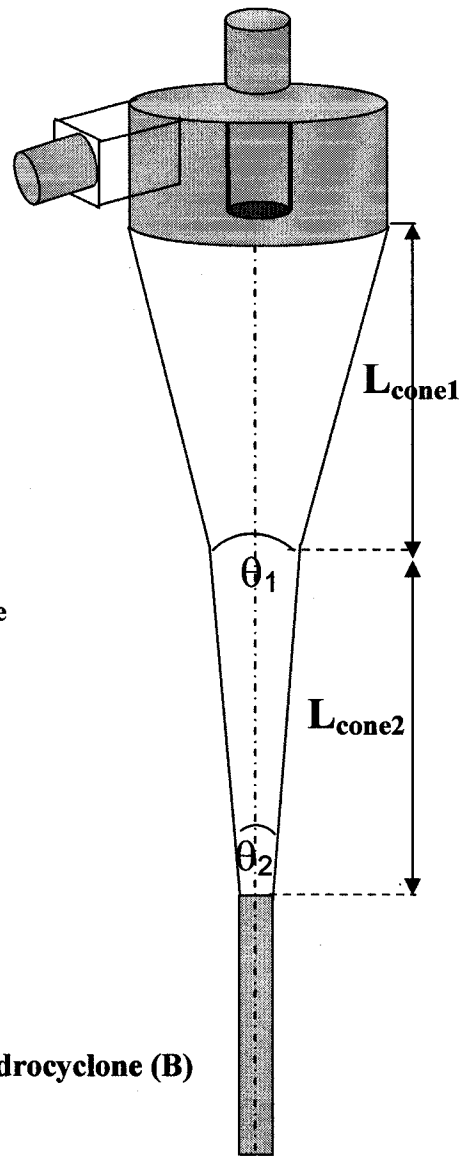

Hydrocyclone (B)

	D_c	D_u	D_o	D_{feed}	L_{vf}	$Lc_{ylinder}$	$L_{cyclone}$	L_{apex}	$L_{cone(1)}$	$L_{cone(2)}$	Θ1	Θ2
Model A	51	10	27	16	38	51	184	25	108		20□	
Model B	51	13	11	16	38	51	269	72	73	73	20□	10□

Note: All dimensions are in "mm"

Figure 3.2: Hydrocyclone model (A) and (B) Specifications

The heavy particles used were silica sand supplied by Manuse Abrasives Canada. The particles have the size distribution presented in Figure 3.6. The mean particle size was 62μm and density, 2650 kg/m^3.

In the case of light particles, two types of materials were selected: 1) Polymeric material and 2) Inorganic cenospheres. Polymer based particles were polyethylene, supplied by Nova Chemicals Canada. These particles due to their hydrophobic nature were not wettable with water so a wetting agent "Triton X 100" was used along with the antifoaming agent "silicon oil, SAG 471" in the slurry preparation. The physical properties of the light and heavy particles used are shown in Table 3.1.

Table 3.1: Physical Properties of Light and Heavy Particles Used

Light Particles			
	Polymer	$\rho = 920$ kg/m^3	$d_{50} = 460$ μm
	Cenospheres (A)	$\rho = (600 - 950)$ kg/m^3	$d_{50} = 360$ μm
	Cenospheres (B)	$\rho = (600 - 950)$ kg/m^3	$d_{50} = 80$ μm
Heavy Particles			
	Sand	$\rho = 2650$ kg/m^3	$d_{50} = 62$ μm

The second type of light particles, "Cenospheres A and B" of two different size ranges, as shown in the Table 3.1, were spherical in shape.

3.3 Particles Size Analysis

The particle size distribution of solids in the feed, overflow and underflow streams were determined by using "Malvern Mastersizer 2000" which is based on light

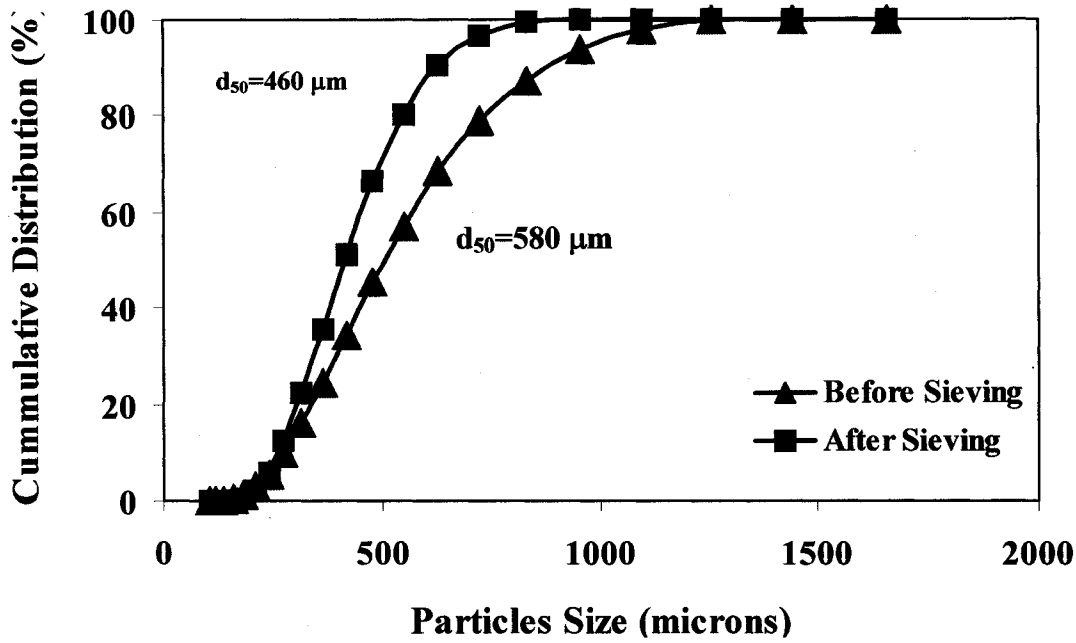

Figure 3.3: Light Polymer Particles Size Distribution

scattering principle (Napier Munn et al.,1996). It is commonly called Low Angle Laser Scattering and is widely used in the industry for characterization and quality control of particle sizes. It measures 0.02-2000 microns particles. To determine the particles size, the refractive index of the medium and solids need to be provided as input data to the instrument. The sample particles were dispersed in the de-ionized water in a beaker and placed in a 100-ml capacity sample cell of the analyzer. In the cell there is a mechanical stirrer to keep the dispersion in the suspension form. In this way particles size distribution

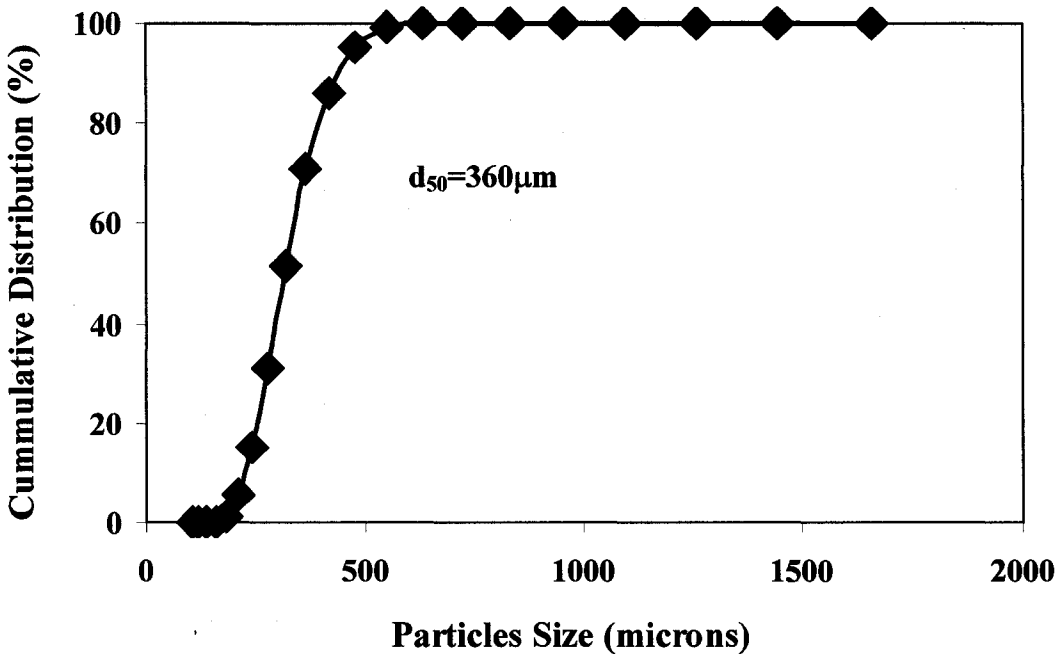

Figure 3.4: Particles Size Distribution of Light Cenospheres (A)

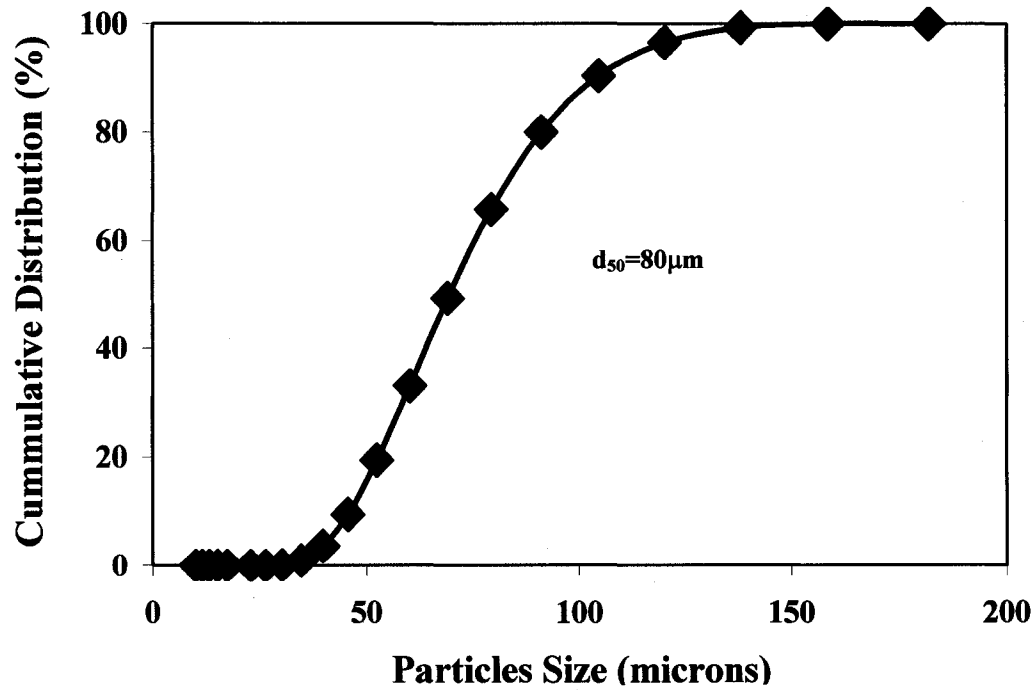

Figure 3.5: Particles Size Distribution of Light Cenospheres (B)

of the feed, underflow and overflow of hydrocyclone was recorded. The size distribution of light particles (polymeric and cenospheres) and heavy particles (sand) is shown in Figures 3.3, 3.4, 3.5 and 3.6, respectively.

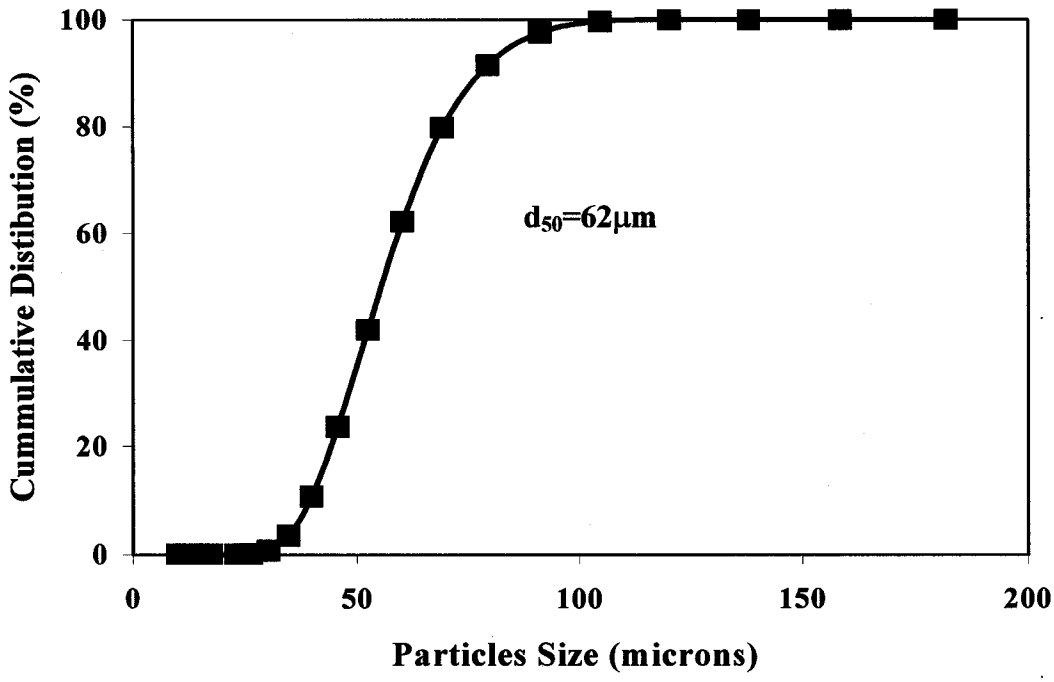

Figure 3.6: Particle Size Distribution of Heavy Sands

3.4 Density Measurement of Light and Heavy Particles

The density difference of the continuous medium and dispersed particles plays an important role in the recovery of light and heavy particles in the product streams. The densities of these particles were measured by a gravimetric method. In the case of light polymer particles, a graduated cylinder was filled with known weight and volume of methanol. Then a known weight of the light particles was placed in the cylinder. The mixture was stirred vigorously to disperse the light particles. The change in volume was recorded and densities were calculated. Similar procedure was used for the heavy

particles but with water as the solvent. The polymer density determined by this method is in Table A1 in Appendix A. Light cenosphere particles have density distribution (600 – 950) kg/m^3, as shown in Table A2 and Figure A1 in appendix A. To determine the density distribution of light cenospheres particles, the solvents used were pentane, hexane, heptane, acetone and methanol.

3.5 Procedure

In this study, two different types of hydrocyclones as shown in Figure 3.2 were used. A series of experiments was performed to determine the applicability of these types of hydrocyclones for the separation of light particles from heavy particles in a liquid slurry. The effect of different design and operating variables on recovery and quality of particles in the product streams was examined. The design parameters investigated included hydrocyclone overflow to underflow diameter ratio, cylindrical chamber length, vortex finder length and cone angle, while operating variables included feed flow rate, underflow split ratio, light particles size distribution and feed solids concentration.

Initially, the slurry holding tank was filled with 150-liters of tap water. The pump was turned on and water was circulated through the closed loop during which the density and temperature of the water were recorded from the calibrated coriolis meter as shown in the Figure 3.1. The mixer was switched on and pre-weighed light and heavy solids at 1:2 mass ratio were added slowly into the tank to prepare homogeneous slurry of 5% (by weight) total solids. Particles used for the experiments were of two different characteristics; light particles were hydrophobic polymeric material less dense than the continuous medium. To increase the wetability of the particles by water, 25 ml of wetting

agent "Triton X 100" was used. The wetting agent addition caused foaming in the slurry. To overcome this problem, 25 ml of antifoaming agent "silicon oil, SAG 471" was added. Both the wetting and the antifoaming agents were very active in their respective functions and did not have any effect on the density and the viscosity of the water. The hydrophilic silica particles were denser than the continuous medium.

A hand operated control valve at the overflow stream was used to adjust the feed flow rate split ratio. The slurry was kept circulating for few minutes at constant feed flow rate. Overflow and underflow samples were taken at the same time to determine the solids concentration in the feed line. Five samples were taken for consistency purposes. The feed solid concentration was calculated by using the equations 3.1 and 3.2 below:

Overall material balance is:

$$M_f = M_o + M_u \tag{3.1}$$

Component balance is:

$$M_f \alpha_{if} = M_o \alpha_{io} + M_u \alpha_{iu} \tag{3.2}$$

where, i, represents light or heavy particles.

At steady state, the feed rate and total solids concentration in the feed line was constant. Slurry samples were also taken before and after starting the pump to note the effect of crushing by the mixer and the pump on the size distribution of the light cenospheres particles as shown in Figures B1 and B2 (appendix, B). The mixer and pump had little effect on the particle size distribution of silica and polymer particles.

Before starting the main experiment, 20 empty polypropylene beakers of 1000 ml were weighed for 10 sets of overflow and underflow samples collected at the particular operation and design conditions. The speed of the pump was set at a pre-calibrated reading of the ampere meter according to the required feed flow rate. The position of the overflow valve was also adjusted to control the split ratio. At the steady state, the inlet feed pressure and overflow pressure were recorded. Underflow and overflow stream samples were collected into 1000 ml beakers and the time of sample collection was recorded. The samples were taken at different split ratios by changing the position of the overflow valve. Feed concentration was determined for each set of experiment. To verify the data three samples were taken: one at the start, second at the mid point and the last one at the end of each set of runs.

All the samples were weighed and the volume was recorded. Using a float and sink method, light and heavy particles in each sample were separated and collected on the pre-weighed Wattman # 42. All solid particles in each sample were collected on the filter paper. The filter paper and solid particles were dried in open atmosphere over night. Then the concentration of "light and heavy" particles in each sample of the feed, overflow and underflow was calculated.

Recovery of light particles in the overflow is defined as the ratio of the mass of light particles recovered in the overflow to the mass of light particles in the feed and is calculated by equation;

$$R_{lo} = \frac{M_o \alpha_{lo}}{M_f \alpha_{lf}} \qquad 3.3$$

Similarly, the recovery of heavy particles in the underflow is defined as,

$$R_{hf} = \frac{M_u \alpha_{hu}}{M_f \alpha_{hf}} \qquad 3.4$$

Quality of the overflow product stream is calculated by using the equation;

$$q_o = \frac{\frac{\alpha_{lo}}{\alpha_{ho}}}{\frac{\alpha_{lf}}{\alpha_{hf}}} \qquad 3.5$$

On average, 10% slurry by volume was removed from the tank for the 10 sample sets after a total time of about 1 hr. After taking each set of samples, the system was run for 5 minute to reach a new steady state. It was found that when removing the 10% slurry by volume, the change of total solid concentration was only 0.01%. In each test, the inlet concentration was determined by the mass balance of the product streams, verified periodically by taking the sample of the feed stream.

In addition, the particle size distribution of the product streams and feed was measured by using the Malvern Master-sizer, to determine breakage of the particles by the pump. It was found that the pump did not break the polymeric and heavy solid particles, while 360μm cenospheres experienced the greater degree of breakage than 80μm. To overcome this problem, the whole slurry was replenished by fresh particles slurry after each set of runs and size distribution was corrected by measuring the particle size distribution of the product streams of each run.

Chapter 4

RESULTS AND DISCUSSION

The main objective of this research was to develop a hydrocyclone capable of separating "light/heavy" particles, to mimic primary separation of bitumen from coarse solids and water. In the current study, two designs of hydrocyclones were used. The details on hydrocyclones dimension and the experimental set-ups were described in Chapter 3. In this chapter, the results are discussed in the context of the operation and design variables.

Presentation of Results

The separation efficiency of both hydrocyclone models A and B is presented by evaluating the following parameters;

1) Recovery of light particles in overflow
2) Recovery of heavy particles in underflow
3) Quality of overflow product

4.1 Hydrocyclone Model A

Initially hydrocyclone model A was used to check the effect of different parameters on the separation efficiency and the results are described as follows.

4.1.1 Effect of Underflow Split Ratio

The flow enters the hydrocyclone tangentially, creating a swirling motion in the cono-cylindrical chamber from the top to the bottom. This spinning fluid creates different pressure zones inside the cyclone: a high-pressure zone near the walls and a low-pressure

zone in the centre. This differential pressure splits the flow into the overflow and underflow streams. The underflow split ratio is the volume fraction of the feed flowrate which reaches the underflow stream. This volume fraction can be controlled by a control valve in the overflow or underflow stream and by varying the dimensions of hydrocyclones. Many correlations, such as Plitt equation 2.16, have been proposed to describe the dependence of the flow split ratio on operation and design variables. In general, increasing the pressure drop or the overflow diameter or decreasing hydrocyclone diameter, decreases the underflow split ratio. On the other hand, increasing the underflow diameter, feed solids concentration and/or free space length in the hydrocyclone increases the underflow split ratio. According to Dale and Charles (1994), decreasing the underflow split ratio improves the purity of the underflow stream because a larger quantity of water and light particles reach the overflow stream and vice versa.

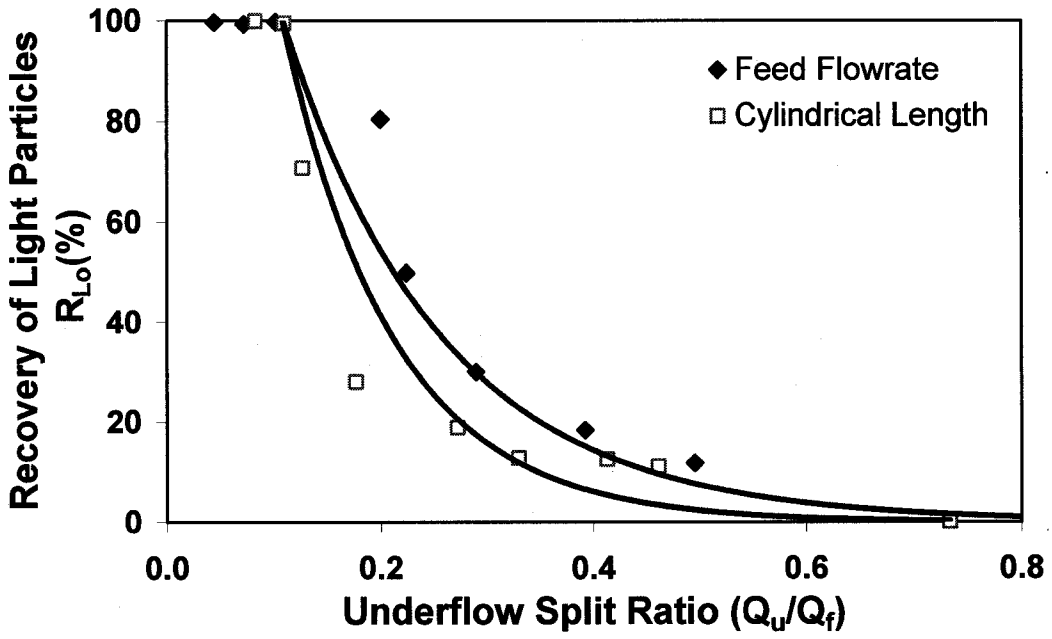

Figure 4.1: Effect of Underflow Split Ratio on Light Particles Recovery in Overflow Q_f = 33L/min; α_{lf} = 1.4%; α_{hf}= 1.9%; D_o = 27mm; θ = 20°, Model (A)

The effect of underflow split ratio on the recovery of light particles in the overflow is common under different operation and design conditions, as shown in all next figures. As a result, it is explained in Figure (4.1). Figure 4.1 shows that the recovery of the light particles in the overflow stream clearly increased as decreasing underflow split ratio from 0.8-0.1. The underflow split ratio can be controlled either by changing the underflow/overflow orifice or by changing the back pressure on either or both outlet streams (Svarovsky, 1984). Decreasing the underflow split ratio increases the axial velocity in the inner helical vortex, and its direction is upwards. The spinning fluid causes the light particles to move into the inner helical vortex and is removed through the overflow. If the overflow backpressure is increased slowly by closing the overflow valve, the pressure differential inside the hydrocyclone body decreases. As a result, the air core in the conical section elongates, and the light particles get remixed with the heavy particles (Colman and Thew, 1980; Young et al., 1994), ultimately resulting in a decrease in the recovery of light particles to overflow. As the overflow valve is opened slowly, the backpressure in the overflow stream is reduced. The pressure differential is again developed along with the air core formation inside the hydrocyclone body. The light particles, due to the strong radial centripetal force, are moved toward the central axis of the hydrocyclone and are trickled up by the central air core to the overflow stream, resulting in an increase in the recovery of the light particles to the overflow by decreasing the underflow split ratio.

In the overflow stream, light particles arrive along with the water. Their quality in the overflow is improved as the underflow split ratio is decreased as shown in all next figures, but the improvement in quality is insignificant due to the increase in the water

split ratio to the overflow stream. In order to reduce the water content in the overflow, the underflow diameter should be increased or the overflow diameter should be reduced (Slechta and Firth, 1984; Shah et al., 2006).

4.1.2 Effect of Feed Flow Rate

The performance of hydrocyclones is directly related to the feed flowrate and pressure drop. In general, increasing the feed flowrate increases the pressure drop. When the feed is introduced tangentially into the upper cylindrical part of the hydrocyclone, the rotational motion results in different pressure zones. The high-pressure zone and low-pressure zone are near the walls and in the centre, respectively. The migration of the light and heavy particles in the pressure zones depends on the forces acting on the particles in the radial and axial directions. The direction and magnitudes of the forces depend on the feed flowrate and the physical properties of particles, such as size, shape and density.

Figures 4.2-4.4 show the effect of the feed flow rate on the recovery and the quality of the light and heavy particles in the overflow and underflow streams, respectively. In this set of tests d_{50} for the light "polymer" and heavy "sand" particles was 460μm and 62μm, respectively. The concentration of the light and heavy particles in the feed was 1.4% and 1.9% by weight, respectively. The hydrocyclone's overflow diameter was D_o=27mm, and the cone angle θ was 20°. Figure 4.2 shows that the recovery of light particles in overflow decreased when the feed flow rate was increased from 17 L/min. to 46 L/min. The feed flowrate affected the separation of the light/heavy particles. When the feed was introduced tangentially, the rotational field was developed inside the hydrocyclone. The separation of the light and heavy particles in the swirl chamber of the hydrocyclone was a

result of the centrifugal and centripetal forces acting on the particles and their residence time in that chamber (Dwari et al., 2004; Young et al., 1994). A lower flowrate results in a longer residence time, lower centrifugal forces, and higher centripetal forces. Conversely, a higher flowrate results in higher centrifugal forces, lower centripetal forces and shorter residence time (see Equations 2.22, 2.23 and 2.25).

At a high feed flow rate, the centrifugal force acting on the feed particles increases due to the strong tangential motion of feed particles (King, 2000), but the centripetal buoyancy

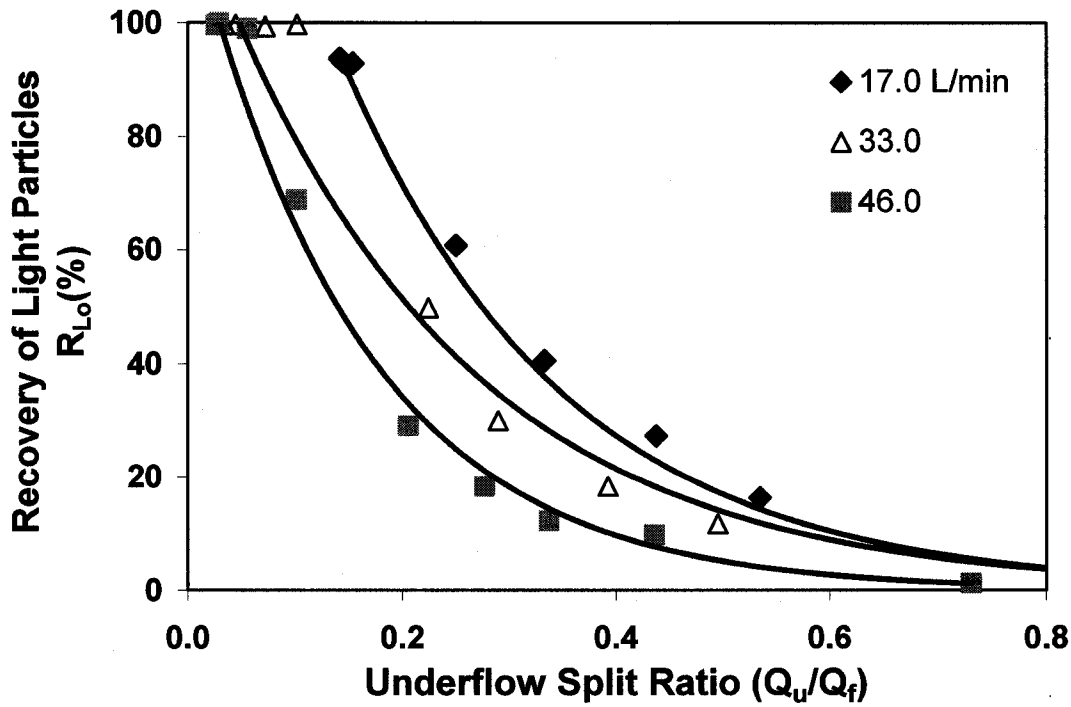

Figure 4.2: Effect of Feed Flowrate on Light Particles Recovery in Overflow
α_{lf} = 1.4%; α_{hf}= 1.9%; d_{50}= 460μm; D_o = 27mm; θ = 20° , Model (A)

and drag forces do not increase significantly. At low centripetal forces, the particles move towards the wall of the hydrocyclone. Light particles, due to a short residence time within the hydrocyclone's body and cloud of heavy particles, cannot migrate quickly to the centre, so the recovery of the light particles in the overflow is decreased.

Figure 4.2 shows that the recovery of the light particles in the overflow stream increased as the underflow split ratio Q_u/Q_f dropped below 0.4 and reached 98% at 0.1. The air core developed at 0.8 underflow split ratio. With an underflow split ratio between 0.4-0.8, the fluid downward velocity was greater than the rising velocity of light particles. As a result, the recovery of the light particles in the overflow was low and changed only marginally. At a high underflow split ratio, the axial velocity of the light particles in the outer helical flow was higher than in the inner helical flow (Chu et al., 2002), and the back pressure in the overflow stream was high due to the nearly closed overflow valve.

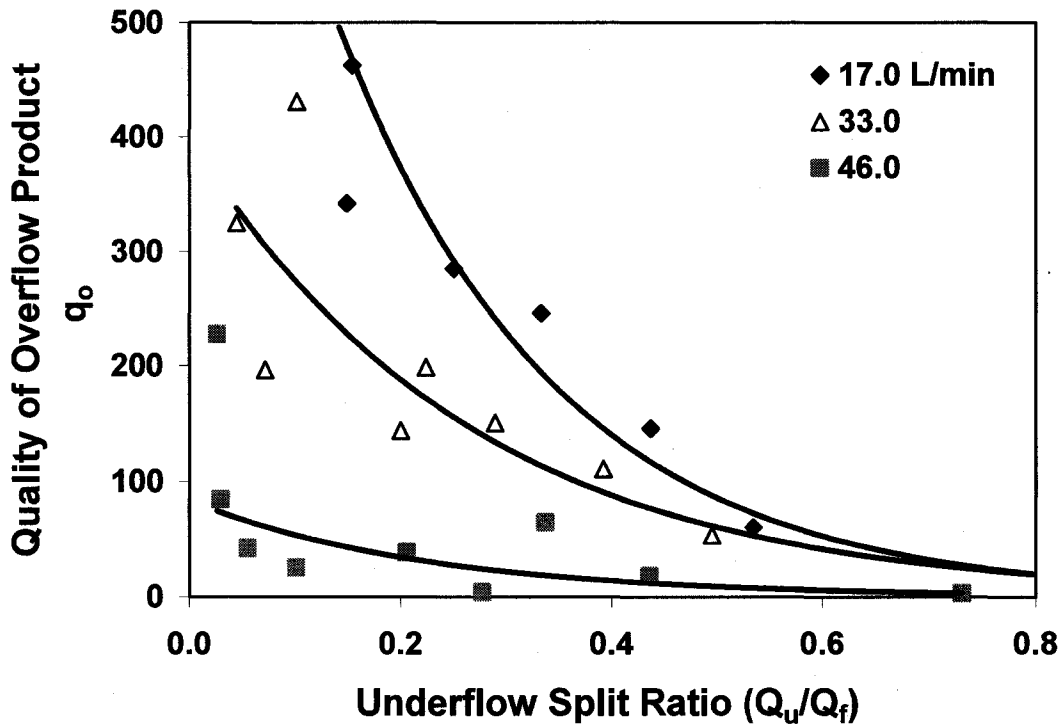

Figure 4.3: Effect of Feed Flowrate on Quality of Overflow Product
α_{lf} = 1.4%; α_{hf}= 1.9%; d_{50}= 460μm; D_o = 27mm; θ = 20°, Model (A)

As a result, the pressure differential inside the cyclone's body become negligible, and the air core formation dropped. Under this condition, the light particles were pushed back along with the heavy ones to the underflow stream, leading to very low recovery of the

light particles in the overflow. When the overflow valve was slightly opened, the back pressure in the overflow stream was reduced and the underflow split ratio was decreased.

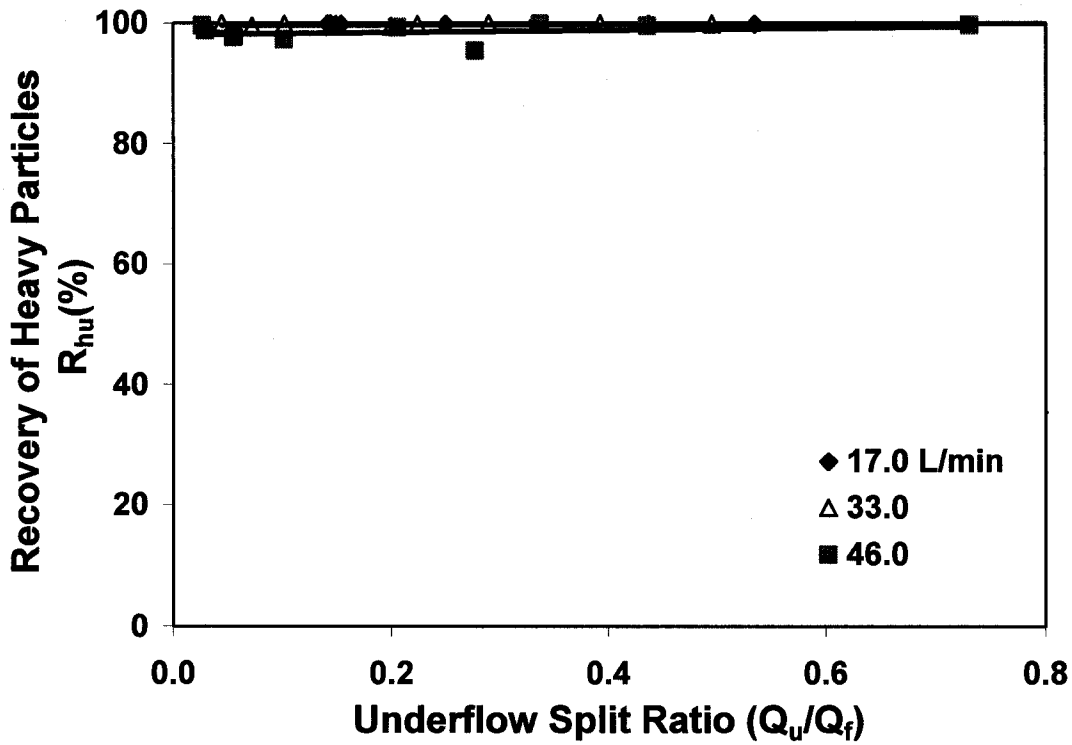

Figure 4.4: Effect of Feed Flowrate on Heavy Particles Recovery in Underflow α_{lf} = 1.4%; α_{hf}= 1.9%; d_{50}= 460μm; D_o = 27mm; θ = 20°, Model (A)

The migration probability of the light particles towards the central axis was increased. The axial velocity of the light particles in inner helical flow was increased with a decreased underflow split ratio (Chu et al., 2002), so the recovery of the light particles in the overflow was increased.

The quality of the overflow stream was decreased when the feed flowrate and underflow split ratio were increased as shown in Figure 4.3. Increasing the feed flowrate results in an increase in the overflow slurry and water split ratio (Narasimha et al., 2004). Increasing the feed flowrate also decreases the residence time. Eventually, the overflow quality was decreased.

The recovery of heavy particles in the underflow was nearly 99% at all feed flow rates and underflow split ratios as shown in Figure 4.4. The recovery of the heavy particles in the underflow was not affected by either increasing the feed flowrate or underflow split ratio due to the greater density differential between the heavy particles and the carrier fluid than that between the light particles and the carrier fluid, i.e., $d_h^2(\rho_h - \rho_m) > d_l^2(\rho_l - \rho_m)$, leading to stronger outward centrifugal forces than the inward centripetal buoyancy and drag forces. Eventually, the majority of the heavy particles reached to the underflow stream.

4.1.3 Effect of Feed Solids Concentration

The feed solids concentration is the most critical operating variable and significantly affects the hydrocyclone's separation efficiency, which directly depends on the particles settling velocity. At a relatively low total solids concentration, the settling velocities of the light and heavy particles are slightly retarded. However, at high enough solids concentrations, the settling rate declines with increasing concentrations due to the return flow being more uniformly distributed (Changirwa, 1997).

Figures 4.5 and 4.6 show the recovery and quality of the light particles in the overflow stream as a function of the underflow split ratio at two different solid concentrations 3.3% and 7.5% by weight. The feed solids concentration was increased by adding light and heavy particles at a 1:2 ratio by weight. In this set of tests d_{50} for the light "polymer" and heavy "sand" particles was 460μm and 62μm, respectively. The operation and design conditions are described in the figure captions.

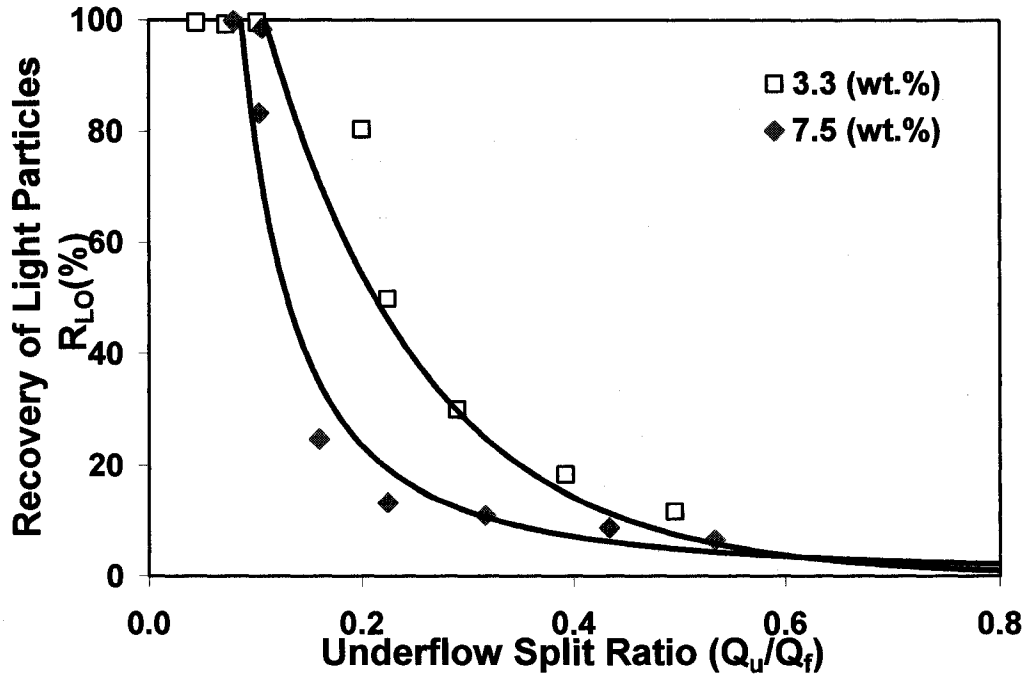

Figure 4.5: Effect of Feed Solids Concentration on Light Particles Recovery in Overflow, α_{lf1} = 1.4%; α_{hf1}= 1.9%; α_{lf2} = 2.8%; α_{hf2}= 4.7%; d_{50}= 460μm; D_o = 27mm; θ = 20°, Model (A)

Figure 4.5 reveals that by changing the feed solids concentration from 3.3 to 7.5 % by weight, the recovery of the light particles in the overflow was decreased by about 20% over a 0.08 to 0.50 underflow split ratio (Q_u/Q_f). According to Changirwa's (1997) explanation, at high solids concentrations, the rising (in-ward migration) velocity of light particles was retarded, due to the hindrance of light particles moving in cloud of heavy particles. As a result, the light particles overflow recovery was decreased.

The quality of the overflow was decreased significantly by changing the feed solids concentration from 3.3 to 7.5% over a 0.08 to 0.50 underflow split ratio as shown in Figure 4.6.

The recovery of the heavy particles in the underflow stream was not affected by increasing the feed solids concentration or the underflow split ratio as shown in Figure 4.7.

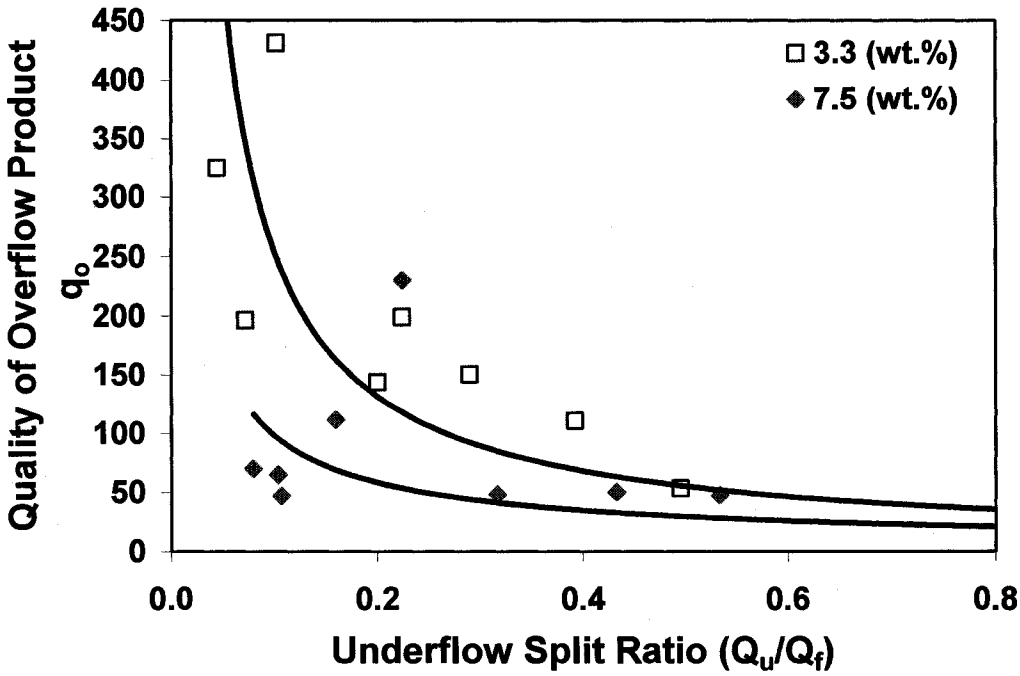

Figure 4.6: Effect of Feed Solids Concentration on Quality of Overflow Product α_{lf1}=1.4%; α_{hf1}=1.9%; α_{lf2}=2.8%; α_{hf2}= 4.7%; d_{50}= 460μm; D_o= 27mm; θ= 20°, Model (A)

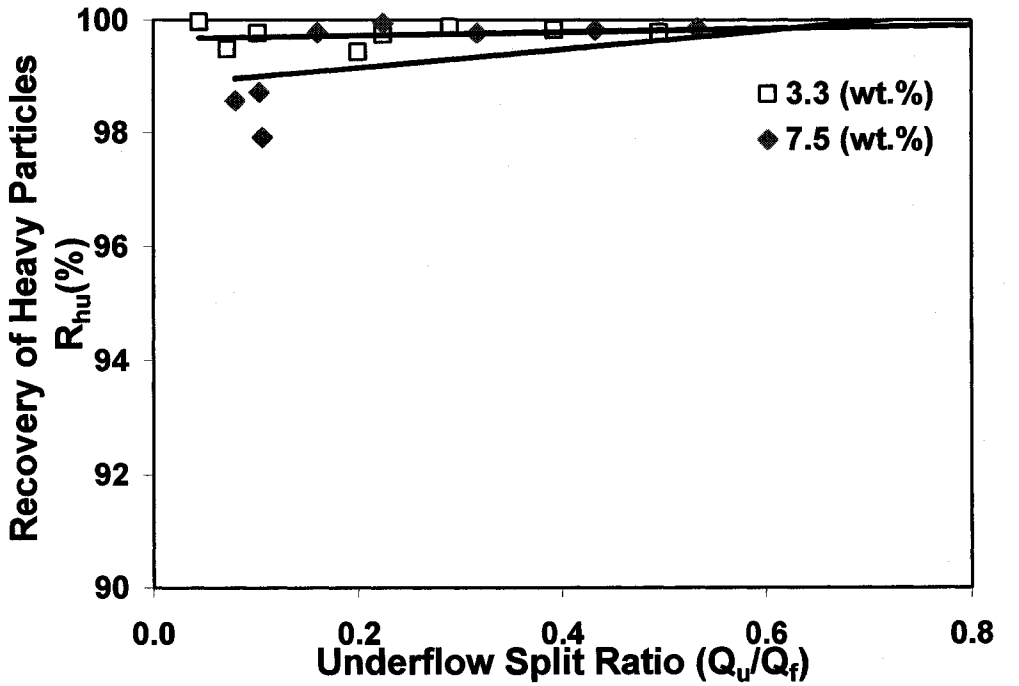

Figure 4.7: Effect of Feed Solids Concentration on Heavy Particles Recovery in Underflow, α_{lf1} = 1.4%; α_{hf1}= 1.9%; α_{lf2} = 2.8%; α_{hf2}= 4.7%; d_{50}= 460μm; D_o= 27mm; θ = 20°, Model (A)

4.1.4 Effect of Light Particles Size

The physical properties of the particles dispersed in continuous medium "water" have a vital affect on the hydrocyclone's separation efficiency. First, for the separation process to take place, a finite density difference must exist between the phases to be separated. In the current case, the absolute value of density differential for the light particles $(\rho_m - \rho_l)$ was less than that for the heavy particles $(\rho_h - \rho_m)$.

According to Stokes law,

$$\left(V_{settling} = \frac{\Delta\rho.g.d_s^2}{18\mu} \right) \qquad 4.1$$

The settling velocity of the particles is directly proportional to the square of their size. Increasing the size of the light particles increases the radial centripetal forces acting on the particles and hence the axial velocity of the particles, resulting in a faster mobility of the larger-sized light particles towards the central axis of the cyclone, where they are removed from the overflow. Similarly, increasing the size of the heavy particles increases the centrifugal force acting on the larger-sized heavy particles, resulting an improvement in the heavy particles reporting to the underflow.

Figure 4.8 shows the effect of the size of light particles on the separation of the light and heavy particles. In this set of tests, two different light particles were used in combination with the heavy particles. The d_{50} of light "Cenosphere A" particles was 360μm and the d_{50} of light "Censophere B" was 80μm. The d_{50} of heavy "sand" particles was 62μm.

The concentration of the light and heavy particles in the feed was 1.4% and 1.9% by weight, respectively. The recovery of the larger-sized light particles in the overflow was

improved at all underflow split ratios (Q_u/Q_f) from 0.1 to 0.7, and reached a maximum 99% at 0.1. The rising velocity of the larger-sized light particles is greater than the settling velocity at any underflow split ratio value. Based on Eq.4.1 the migration probability for the larger-sized light particles towards the centre was greater than that of the smaller-sized light particles (Dale and Charles, 1994; Hashmi et al., 2004).

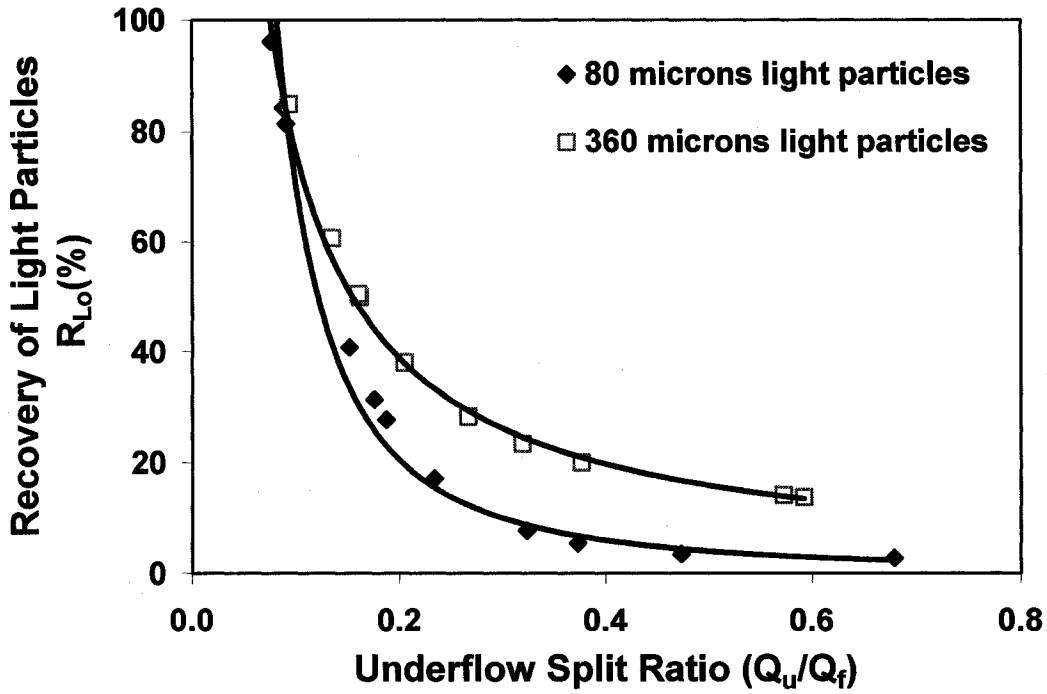

Figure 4.8: Effect of Light Particles Size on Recovery in Overflow
Q_f = 33L/min; α_{lf} = 1.4%; α_{hf}= 1.9%; D_o = 27mm; θ = 20°, Model (A)

The quality or the purity of the overflow stream was decreased with an increase in the size of light particles as shown in Figure 4.9. This result shows that the quality of the overflow product for larger-sized light particles was smaller than that of the smaller-sized light particles. Considering that the larger-sized light cenospheres, after dipping into water become heavier and also break during operation than smaller-sized light cenospheres.

Figure 4.10 shows the recovery of heavy particles in the underflow stream. The use of cenospheres actually has no effect on heavy particles recovery. The breakage of cenospheres, lead to an increase in underflow density. For this reason, the recovery and quality of heavy particles is not reported for the cases in which cenosphere particles were used.

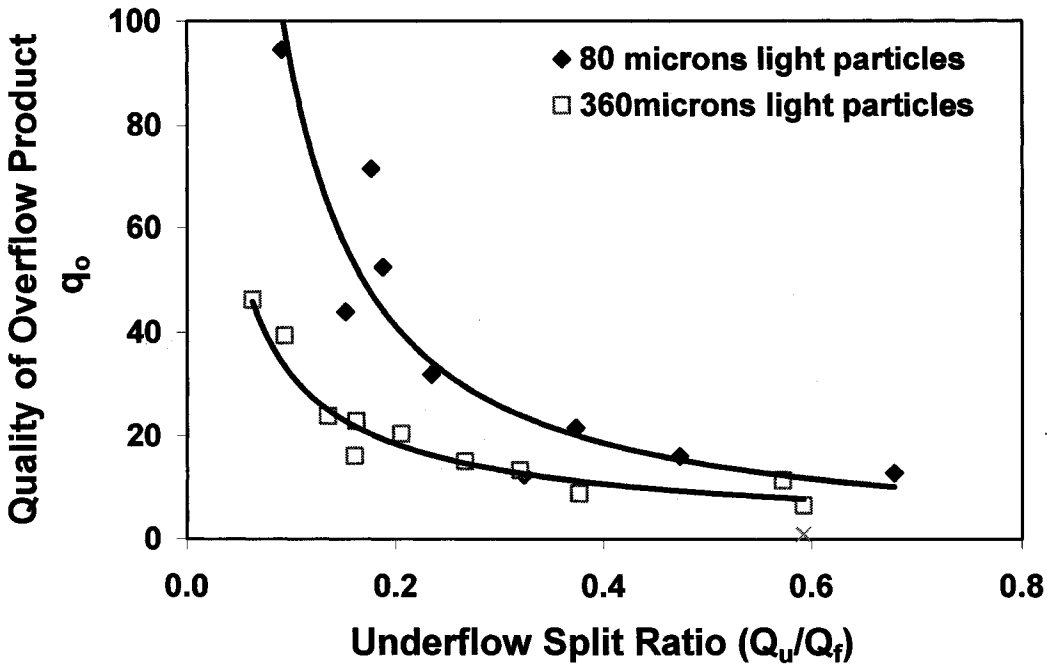

Figure 4.9: Effect of Light Particles Size on Quality of Overflow Product
Q_f = 33L/min; α_{lf} = 1.4%; α_{hf}= 1.9%; D_o = 27mm; θ = 20°, Model (A)

4.1.5 Effect of Overflow to Underflow Diameter Ratio

The overflow to underflow diameter ratio (D_o/D_u) is one of the important design variables affecting the performance and characteristics of hydrocyclones, such as capacity, cut size, sharpness of classification, split ratio, recovery, and quality of the product. (Lynch and Rao, 1975; Plitt, 1976; Nageswararao, 1978).

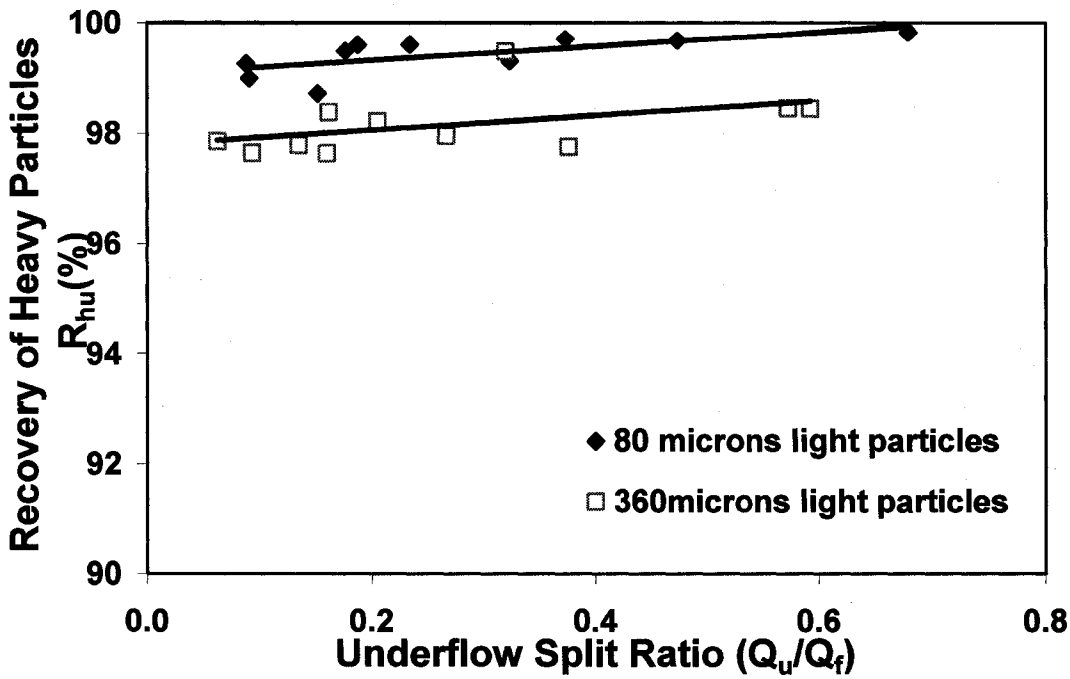

Figure 4.10: Effect of Light Particles Size on Heavy Particles Recovery in Underflow, Q_f = 33L/min; α_{lf} = 1.4%; α_{hf}= 1.9%; D_o = 27mm; θ = 20°, Model (A)

To analyze the effect of the overflow to underflow diameter ratio on the separation of light and heavy particles, a set of experiments was conducted by using the light polymer particles and heavy sand particles. The d_{50} of light polymer and heavy sand particles used was 460 and 62μm, respectively. The concentration of light and heavy particles in the feed was 2.8% and 4.7% by weight. The cone angle of hydrocyclone was 20°. The D_o/D_u ratio was decreased from 2.7 to 0.85 by changing the overflow diameter from 27mm to 11mm. The results are shown in Figures 4.11 to 4.13. Figure 4.11 shows that the recovery of light particles in the overflow stream is inversely proportional to D_o/D_u ratio at higher underflow split ratio. At the higher underflow split ratio, the pressure drop between the overflow and feed stream was higher and the residence time was increased due to larger volume available inside the hydrocyclone (Mukherjee et al., 2003). But at low underflow split ratios, the recovery was higher for the larger D_o/D_u ratio. Increasing the D_o/D_u ratio

by increasing the vortex finder diameter increased the air core diameter from top to bottom, increased the upward axial velocity, and decreased the radial velocity (Balaji, 1997; Chu et al., 2002; Narasimha et al., 2006). Increasing the D_o/D_u ratio also results in an increase of the water recovery in the overflow stream and a denser underflow stream (Brooks et al., 1984). Figure 4.11 shows that the recovery of the light particles is inversely proportional to the underflow split ratio reaching the maximum of 98% at a $Q_u/Q_f = 0.10$ for $D_o/D_u = 2.7$. In the case of the smaller ratio $D_o/D_u = 0.85$, the maximum recovery is 88% achieved at a $Q_u/Q_f = 0.58$.

In the case of a smaller overflow to underflow diameter ratio of the hydrocyclone, the quality of the light particles in the overflow stream was improved significantly as shown in Figure 4.12. Based on Eq. 2.19, a larger volume of water is pulled into the underflow (Brooks et al., 1984; Shah et al., 2006) at smaller D_o/D_u ratio. As a result, the quality is increased due to the smaller volume of water in the overflow stream. The water overflow split ratio can be controlled further by putting a back pressure on the overflow stream by means of a valve (Bradley, 1965; Patil and Rao, 1999).

Figure 4.13 shows that the recovery of heavy particles in the underflow stream was not affected by changing the overflow to underflow diameter ratios D_o/D_u.

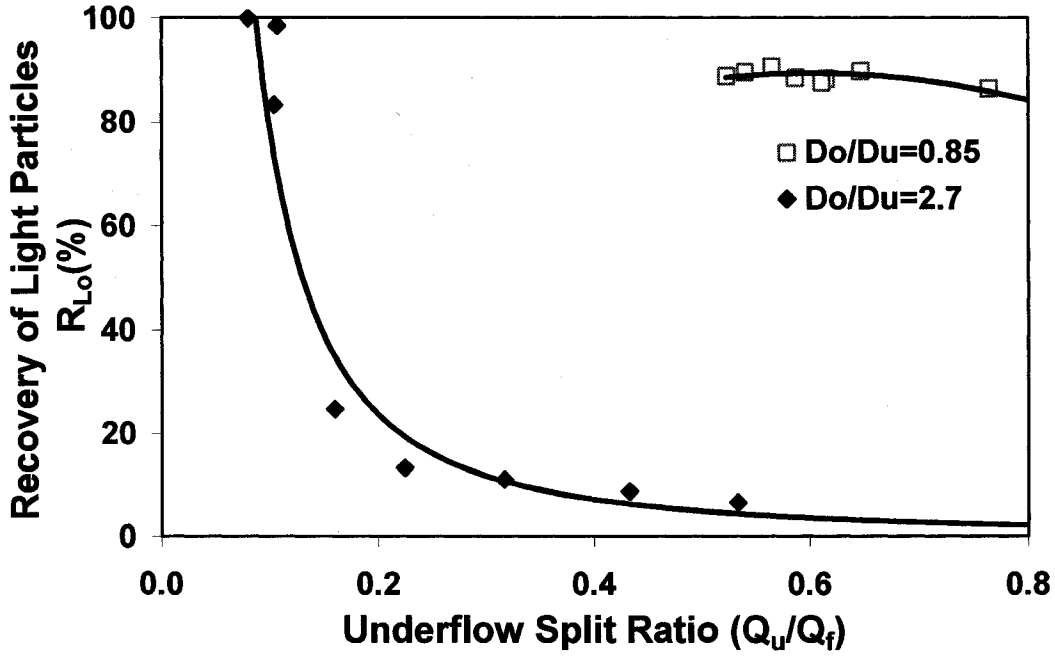

Figure 4.11: Effect of Overflow to Underflow Diameter Ratio on Light Particles Recovery in Overflow, α_{lf} = 2.8%; α_{hf} = 4.7%; d_{50} = 460μm; θ = 20°, Model (A)

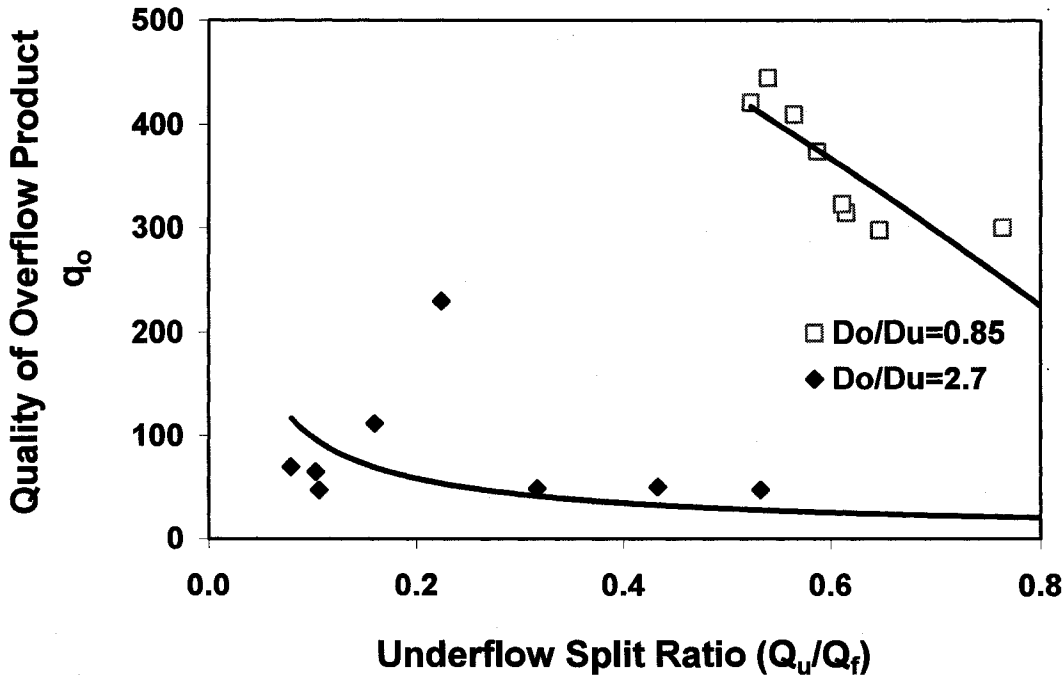

Figure 4.12: Effect of Overflow to Underflow Diameter Ratio on Quality of Overflow Product, α_{lf} = 2.8%; α_{hf} = 4.7%; d_{50} = 460μm; θ = 20°, Model (A)

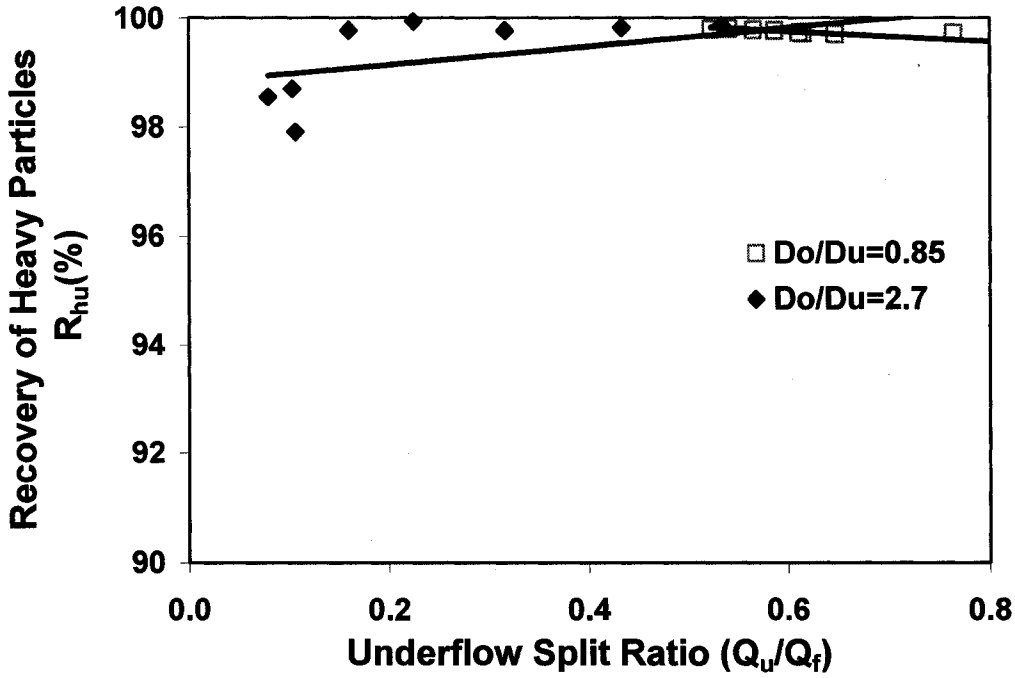

Figure 4.13: Effect of Overflow to Underflow Diameter Ratio on Recovery of Heavy Particles in Underflow, α_{lf} = 2.8%; α_{hf} = 4.7%; d_{50} = 460μm; θ = 20°, Model (A)

4.1.6 Effect of Vortex Finder Length

The vortex finder length has very little effect on the separation efficiency but plays a major role in controlling the short circuit of flow. According to Bradley (1965), the vortex finder should not be parallel to the inlet opening or the joint of the cylindrical and conical section. Otherwise, the short circuit flow and turbulence will affect the hydrocyclone's separation efficiency. According to Plitt (1976), the pressure drop is inversely proportional to the length of the free vortex in the cyclone. To achieve a higher pressure drop and better separation, the length of vortex finder should be minimized, but within the limits to avoid turbulence and short circuiting of feed flow (Bradley, 1965).

When the vortex finder's length is increased, the strength and length of the forced vortex inside the cyclone body is decreased. As a result, the hydrocyclone separation efficiency is improved (Svarovsky, 1984).

The effect of vortex finder's length on separation of the light and heavy particles is shown in Figures 4.14 - 4.16. In this set of tests, two vortex finder lengths of 37mm and 84mm were used. The operation and design conditions are given in captions of Figures 4.14 – 4.16. Figure 4.14 shows that the recovery was increased slightly by increasing the vortex finder's length from L_{vf1}=37mm to L_{vf2}=84mm. Extending the vortex finder's length into the conical section (L_{vf2}=84mm) where the radial velocity increases from the wall to the centre of the hydrocyclone and higher radial velocity gradient is in the inner

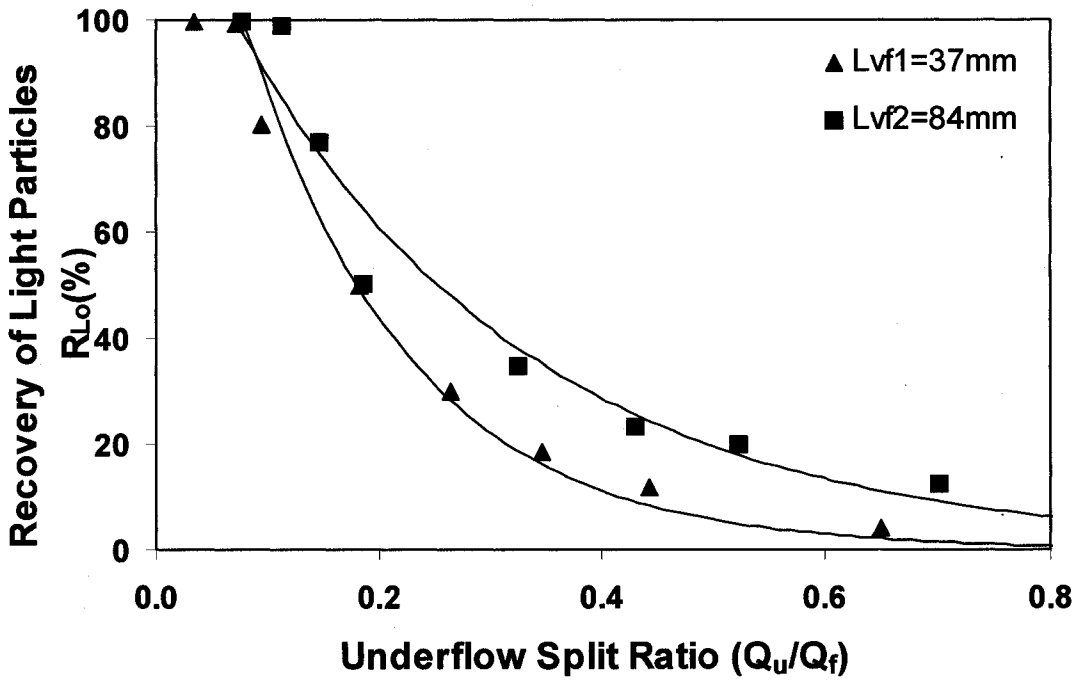

Figure 4.14: Effect of Vortex Finder Length on Light Particles Recovery in overflow Q_f= 33L/min; α_{lf} = 1.4%; α_{hf}= 1.9%; d_{50}= 460μm; D_o = 27mm; θ = 20°, Model (A)

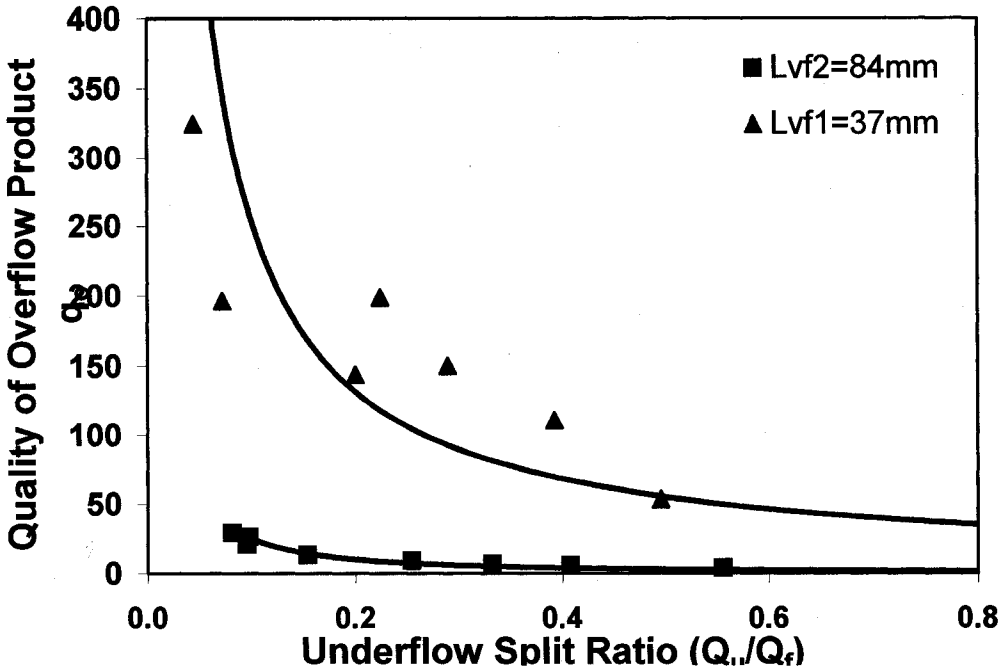

Figure 4.15: Effect of Vortex Finder Length on Quality of Overflow Product Q_f = 33L/min; α_{lf} = 1.4%; α_{hf}= 1.9%; d_{50}= 460μm; D_o = 27mm; θ = 20°, Model (A)

helical flow than the outer (Zhao and Xia, 2006). Higher radial velocity gradient in the inner helical flow helps the light particles to get separated from the heavy ones and recovery of light particles in the overflow is increased.

Figure 4.14 shows a general decrease in the recovery of the light particles with increasing the underflow split ratio. At any underflow split ratio, the recovery of light particles in the overflow was higher with a larger vortex finder length L_{vf2} = 84mm, reaching a maximum of 99% at a Q_u/Q_f value of 0.08.

Increasing the length of vortex finder decreased the quality of overflow product as shown in Figure 4.15. In this case, a fraction of fine heavy particles reported to the overflow along with the water and light particles, thereby decreasing the quality.

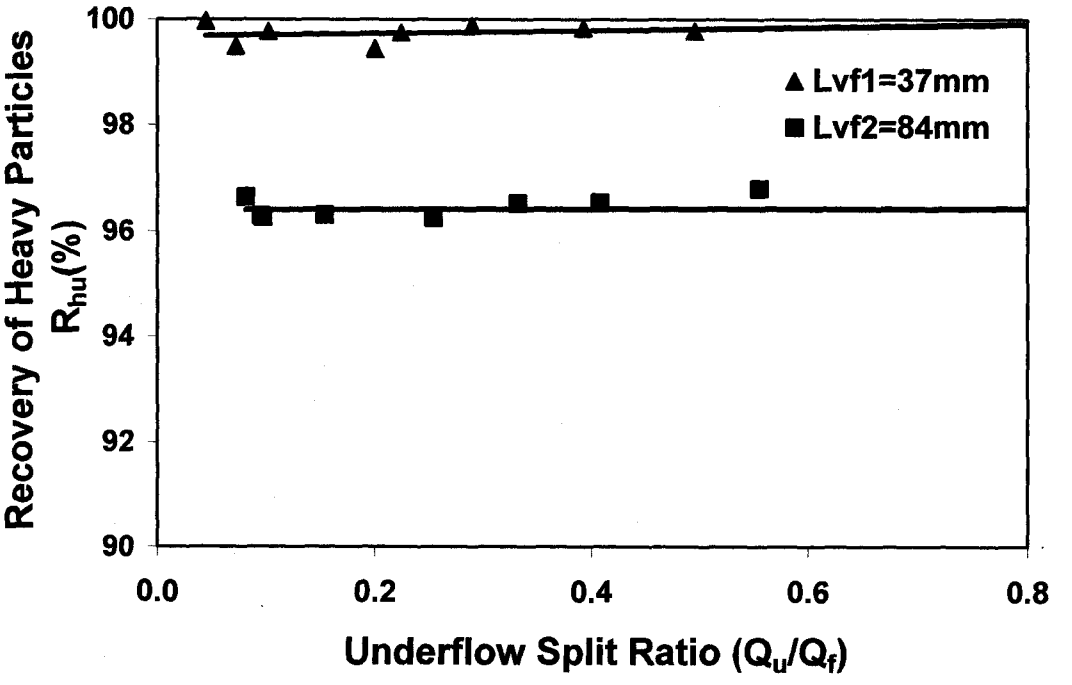

Figure 4.16: Effect of Vortex Finder Length on Heavy Particles Recovery in Underflow $Q_f = 33$L/min; $\alpha_{lf} = 1.4\%$; $\alpha_{hf} = 1.9\%$; $d_{50} = 460\mu$m; $D_o = 27$mm; $\theta = 20°$, Model (A)

The recovery of the heavy particles in the underflow stream was reduced by increasing the vortex finder length as shown in Figure 4.16. It appears that some heavy fine particles reached the overflow along with the light particles during transfer of the light particles from outer helical flow to inner in the conical section.

4.1.7 Effect of Upper Body (Cylindrical Chamber) Length

The cylindrical chamber is the upper body of the cono-cylindrical cyclones. Typically, the length of cylindrical section is equal to the cyclone diameter and can be a separate part or integral part of the inlet orifice. In the cylindrical chamber, the fluids change tangential motion into rotational motion. In general, the shorter the cylindrical length, the better is the separation (Svarovsky, 1984).

Figures 4.17-4.19 show the effect of cylindrical length on the separation of the light and heavy particles in the product streams. In this set of tests, two cylindrical lengths, 51mm and 135mm, were used. The light particles used were made of polymer.

As shown in Figure 4.17, increasing the cylindrical length decreased the recovery of the light particles in the overflow stream. In the cylindrical section, the fluid does not spin fast enough compared to that in the conical section. When the cylindrical length is increased, the residence time is increased, while the strength of the tangential velocity is decreased and angular momentum is lost by the drag against the walls of this region. As a result the separation efficiency becomes poor (Young et al., 1994).

The quality of the overflow on the other hand, was also decreased marginally with increasing the cylindrical length at normal operating Q_u/Q_f ratio greater than 0.1, as shown in the Figure 4.18.

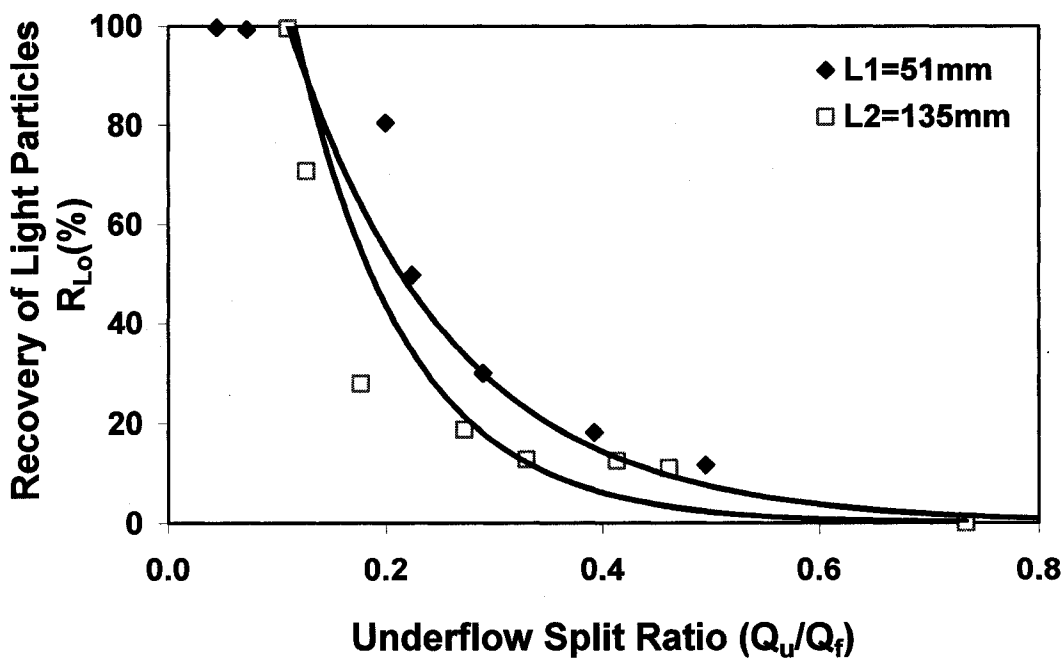

Figure 4.17: Effect of Cylindrical Length on Light Particles Recovery in Overflow, Q_f = 33L/min; α_{lf} = 1.4%; α_{hf}= 1.9%; d_{50}= 460μm; D_o = 27mm; θ = 20°, Model (A)

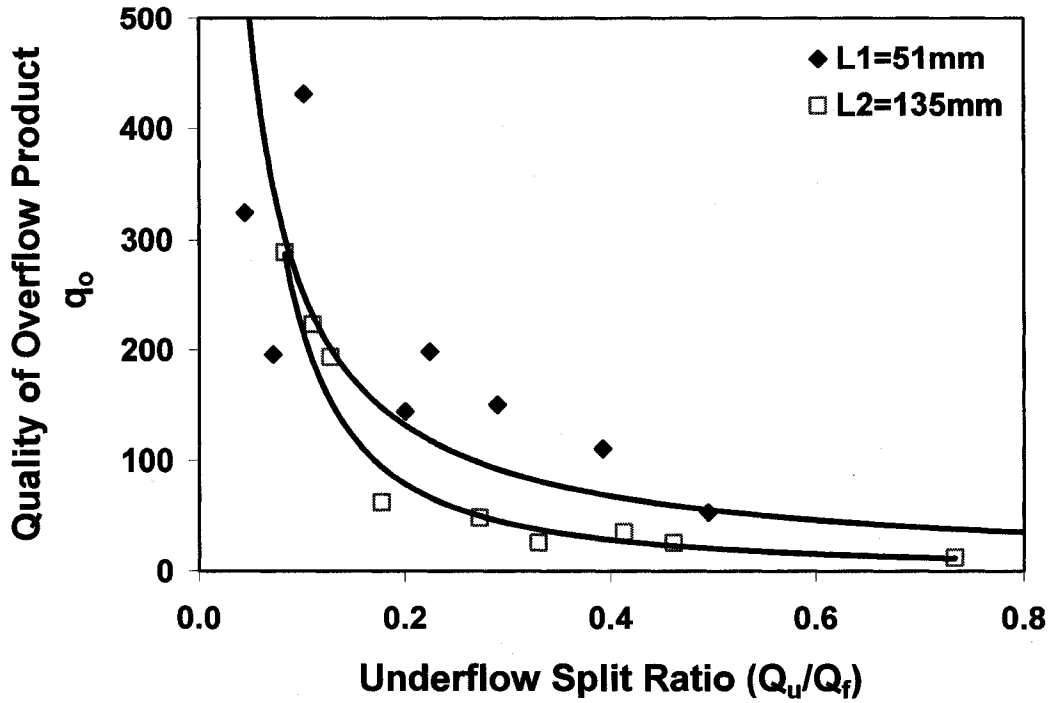

Figure 4.18: Effect of Cylindrical Length on Quality of Overflow Product Qf = 33L/min; α_{lf} = 1.4%; α_{hf}= 1.9%; d_{50}= 460μm; D_o = 27mm; θ = 20°, Model (A)

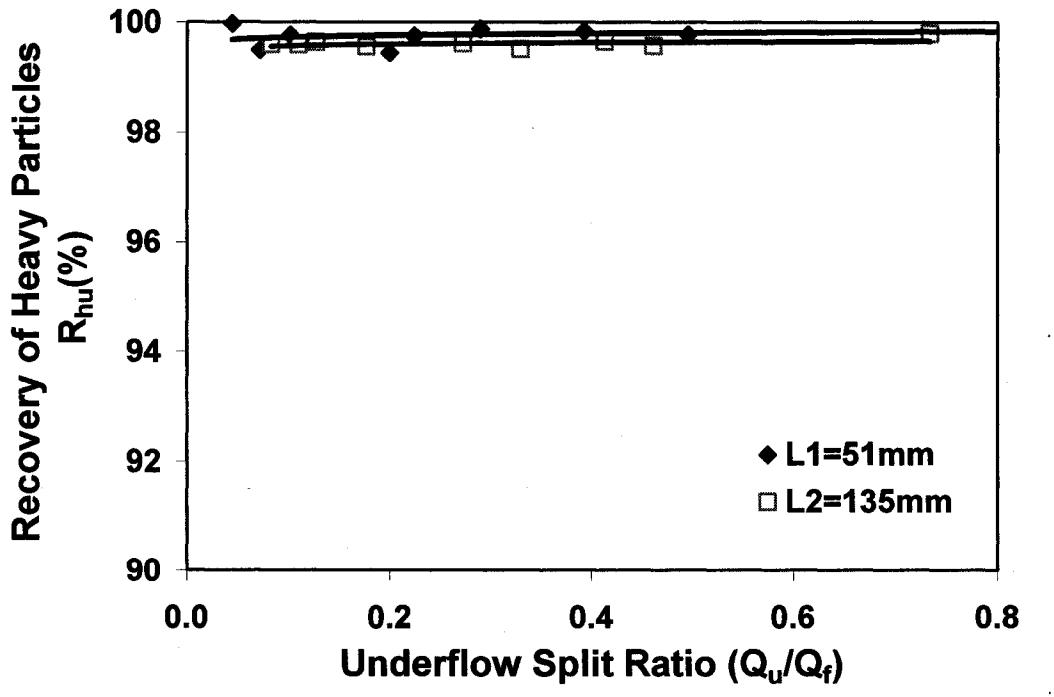

Figure 4.19: Effect of Cylindrical Length on Heavy Particles Recovery in Underflow, Q_f = 33L/min; α_{lf} = 1.4%; α_{hf}= 1.9%; d_{50}= 460μm; D_o=27mm; θ = 20°, Model (A)

The volume split ratio of the water and slurry in the underflow was increased by increasing the cylindrical length, as presented by Nageswararao equations 2.19 and 2.20. This increase increased the concentration of light particles in the underflow stream, leading to a decreased overflow quality.

Figure 4.19 shows the effect of the cylindrical length on the recovery of heavy particles in the underflow stream, as a function of the underflow split ratio. This figure shows that the recovery of the heavy particles was not affected by increasing the cylindrical length. The overall recovery of the heavy particles in the underflow stream was higher than that of the light particles because of the higher centrifugal forces acting on the heavy particles and hence high settling velocity.

4.1.8 Heavy Particles Recovery in Underflow Stream

According to Stokes law (see Equation 4.1), separation efficiency directly depends on the particles settling velocity. The particles with a high settling velocity are centrifuged to the cyclone's walls and are removed through the conical part called the apex, and the particles with a low settling velocity are carried away by an upward vortex through the vortex finder (Puprasert et al., 2004).

Figure 4.20 shows the effect of the operation and design variables on the recovery of the heavy particles in the underflow stream. The recovery is nearly 99% for all operation and design variables except for the length of vortex finder. Increasing the length of vortex finder causes the entrainment of fine heavy particles in the overflow, leading to a decrease in heavy particles recovery in underflow stream. In most of the cases, the heavy particle recovery is not affected by either the design or operation variables or the

underflow split ratio. The equation 4.1 shows that the density differential has a significant impact on the settling velocity and separation efficiency. For the particles to be separated, a finite density difference must exist; otherwise, the buoyancy force will equal the centrifugal force, and no separation would take place.

The density differential between the heavy particles and the carrier fluid is greater than that between the carrier fluid and the light particles. As the particles density differential increases relative to the carrier fluid density, their mobility will increase when subjected to a centrifugal force. The radial velocity of the greater density differential of the heavy particles is higher than that of the smaller density differential of the light particles. For this reason, the mobility of heavy particles toward the walls is greater. In our system, the outward centrifugal forces are significant so that the majority of the heavy particles reach the underflow stream.

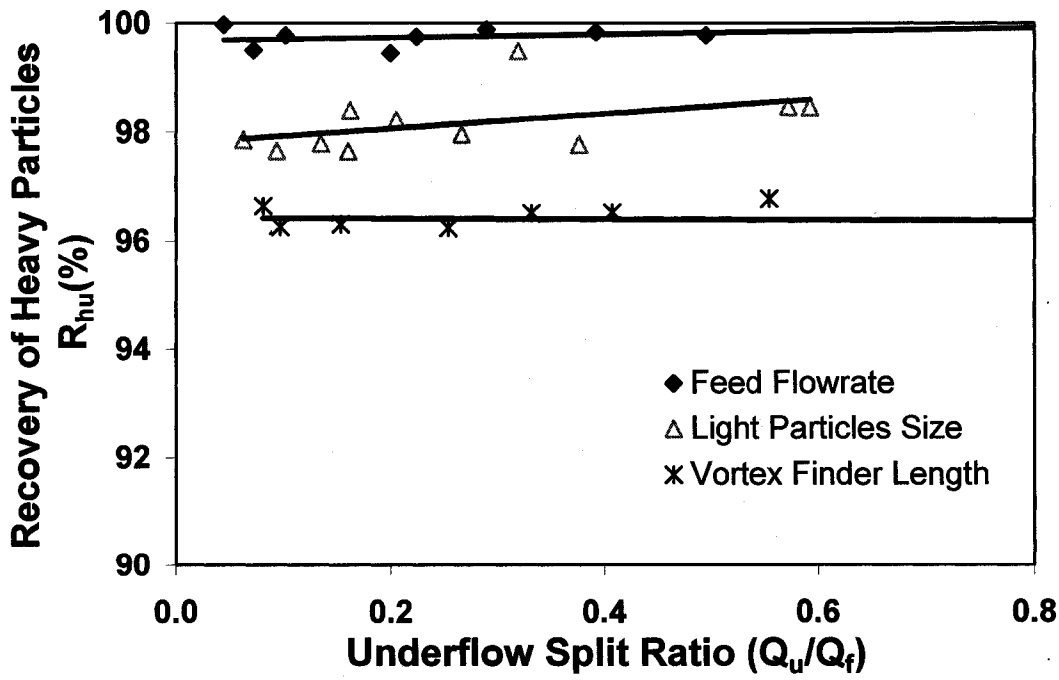

Figure 4.20: Effect of Operation and Design Variables on Heavy Particles Recovery in Underflow, Q_f = 33L/min; α_{lf} = 1.4%; α_{hf}= 1.9%; D_o = 27mm; θ = 20°, Model (A)

4.2 Hydrocyclone Model B

Hydrocyclone model B is a modification of hydrocyclone model A. The model was developed by Changirwa in 1997 for three-phase separation. The main design modifications are such that it consists of two conical sections with different cone angles of 20° and 10°. The two cones are structured coaxially with the principal axis of hydrocyclone. Due to the different cone angles, the length of its conical section is increased to 256 mm. It has a long underflow aperture. The vortex finder diameter is less than the apex diameter. The main purpose for increasing the conical length by decreasing the cone angle is to increase the residence time, the tangential motion and the angular momentum in the conical section to facilitate particles separation. The purpose of decreasing the diameter of vortex finder is to improve quality and overflow recovery of the light particles at a higher underflow split ratio. All the other dimensions are described in Figure 3.2.

4.2.1 Effect of Feed Flow Rate

Figures 4.21-4.23 show the effect of the feed flow rate and the underflow split ratio (Q_u/Q_f) on the recovery, and the quality of the light and heavy particles in the overflow and underflow streams, respectively. In this set of tests, the d_{50} for the light "Censophere" and heavy "sand" particles was 80μm and 62μm, respectively. The concentration of the light and heavy particles in the feed was 2.8% and 4.7% by weight, respectively. The vortex finder diameter used was 27mm. Figure 4.21 shows that the recovery of the light particles in the overflow was increased when the feed flow rate was increased from 33 L/min. to 46 L/min. In hydrocyclone B, the smaller cone angle increased the length of

the cyclone and hence the air core diameter from the top to the bottom. As a result of this increase, when the feed flow rate was increased the tangential velocity and the

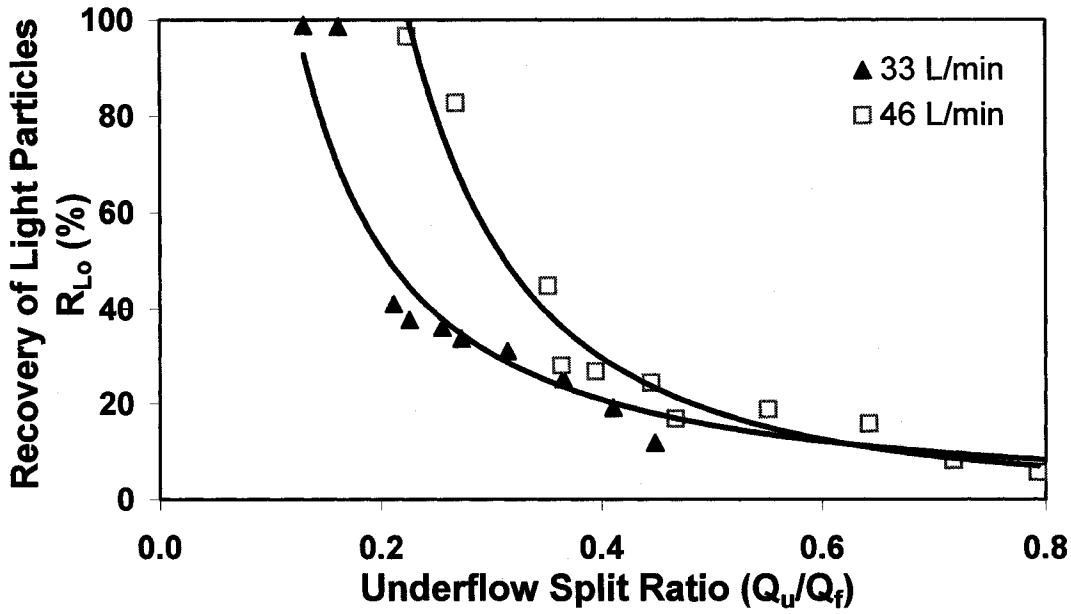

Figure 4.21: Effect of Feed Flow Rate on Light Particles Recovery in Overflow
α_{lf} = 2.8%; α_{hf}= 4.7%; d_{50}= 80μm; D_o = 27mm; θ = 10°, Model (B)

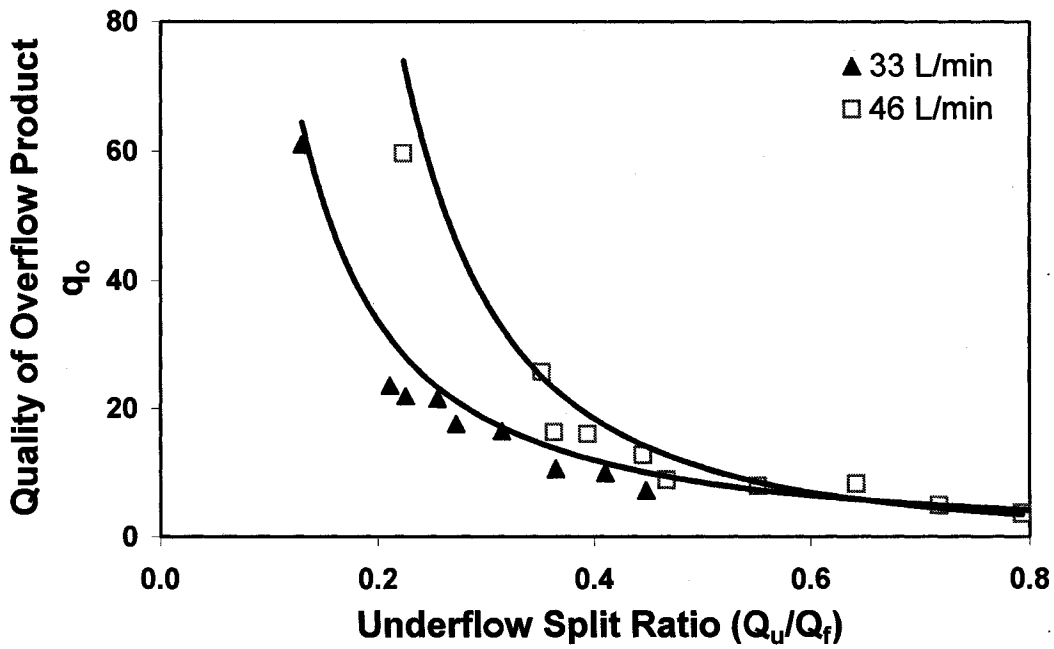

Figure 4.22: Effect of Feed Flow Rate on Quality of Overflow Product
α_{lf} = 2.8%; α_{hf}= 4.7%; d_{50}= 80μm; D_o = 27mm; θ = 10°, Model (B)

acceleration forces in the conical section were increased. The increased length of the cyclone gave the particles enough residence time to get stratified in the respective zones, leading an increase recovery of the light particles to the overflow stream.

Figure 4.21, also shows that the recovery of the light particles in the overflow stream was increased as the underflow split ratio was decreased from 0.6 to 0.18 reaching 92% at 0.18, but was constant in the range of a underflow split ratio of 0.8-0.6.

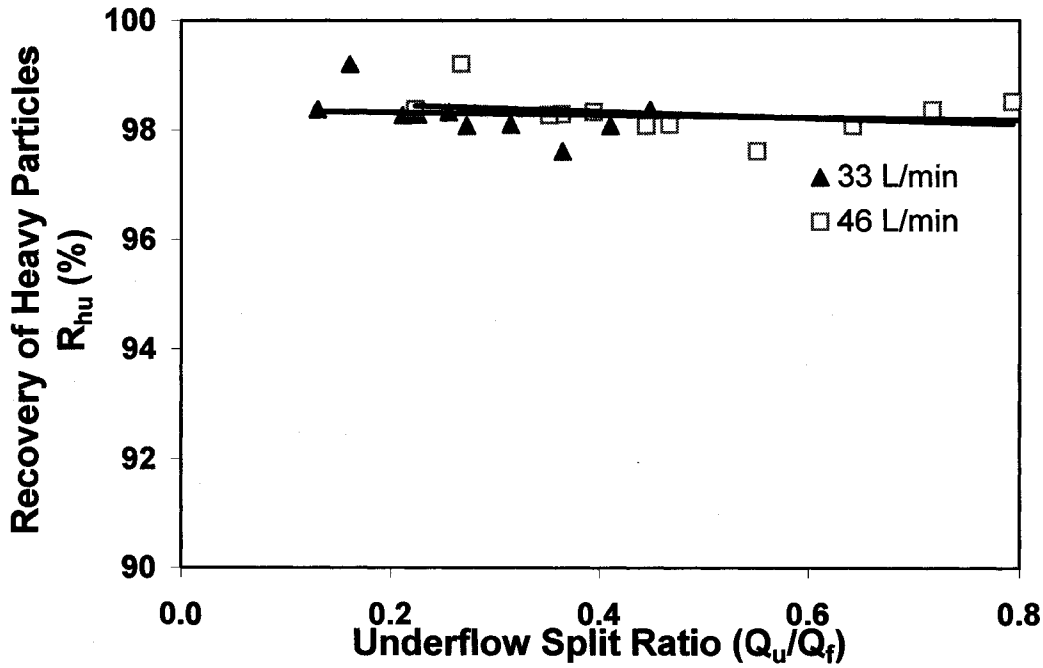

Figure 4.23: Effect of Feed Flow Rate on Heavy Particles Recovery in Underflow, α_{lf} = 2.8%; α_{hf}= 4.7%; d_{50}= 80μm; D_o = 27mm; θ = 10°, Model (B)

Figure 4.22 shows the effect of the feed flowrate and the underflow split ratio on the quality of the overflow stream. Increasing the feed flowrate increased the quality of the overflow stream, and the overall quality was improved. But this was less than expected because increasing the feed flowrate increased the vortex finder flowrate and water split ratio to the overflow (Slechta and Firth, 1984; Narashimha et al., 2004). As well, the

density of the light particles was close to the density of the continuous medium "water". The majority of the water reported to the overflow, along with the light particles.

The recovery of heavy particles in the underflow was nearly 98% at all feed flow rates and underflow split ratios as shown in Figure 4.23. The recovery of the heavy particles in the underflow was not affected by either increasing the feed flowrate or underflow split ratio due to their higher settling velocity.

4.2.2 Effect of Light Particles Size

The particle size plays a major role in the separation of light and heavy, within the slurry. To check the effect of the particles size on the separation of the light and heavy phases in the product streams, a set of experiments was conducted. The operation and design conditions were maintained as such that the d_{50} of heavy particles was 62μm and the feed volumetric flow rate was 33 L/min. The overflow diameter was 11mm, and the cone angle was 10°. The two different sizes of light "Censophere" particles were used. The d_{50} was 80 and 360 μm. The underflow split ratio (Q_u/Q_f) varied from 0 to 1.0. The air core formation started at a 0.80 underflow split ratio.

Figure 4.24 shows that when the size of light particles was increased from 80 to 360 μm, the recovery of the larger-sized light particles in the overflow was improved when the underflow split ratio (Q_u/Q_f) was from (0.45 – 0.80). In the case of the smaller-sized light particles, the maximum recovery was 88% at 0.52 underflow split ratio, while in the case of the larger-sized light particles, the maximum recovery was 92% at a 0.72 underflow split ratio. With an underflow split ratio from 0.0-0.45, no change was observed in the recovery with slurry split ratio for both types of particles.

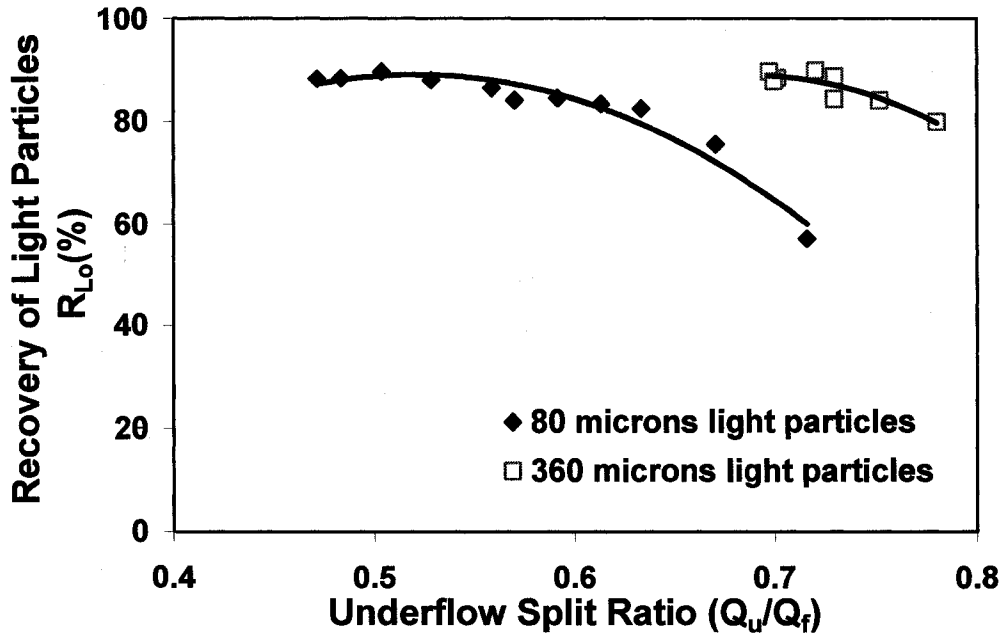

Figure 4.24: Effect of Light Particles Size on Recovery in Overflow
Q_f = 33L/min; α_{lf} = 2.8%; α_{hf}= 4.7%; D_o = 11mm; θ = 10°, Model (B)

The quality or the purity of the overflow stream with respect to the light particles was not reported because the breakage of light cenosphere particles was significant.

4.2.3 Effect of Overflow to Underflow Diameter Ratio

As illustrated with hydrocyclone model A, the overflow to the underflow diameter ratio D_o/D_u plays a major role in the concentration and separation of light/heavy particles in the hydrocyclone. This ratio can be varied by changing either the overflow diameter or the underflow diameter. In the hydrocyclone model B, the overflow diameter was varied, and the underflow diameter was fixed. The effect of the overflow to underflow diameter ratio on the recovery and quality of the light particles in the overflow stream is shown in Figures 4.25 and 4.26. Figure 4.25 shows that the recovery of the light particles increased

as the underflow split ratio decreased and reached a maximum of 98% at a split ratio 0.15 for $D_o/D_u = 2.7$. With the smaller overflow to underflow diameter ratio of $D_o/D_u = 0.85$, the maximum recovery was 90% at a corresponding value for the underflow split ratio of 0.58. However, as the underflow split ratio was increased, the recovery decreased sharply because the Cenospheres were broken down at the higher underflow rate. At fully opened overflow valve, the overall recovery was higher for the larger D_o/D_u ratio hydrocyclone.

In the case of the hydrocyclone with a smaller overflow to underflow diameter ratio, the quality of the light particles in the overflow stream was improved very significantly (see Figure 4.26). In this case, the axial velocity of the light particles was increased, and the air core formed was more stable and strong, which helped to pull the light particles upwards. In addition, a larger amount of the dilution water reached the underflow, thereby leading to improve the quality by decreasing the overflow diameter.

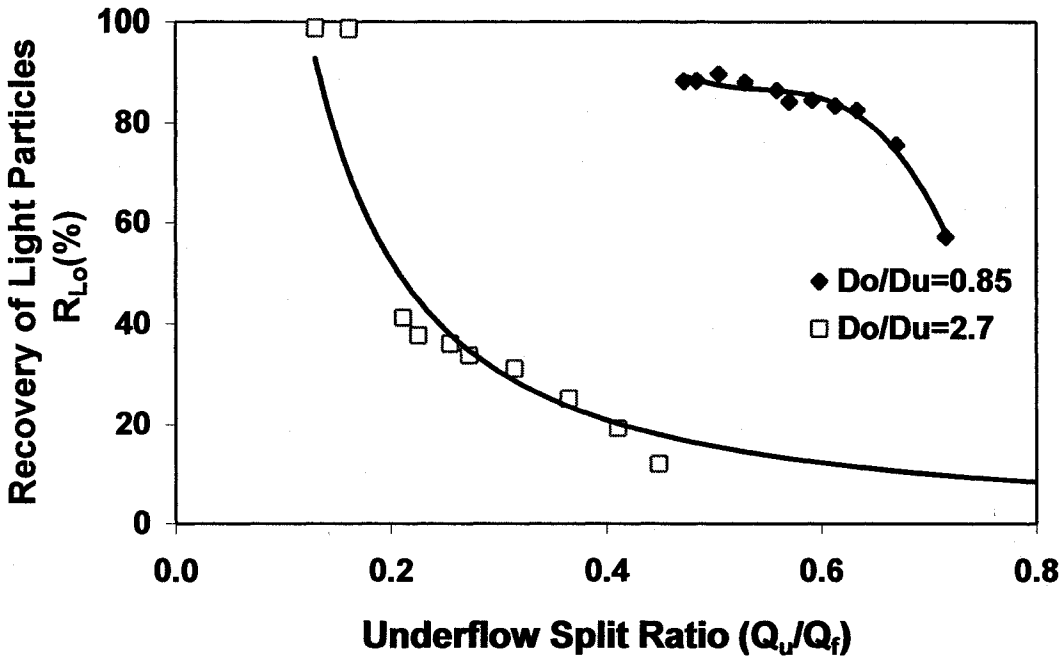

Figure 4.25: Effect of Overflow to Underflow Diameter Ratio on Light Particles Recovery in Overflow, Q_f = 33L/min; α_{lf} = 2.8%; α_{hf}= 4.7%; d_{50}= 80μm; θ = 10°, Model (B)

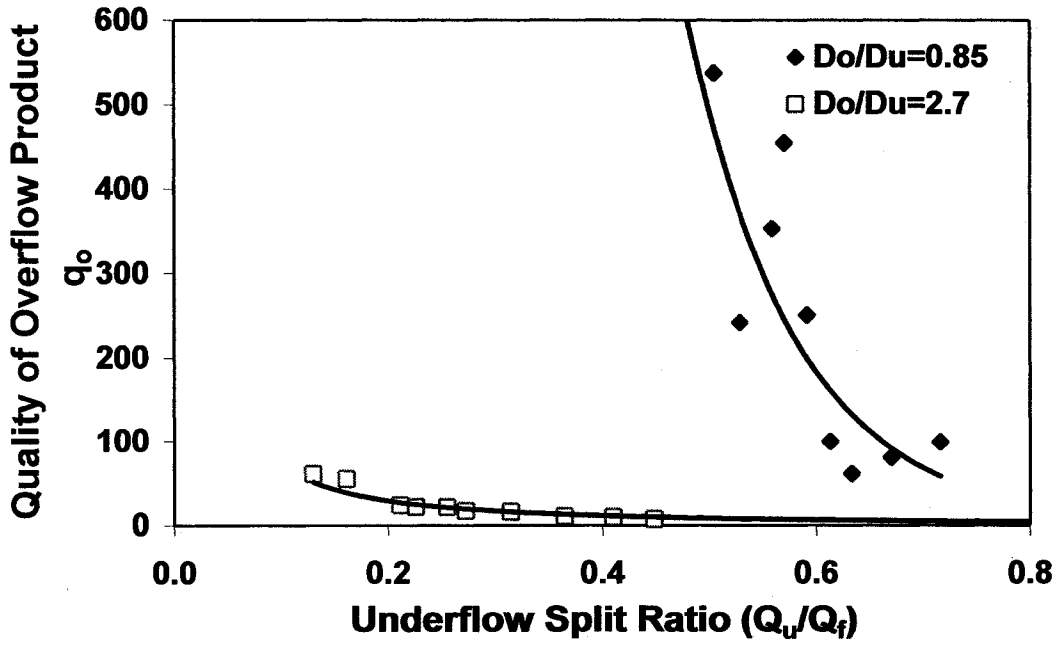

Figure 4.26: Effect of Overflow to Underflow Diameter Ratio on Quality of Overflow Product, Q_f = 33L/min; α_{lf} = 2.8%; α_{hf}= 4.7%; d_{50}= 80μm; θ = 10°, Model (B)

4.3 Comparison of Hydrocyclone Model A and Model B

The hydrocyclone models A and B were operated under the same operation conditions, such as feed flowrate, particle-size distribution, and solid concentrations. The design variables such as the overflow diameter, length of the conical section and the cone angle were varied.

4.3.1 Feed Flowrate

Figure 4.27 and 4.28 shows the comparison of hydrocyclone model A and model B under the same operation and design conditions. The feed flowrate was maintained at 33 L/min. The d_{50} for the light "Censophere" and heavy "sand particles was 80 and 62 μm, respectively. The recovery of light particles and quality of overflow product for hydrocyclone model B was greater than that of the hydrocyclone model A at a given

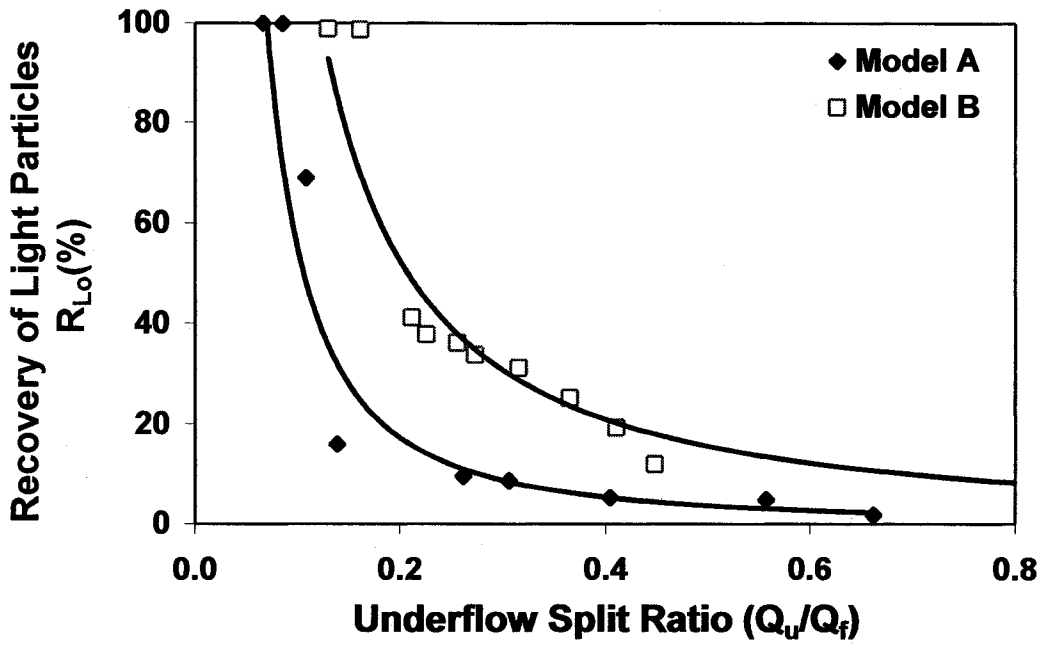

Figure 4.27: Hydrocyclone Model A and B, Light Particles Recovery in Overflow Q_f = 33L/min; α_{lf} = 2.8%; α_{hf}= 4.7%; d_{50}= 80μm; D_o/D_u = 2.1

underflow split ratio of 0.15-0.40. The recovery and quality for both model hydrocyclones merged when the underflow split ratio varied from 0.4 to 0.8. This is attributed to the smaller pressure differential under a higher underflow split ratio. Decreasing the cone angle from 20° to 10° increased the length of conical section, leading to a greater radial and axial velocity of the light particles in the conical region than in the upper and lower sections of the hydrocyclone. With such a configuration, the separation zone was increased, leading to an increase in the recovery of the light particles in the overflow.

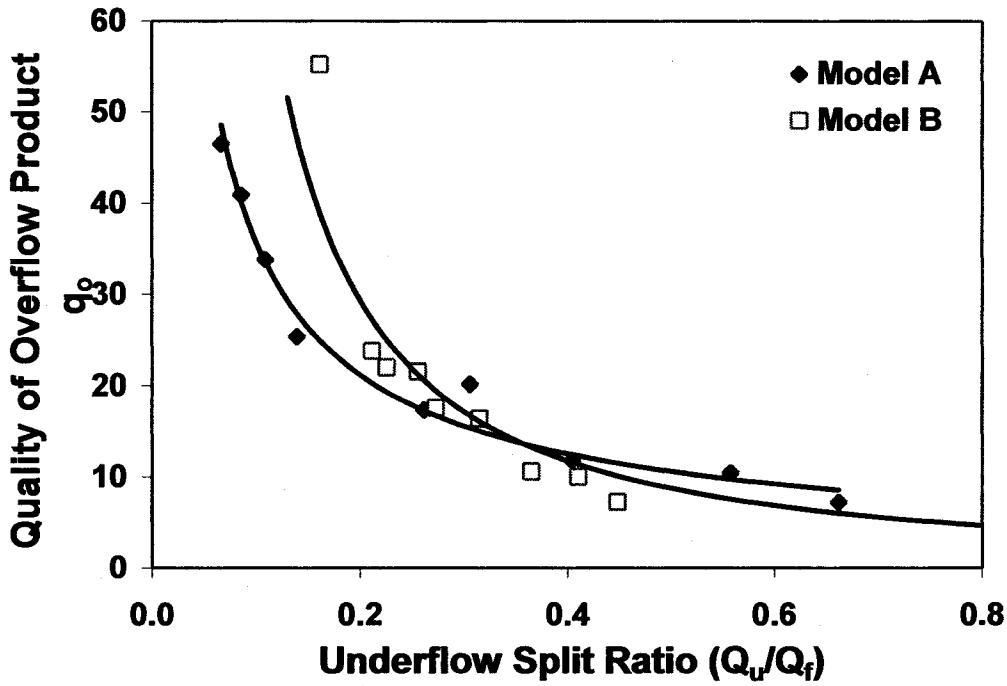

Figure 4.28: Hydrocyclone Model A and B, Quality of Overflow Product
Q_f = 33L/min; α_{lf} = 2.8%; α_{hf}= 4.7%; d_{50}= 80μm; D_o/D_u = 2.1

4.3.2 Overflow to Underflow Diameter Ratio

Figures 4.27-4.29 show that when the overflow to underflow diameter ratios D_o/D_u are changed from 2.1 to 0.85, the recovery of light particles in the overflow of hydrocyclone

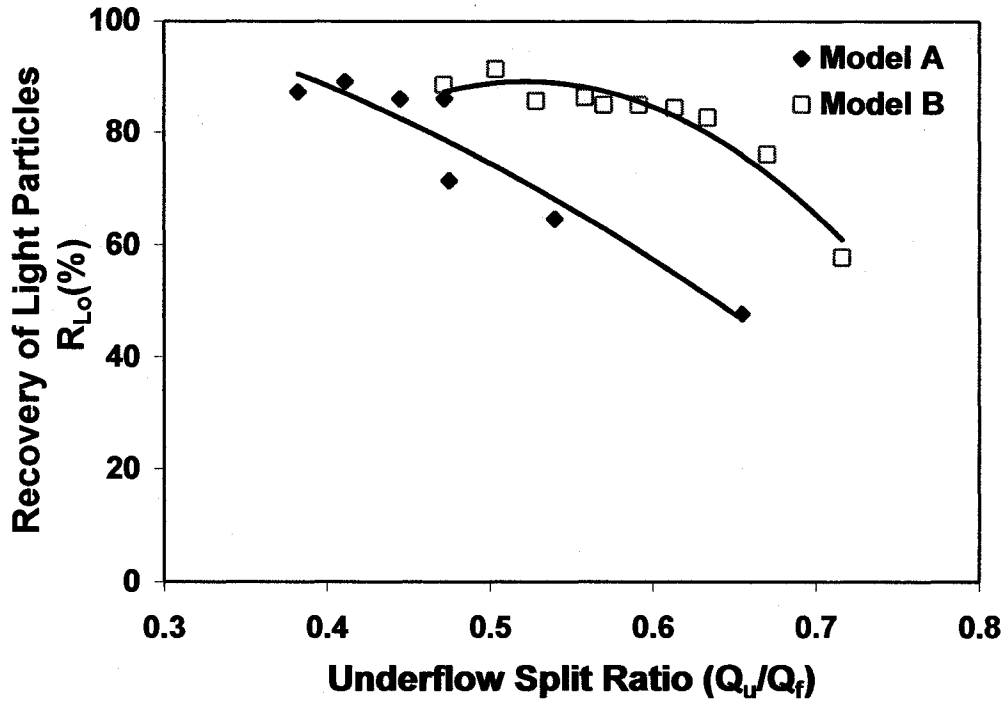

Figure 4.29: Hydrocyclone Model A and B, Light Particles Recovery in Overflow
Q_f = 33L/min; α_{lf} = 2.8%; α_{hf}= 4.7%; d_{50}= 80μm; D_o/D_u = 0.85

B is greater than that of the hydrocyclone A. This is due to increased residence time by increasing the conical length of hydrocyclone. As a result, the recovery of the light particles in the overflow was higher.

Chapter 5

CONCLUSIONS

The separation of light and heavy particles in a liquid slurry can be achieved quite efficiently by the use of a hydrocyclone with a short residence time, low capital and operation cost and with high recovery. The main concerns in considering this technique for separating of light "bitumen" and heavy "sand" particles within the liquid slurry are

- Solving the problem of transporting the high specific gravity slurry from the mine area to the oilsand extraction plant, to save huge maintenance costs for the hydrotransport lines.
- Eliminating the development of a huge tailings pond by disposing of the slurry at the mining site.

As a result of this research work, two hydrocyclone models were built and operated by varying the operation variables. The conclusions of this research work are summarized as;

5.1 Design Variables

The effect of the design variables on the recovery and quality of the light and heavy particles in the overflow and underflow streams is as follows:

- For hydrocyclone model A, increasing the cylindrical chamber length decreases the recovery of the light particles in the overflow and the recovery of heavy particles in the underflow stream is not affected. The quality of the overflow

product is reduced slightly because more of the water in the feed stream splits into the overflow.

- For hydrocyclone model A, increasing the vortex finder length increases the recovery of the light particles in the overflow and the recovery of heavy particles in the underflow stream is decreased. The quality of the overflow product is reduced due to the entrainment of heavy fine particles in the overflow.
- Decreasing the overflow to underflow diameter ratio changes the behavior of the hydrocyclone from forward to reverse flow. The results of the tests indicate that when the overflow diameter is less than the underflow diameter, the recovery of the light particles and quality of the overflow product stream is increased at a higher underflow split ratio in both the models A and B. Overflow to underflow diameter ratio does not have any effect on the recovery of heavy particles in the underflow stream.
- Increasing the length of the hydrocyclone by increasing the length of the conical section and decreasing the cone angle from 20° to 10° increases the recovery of the light particles and quality of the overflow product stream is improved in hydrocyclone model B either using larger or smaller D_o/D_u ratio.

5.2 Operation Variables

The effect of operation variables on the recovery and quality of the overflow and underflow streams is as follows:

- The feed flowrate is one of the important operating variables and significantly affects the recovery of the light and heavy particles in the overflow and underflow

streams. For the case of hydrocyclone model A, increasing the feed flowrate results in a decrease in the recovery and quality of the overflow product stream; while in the case of hydrocyclone B opposite results are achieved. There is no effect on the recovery of heavy particles in the underflow stream in both the hydrocyclones.

- Increasing the size of the dispersed light particles increased the overflow recovery and quality of the overflow in both A and B hydrocyclones. Larger size light Cenosphere particles break by the pump. Thus, further studies are needed to find the best way to reduce particles breakage.
- Increasing the feed solids concentration by weight results in decreasing the recovery and quality of the light particles in the overflow.

Recommendations for Further Research Work

The following recommendations are made for the hydrocyclone (model B) to further optimize its design for future research work.

Hydrocyclone model B showed better results in both improving the recovery and quality of the overflow. Further experimental work with the operation variables is required. This work would involve changing the total solid concentration and the light and heavy particles ratio according to the bitumen and solids ratio in the low-, average-, and high-grade oilsand ores distribution on site.

More experiments are needed for different design variables such as cone angle and overflow diameter.

Visualization experiments are needed to understand the separation zone and mechanism occurring in the hydrocyclone's body. Such experiments may help to improve further the hydrocyclone's design.

REFERENCES

Balaji, D., "Hydrodynamic Modeling of Solid Liquid Flows in Large Scale Hydrocyclones", PhD Thesis, Dept. of Metallurgical Engineering, University of Utah, 1997.

Bednarski, S., "Hydrocyclones for simultaneous removal of oil and solid particles from ships oily waters", 3rd International Conference on Hydrocyclones, BHRA, Cranfield, G2: 181, 1987.

Bohnet, M., "Separation of two liquids in the hydrocyclones", Chem. Eng. Techn. 41: No. 5 and 6, 1969.

Bradley, D., "The Hydrocyclone", Pergamon Press, 1965.

Brookes, G. F., Miles, N. J. and J. S. Clayton, "Hydrocyclone performance related to velocity parameters", 2nd International Conference on Hydrocyclones, Oxford, England, C1: 67, 1984.

Changirwa, R. M. M. and M. C. Rockwell, "Hybrid simulation for oil-solids-water separation in oilsands production", Minerals Engineering, Vol. 12, No. 12: 1459, 1999.

Changirwa, R. M. M., "Modelling of a Three-Phase Separation Hydrocyclone", M.A.Sc. Thesis, Dept. of Mining and Metallurgical Engineering, TUNS, Halifax, NS, Canada, 1994.

Changirwa, R. M. M., "Phenomenological Separation in a Three-Phase Hydrocyclone", PhD Thesis, Dept. of Mining and Metallurgical Engineering, TUNS, Halifax, NS, Canada, 1997.

Chu, L. Y., Chen, W. M. and X. Z. Lee, "Effects of geometric and operating parameters and feed characters on the motion of the solid particles in hydrocyclones", Separation and

Purification Technology, 26: 237, 2002.

Colman, D. A. and M. T. Thew, "Hydrocyclone to give highly concentrated samples of a lighter dispersed phase", 1st International Conference on Hydrocyclones, BHRA, Cranfield, 15: 209, 1980.

Colman, D. A. and M. T. Thew, "The concept of hydrocyclones for separating light dispersions and a comparison of field data with laboratory work", 2nd International Conference on Hydrocyclones, BHRA, Bath, F2: 217, 1984.

Colman, D. A., "The Hydrocyclone for Separating Light Dispersions", PhD Dissertation, University of Southampton, UK, 1981.

Colman, D. A., Thew, M. T. and D. R. Corney, "Hydrocyclones for oil/water separation", 1st International Conference on Hydrocyclones, BHRA, Cranfield,11: 143, 1980.

Dai, G. Q., Chen, W. M., Li, J. M. and L. Y. Chu, "Experimental study of solid-liquid two-phase flow in a hydrocyclone", Chemical Engineering Journal, 74: 211, 1999.

Dale, G. W. and A. P. Charles, "Process engineering of produced water treatment facility based on hydrocyclone technology", Proceedings of the International Petroleum Environmental Conference, Houston, Texas, March 2-4, 1994.

Devulapalli, B. and R. K. Rajamani, "A comprehensive CFD model for particle-size classification in industrial hydrocyclones", Proceedings Hydrocyclones '96, Cambridge, 83, 1996.

Dwari, R. K., Biswas, M. N. and B. C. Meikap, "Performance characteristics for particles of sand FCC and fly ash in a novel hydrocyclone", Chemical Engineering Science, 59: 671, 2004.

Hashmi, K. A., Hamza, H. A. and J. C. Wilson, "An emerging alternative for the

treatment of oily waste streams", Minerals Engineering, 17: 643, 2004.

Hashmi, K. A., Hamza, H. A., Kar, K. L., Zalischuk, J. L. and M. T. Thew, "Liquid-liquid hydrocyclone for removing oil from produced waters in heavy oil recovery", Joint Technical Seminar, Arctic and Marine Oil spill Program (AMOP) and Chemical Spills, June 9, 1992.

Hitchon, J. W., "Cyclones as liquid-liquid contractor-separators", AERE-CE/r 2777, 1959.

Kelsall, D. F., "A study of the motion of solid particles in a hydraulic cyclone", Trans. Inst. Chem. Eng. 30: 87, 1952.

Kimber, G. R. and M. T. Thew, "Experiments on oil/water separation with hydrocyclone", Proc. 1st European Conf. on Mixing and Centrifugal Separation, Cambridge, BHRA, Cranfield, E1, 1975.

King, R. P., "Technical Notes on MODSIM", University of Utah, 2000.

Lynch, A. J. and T. C. Rao, "Modeling and scale-up of hydrocyclone classifiers", Proceedings XI Int. Min. Proc. Congress, Cagliari, 9, 1975.

Masliyah, J. H., "Intensive Short Course on Extraction of Oilsands Bitumen", Department of Chemical and Materials Engineering, University of Alberta, 2000.

Mukherjee, A. K., Sripriya, R., Rao, P. V. T. and P. Das, "Effect of increase in feed inlet pressure on feed rate of dense media cyclone", International Journal of Mineral Processing, 69: 259, 2003.

Nageswararao, K., "Further Developments in the Modeling and Scale-up of Industrial Hydrocyclone", PhD Thesis, University of Queensland (JKMRC), 1978.

Napier-Munn, T. J., Morrell, S., Morrison, R. D. and T. Kojovic, "Mineral comminution

circuits, their operation and optimisation", Julius Kruttschnitt Mineral Research Centre, Australia, 1996.

Narasimha, M., Brennan, M. and P. N. Holtham, "Large eddy simulation of hydrocyclone-prediction of air core diameter and shape", International Journal of Mineral Processing, 2006.

Narasimha, M., Sripriya, R. and P. K. Banerjee, "CFD modelling of hydrocyclone–prediction of cut size", International Journal of Mineral Processing, 2004.

Patil, D. D. and T. C. Rao, "Classification evaluation of water injected hydrocyclone", Minerals Engineering, Vol. 12, No. 12: 1527, 1999.

Plitt, L. R., "A mathematical model of the hydrocyclone classifier", CIM Bulletin, 114, 1976.

Plitt, L. R., "Roping in hydrocyclones", 3rd Int. Conference on Hydrocyclones, Oxford, England, A3: 21, 1987.

Puprasert, C., Hebrard, G., Lopez, L. and Y. Aurelle, "Potential of using hydrocyclone and hydrocyclone equipped with grit pot as a pre-treatment in run-off water treatment", Chemical Engineering and Processing, 43: 67, 2004.

Shah, H., Majumder, A. K. and J. P. Barnwal, "Development of water split model for a 76 mm hydrocyclone", Minerals Engineering, 19: 102, 2006.

Simkin, D. J. and R. B. Olney, "Phase separation and mass transfer in a liquid-liquid cyclone", AICHEJ, 2, 1956.

Slechta, J. and B. A. Firth, "Classification of fine coal with a hydrocyclone", International Journal of Mineral Processing, 12: 213, 1984.

Statie, E., Salcudean, M., Gartshore, I. and E. Bibeau, "A computational study of particle separation in hydrocyclones", Journal of Pulp and Paper Science, Vol. 28, No.3: 84, 2002.

Svarovsky, L., "Hydrocyclones", Technomic Publishing Co. Inc, New York, 1984.

Symth, I. C. and M. T. Thew, "A comparison of the separation of heavy particles and droplets in a hydrocyclone", 3rd International Conference on Hydrocyclones, BHRA, Cranfield, G3: 193, 1987.

Young, G. A. B., Wakley, W. D., Taggart, D. L., Andrews, S. L. and J. R. Worrell, "Oil-water separation using hydrocyclones", An experimental search for optimum dimensions, Journal of Petroleum Science and Engineering, 11: 37, 1994.

Zhao, Q. G. and G. D. Xia, "A theoretical model for calculating pressure drop in the cone area of light dispersion hydrocyclone", Chemical Engineering Journal, 117: 231, 2006.

APPENDICES

APPENDIX A

PHYSICAL PROPERTIES OF TEST MATERIALS

Materials used for the test runs were categorized as

Category (A)
Light Particles

Polymer	$\rho = 920$ kg/m^3

Heavy Particles

Sand	$\rho = 2650$ kg/m^3

Category (B)
Light Particles

Hollow Cenosphere (A)	$\rho = (600 - 950)$ kg/m^3
Hollow Cenosphere (B)	$\rho = (600 - 950)$ kg/m^3

Heavy Particles

Sand	$\rho = 2650$ kg/m^3

Table A.1: Polymer Particles Average Density

Trial #	Density (kg/m^3)
1	900
2	890
3	895
4	904
5	880

Table A.2: Light Particles Density Distribution (Censophere A)

Density (kg/m^3)	Weight%
867	11.7
803	21.9
791	3.8
786	2.7
743	11.8
684	10.3
673	16.1
626	9.6
500	12.0

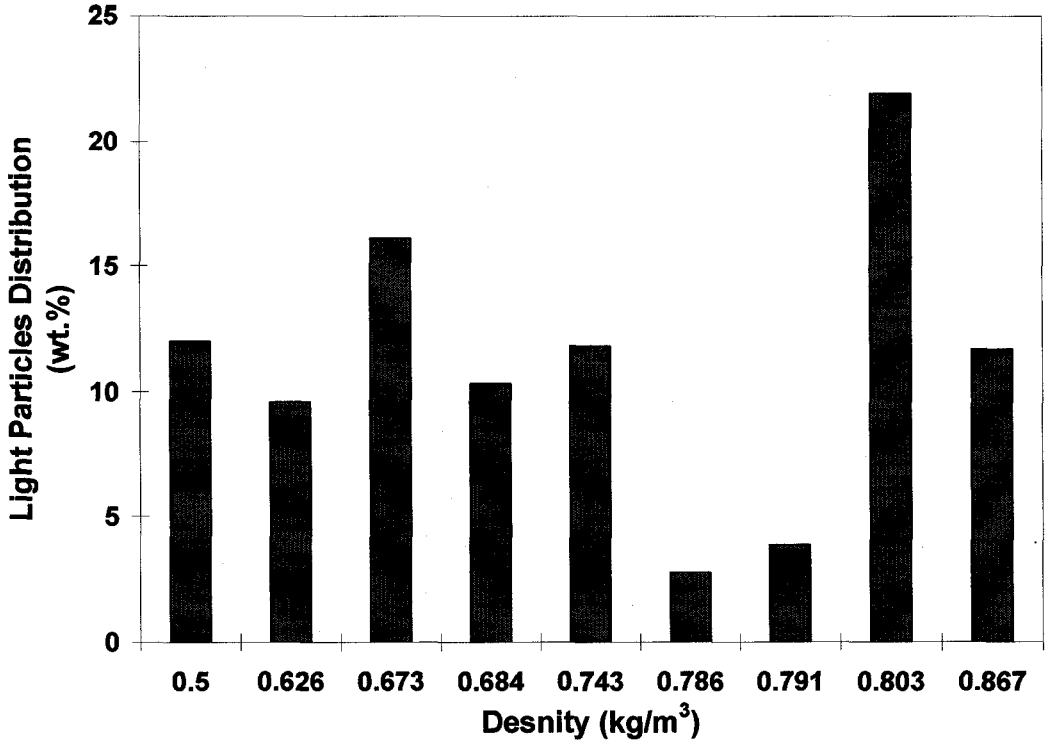

Figure A1: Density Distribution of Light Cenospheres Particles

APPENDIX B

Table B.1: Polymer Particles Size Distribution (Before Sieving)

Size (μm)	Volume (%)	Cumulative (%)
104.7	0	0
120.3	0	0
138.1	0.02	0.02
158.5	0.29	0.31
182.0	0.78	1.09
208.9	1.62	2.71
239.9	2.86	5.57
275.4	4.44	10.01
316.2	6.28	16.29
363.1	8.18	24.47
416.9	9.9	34.37
478.6	11.15	45.52
549.5	11.69	57.21
631.1	11.4	68.61
724.5	10.26	78.87
831.8	8.46	87.33
955.0	6.31	93.64
1096.5	4.17	97.81
1258.9	2.1	99.91
1445.4	0.07	99.98
1659.6	0.02	100

d_{50} = 580 μm

Table B.2: Polymer Particles Size Distribution (After Sieving)

Size (μm)	Volume (%)	Cumulative (%)
104.7	0	0
120.2	0	0
138.0	0	0
158.5	0.01	0.01
181.9	0.39	0.4
208.9	1.53	1.93
239.9	3.66	5.59
275.4	6.66	12.25
316.2	10.15	22.4
363.1	13.32	35.72
416.9	15.32	51.04
478.6	15.47	66.51
549.5	13.63	80.14
630.9	10.27	90.41
724.4	6.35	96.76
831.8	2.82	99.58
954.993	0.42	100
1096.5	0	100
1258.9	0	100
1445.4	0	100
1659.6	0	100

d_{50} = 460 μm

Table B.3: Light Particles Size Distribution (Cenosphere A)

Size (μm)	Volume (%)	Cumulative (%)
104.7	0	0
120.2	0	0
138.0	0	0
158.5	0.11	0.11
181.9	1.2	1.31
208.9	4.22	5.53
239.9	9.68	15.21
275.4	15.94	31.15
316.2	20.12	51.27
363.1	19.77	71.04
416.9	15.19	86.23
478.6	8.95	95.18
549.5	3.86	99.04
630.9	0.88	99.92
724.4	0.08	100
831.8	0	100
954.9	0	100
1096.5	0	100
1258.9	0	100
1445.4	0	100
1659.6	0	100

d_{50} = 360 μm

Table B.4: Light Particles Size Distribution (Cenosphere B)

Size (μm)	Volume (%)	Cumulative (%)
10.0	0	0
11.5	0	0
13.2	0	0
15.1	0	0
17.4	0	0
22.9	0	0
26.3	0	0
30.2	0.09	0.09
34.7	0.89	0.98
39.8	2.73	3.71
45.7	5.84	9.55
52.5	9.83	19.38
60.3	13.72	33.1
69.2	16.24	49.34
79.4	16.46	65.8
91.2	14.23	80.03
104.7	10.34	90.37
120.2	6.14	96.51
138.0	2.79	99.3
158.5	0.7	100
181.9	0	100

d_{50} = 80 μm

Table B.5: Heavy Particles Size Distribution

Size (μm)	Volume (%)	Cumulative (%)
10.0	0	0
11.5	0	0
13.2	0	0
15.1	0	0
17.4	0	0
22.9	0	0
26.3	0.04	0.04
30.2	0.66	0.7
34.7	2.78	3.48
39.8	7.1	10.58
45.7	13.04	23.62
52.5	18.33	41.95
60.3	20.21	62.16
69.1	17.56	79.72
79.4	11.85	91.57
91.2	6.01	97.58
104.7	2.08	99.66
120.2	0.32	99.98
138.0	0.02	100
158.5	0	100
181.9	0	100

d_{50} = 62 μm

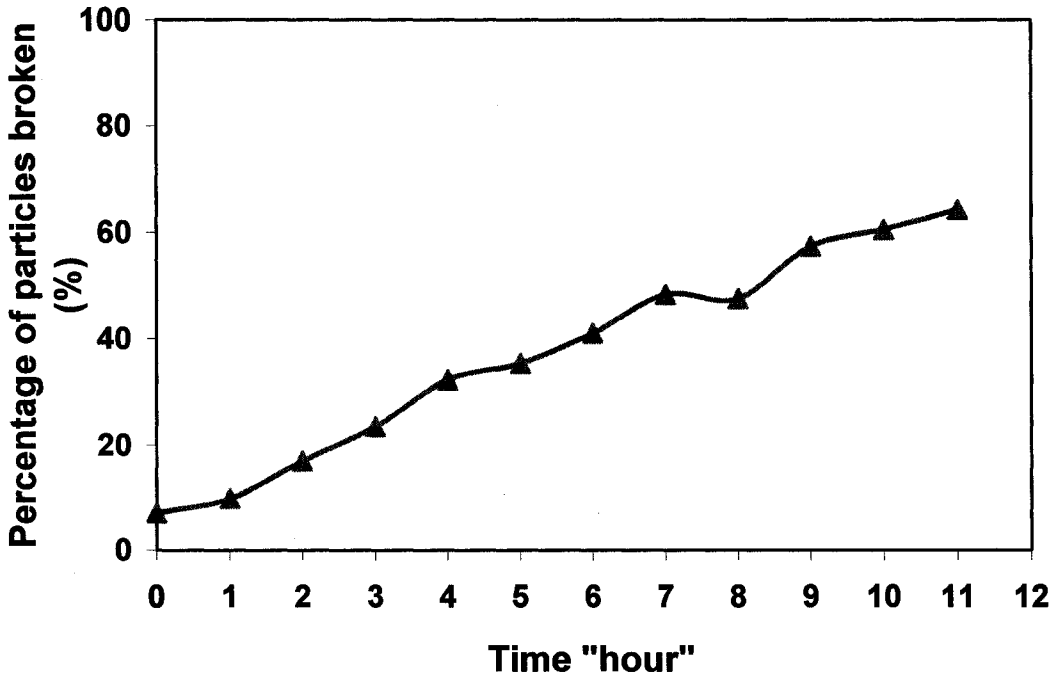

Figure B1: Breakage of Light Cenosphere Particles

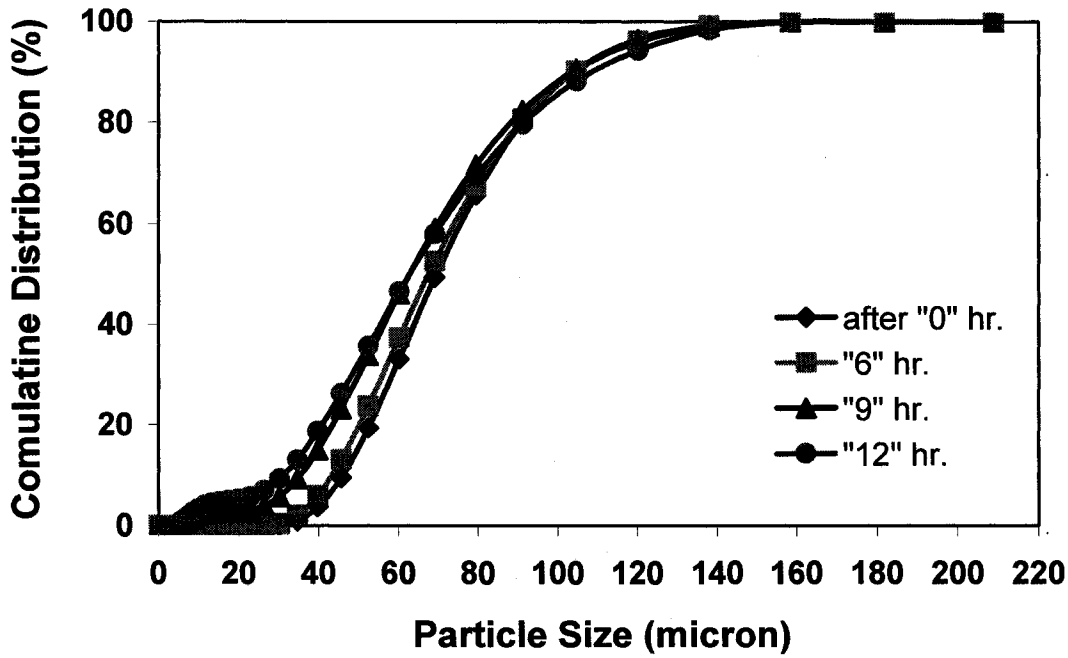

Figure B2: Cenosphere Particles Breaking Effect on Size Distribution

APPENDIX C

SAMPLE CALCULATIONS

SAMPLE CALCULATIONS OF LIGHT AND HEAVY PARTICLES RECOVERY AND QUALITY

Light and heavy particles were dispersed in the continuous medium, which was water in the current case. Concentration of these particles in the feed, overflow and underflow were determined by using float and sink method. These particles were separated by using the separation funnel and filtration technique. The filter paper used was watt man # 42. Most of the time the particles get settled quite quickly and no need to use the multiple funnel-beaker arrangements but some time it was used.

Procedure:

Weigh the empty beakers at each underflow split ratio, which were ten for each overflow and underflow stream.

Weigh the samples from each stream at respective underflow split ratio, along with empty beakers.

Weigh and fold two filter papers for light and heavy particles into the separate funnels for each sample.

Separate the light and heavy particles on respective filter papers and keep them to get dry in open air for whole night.

After dry, weigh each sample and made calculations.

Sample Calculations (Underflow):

1. Weight of empty beaker = 240.5 g
2. Time taken for sample = 2.0 s
3. Volume of the sample = 200 ml

4. Weight of sample (Light + heavy + water) and beaker = 469.64 g
5. Weight of sample (M_u) = 229.14 g
6. Weight of empty filter paper for light particles = 2.328 g
7. Weight of light particles and filter paper = 9.493 g
8. Weight of light particles (M_{lu}) = 7.165 g
9. Weight of empty filter paper for heavy particles = 2.301 g
10. Weight of heavy particles and filter paper = 22.410 g
11. Weight of heavy particles (M_{hu})= 20.109 g

Following the similar procedure, mass of the light and heavy particles in the overflow stream was determined, i.e.

Time taken for sample = 2 s

Volume of the sample = 740 ml

Weight of sample (M_o) = 727.910 g

Weight of light particles (M_{lo}) = 7.118 g

Weight of heavy particles (M_{ho})= 0.051 g

Using the component mass balance equation (3.2)

Weight of the light particles in feed (M_{lf}) = 14.283 g

Weight of the heavy particles in feed (M_{hf})= 20.16 g

Recovery of light particles in the overflow stream was calculated by using equation 3.3;

$$R_{lo} = \frac{M_o \alpha_{lo}}{M_f \alpha_{lf}}$$

$$= \frac{M_{lo}}{M_{lf}} * 100$$

$$= \frac{7.118}{14.283} * 100$$

$$= 49.83\%$$

Quality of overflow product stream was calculated by using equation 3.5;

$$q_o = \frac{\frac{\alpha_{lo}}{\alpha_{ho}}}{\frac{\alpha_{lf}}{\alpha_{hf}}}$$

Following the procedure recovery of heavy particles in the underflow stream was calculated by using the equations 3.4.

APPENDIX D
EXPERIMENTAL DATA

Table D.1: Effect of Feed Flowrate (17 L/min) on Recovery and Quality of Light and Heavy Particles in Overflow and Underflow Streams (Model A)

Time	Overflow Slurry	Underflow Slurry	Feed Slurry*	Light in Feed*	Heavy in Feed*
s	kg	kg	kg	kg	kg
5.6	4.4E-02	1.7E+00	1.70	2.1E-02	2.8E-02
4.1	4.5E-01	6.1E-01	1.05	1.4E-02	1.8E-02
4.1	6.6E-01	5.0E-01	1.16	1.6E-02	2.1E-02
3.9	7.4E-01	3.6E-01	1.10	1.6E-02	1.9E-02
3.8	8.4E-01	2.6E-01	1.10	1.6E-02	1.9E-02
3.4	8.5E-01	1.4E-01	0.99	1.4E-02	1.8E-02
3.0	7.7E-01	1.3E-01	0.89	1.3E-02	1.7E-02
6.1	1.6E+00	2.4E-01	1.79	2.5E-02	3.1E-02
7.1	1.8E+00	2.8E-01	2.06	3.1E-02	3.6E-02

Light		Heavy		Volume	
Overflow	Underflow	Overflow	Underflow	Overflow	Underflow
kg	kg	kg	kg	m3	m3
2.0E-07	2.1E-02	2.6E-08	2.8E-02	4.4E-05	1.7E-03
2.3E-03	1.2E-02	4.8E-05	1.8E-02	4.5E-04	6.1E-04
4.3E-03	1.1E-02	3.9E-05	2.1E-02	6.7E-04	5.0E-04
6.4E-03	9.3E-03	3.1E-05	1.9E-02	7.4E-04	3.6E-04
9.7E-03	6.3E-03	4.0E-05	1.9E-02	8.4E-04	2.6E-04
1.3E-02	1.0E-03	4.9E-05	1.8E-02	8.5E-04	1.4E-04
1.2E-02	8.9E-04	3.4E-05	1.7E-02	7.7E-04	1.3E-04
2.4E-02	1.6E-03	5.6E-05	3.1E-02	1.6E-03	2.4E-04
2.9E-02	2.1E-03	6.2E-05	3.6E-02	1.8E-03	2.8E-04

Flow Rate		Split Ratio	Light Recovery	Heavy Recovery	Product Quality
Overflow	Underflow	Underflow	Overflow	Underflow	Overflow
m^3/s	m^3/s	Q_u/Q_f	R_{LO} (%)	R_{hu} (%)	q_o
7.9E-06	2.9E-04	0.92	0.0	100.0	10.6
1.1E-04	1.5E-04	0.54	16.3	99.7	60.3
1.6E-04	1.2E-04	0.44	27.3	99.8	145.6
1.9E-04	9.2E-05	0.33	40.6	99.8	245.3
2.2E-04	6.9E-05	0.25	60.8	99.8	284.6
2.5E-04	4.1E-05	0.15	92.5	99.7	342.1
2.6E-04	4.2E-05	0.15	93.0	99.8	462.6
2.5E-04	3.9E-05	0.14	93.8	99.8	516.5
2.5E-04	4.0E-05	0.14	93.2	99.8	543.1

Note: 1) (*) From Steady State Mass Balance

2) Table is used in Figure 4.2, 4.3, 4.4

Table D.2: Effect of Feed Flowrate (33 L/min) on Recovery and Quality of Light and Heavy Particles in Overflow and Underflow Streams (Model A)

Time	Overflow Slurry	Underflow Slurry	Feed* Slurry	Light in Feed*	Heavy in Feed*
s	kg	kg	kg	kg	kg
2.2	1.5E-01	1.0E+00	1.2E+00	1.6E-02	2.3E-02
1.8	4.1E-01	4.4E-01	8.5E-01	1.2E-02	1.5E-02
2.6	7.0E-01	5.0E-01	1.2E+00	1.9E-02	2.3E-02
2.4	7.8E-01	3.5E-01	1.1E+00	1.7E-02	2.1E-02
2.0	7.3E-01	2.3E-01	9.6E-01	1.4E-02	2.0E-02
1.7	7.3E-01	1.8E-01	9.1E-01	1.3E-02	1.8E-02
1.7	7.5E-01	6.8E-02	8.2E-01	1.3E-02	1.7E-02
3.5	1.6E+00	9.6E-02	1.7E+00	2.2E-02	3.4E-02
3.3	1.4E+00	7.1E-02	1.4E+00	2.7E-02	2.7E-02

Light		Heavy		Volume	
Overflow	Underflow	Overflow	Underflow	Overflow	Underflow
kg	kg	kg	kg	m3	m3
4.6E-05	1.6E-02	5.7E-06	2.3E-02	1.5E-04	1.0E-03
1.4E-03	1.1E-02	3.2E-05	1.5E-02	4.1E-04	4.3E-04
3.4E-03	1.5E-02	3.8E-05	2.3E-02	7.0E-04	4.9E-04
5.0E-03	1.2E-02	4.3E-05	2.1E-02	7.8E-04	3.4E-04
7.1E-03	7.2E-03	5.1E-05	2.0E-02	7.3E-04	2.2E-04
1.0E-02	2.5E-03	9.8E-05	1.7E-02	7.3E-04	1.7E-04
1.3E-02	8.7E-05	8.6E-05	1.7E-02	7.5E-04	5.8E-05
2.2E-02	7.6E-05	1.0E-04	3.4E-02	1.6E-03	7.5E-05
2.7E-02	7.1E-05	6.2E-05	2.7E-02	1.4E-03	5.5E-05

Flow Rate		Split Ratio	Light Recovery	Heavy Recovery	Product Quality
Overflow	Underflow	Underflow	Overflow	Underflow	Overflow
m3/s	m3/s	Q_u/Q_f	R_{LO} %	R_{hu} (%)	q_o
6.5E-05	4.5E-04	0.93	0.3	100.0	11.4
2.3E-04	2.4E-04	0.50	11.8	99.8	53.4
2.7E-04	1.9E-04	0.39	18.3	99.8	110.9
3.2E-04	1.4E-04	0.29	30.1	99.8	150.1
3.7E-04	1.1E-04	0.22	49.8	99.7	199.0
4.3E-04	9.7E-05	0.20	80.5	99.4	143.8
4.6E-04	3.5E-05	0.07	99.3	99.5	196.4
4.7E-04	2.2E-05	0.04	99.7	99.7	325.3
4.1E-04	1.6E-05	0.03	99.7	99.8	431.3

Note: 1) Table is used in Figure 4.1 – 4.20

Table D.3: Effect of Feed Flowrate (46 L/min) on Recovery and Quality of Light and Heavy Particles in Overflow and Underflow Streams (Model A)

Time	Overflow Slurry	Underflow Slurry	Feed Slurry*	Light in Feed*	Heavy in Feed*
s	kg	kg	kg	kg	kg
2.7	3.5E-01	1.5E+00	1.87	2.0E-02	4.3E-02
1.4	5.1E-01	4.7E-01	0.98	1.3E-02	2.2E-02
1.6	7.5E-01	4.3E-01	1.18	1.7E-02	2.8E-02
1.6	7.9E-01	3.4E-01	1.13	1.7E-02	2.6E-02
1.3	7.3E-01	2.1E-01	0.94	1.5E-02	2.1E-02
2.9	1.8E+00	2.6E-01	2.06	3.4E-02	4.8E-02
3.1	2.2E+00	1.6E-01	2.35	3.9E-02	5.4E-02
2.1	1.5E+00	6.5E-02	1.55	2.5E-02	3.1E-02
1.9	1.4E+00	5.6E-02	1.43	2.5E-02	2.9E-02

Light		Heavy		Volume	
Overflow	Underflow	Overflow	Underflow	Overflow	Underflow
kg	kg	kg	kg	m3	m3
2.5E-04	2.0E-02	1.8E-04	4.3E-02	3.5E-04	1.5E-03
1.3E-03	1.2E-02	1.2E-04	2.2E-02	5.1E-04	4.6E-04
2.1E-03	1.5E-02	5.3E-05	2.8E-02	7.5E-04	4.2E-04
3.1E-03	1.4E-02	1.2E-03	2.5E-02	7.9E-04	3.3E-04
4.3E-03	1.1E-02	1.6E-04	2.1E-02	7.3E-04	2.0E-04
2.4E-02	1.1E-02	1.3E-03	4.6E-02	1.8E-03	2.3E-04
3.8E-02	4.0E-04	1.3E-03	5.2E-02	2.2E-03	1.3E-04
2.5E-02	1.2E-05	3.7E-04	3.1E-02	1.5E-03	4.6E-05
2.5E-02	1.0E-04	1.3E-04	2.9E-02	1.4E-03	3.8E-05

Flow Rate		Split Ratio	Light Recovery	Heavy Recovery	Product Quality
Overflow	Underflow	Underflow	Overflow	Underflow	Overflow
m^3/s	m^3/s	Q_u/Q_f	R_{LO} (%)	R_{hu} (%)	q_o
1.3E-04	5.6E-04	0.73	1.2	99.6	3.0
3.7E-04	3.3E-04	0.44	9.8	99.5	18.4
4.6E-04	2.6E-04	0.34	12.3	99.8	64.3
5.1E-04	2.1E-04	0.28	18.3	95.5	4.0
5.7E-04	1.6E-04	0.21	29.2	99.2	38.5
6.1E-04	7.8E-05	0.10	68.9	97.3	25.4
7.1E-04	4.2E-05	0.06	99.0	97.7	42.5
7.2E-04	2.2E-05	0.03	100.0	98.8	84.3
7.2E-04	2.0E-05	0.03	99.6	99.6	226.9

Note: 1) Table is used in Figure 4.2, 4.3, 4.4

Table D.4: Effect of Feed Solids Concentration (10 wt.%) on Recovery and Quality of Light and Heavy Particles in Overflow and Underflow Streams (Model A)

Time	Overflow Slurry	Underflow Slurry	Feed Slurry*	Light in Feed*	Heavy in Feed*
s	kg	kg	kg	kg	kg
2.04	2.47E-01	1.34E+00	1.58E+00	1.33E-02	5.63E-02
1.97	6.54E-01	8.25E-01	1.48E+00	1.16E-02	4.78E-02
1.88	8.08E-01	6.44E-01	1.45E+00	1.20E-02	4.26E-02
1.69	7.50E-01	4.28E-01	1.18E+00	1.30E-02	3.65E-02
1.72	7.52E-01	3.13E-01	1.07E+00	1.18E-02	3.30E-02
1.28	7.95E-01	1.71E-01	9.66E-01	1.23E-02	2.60E-02
2.82	1.9E+00	2.57E-01	2.14E+00	2.78E-02	5.86E-02
2.04	1.4E+00	1.90E-01	1.59E+00	1.89E-02	4.13E-02
1.97	1.4E+00	1.44E-01	1.55E+00	1.98E-02	4.00E-02

Light		Heavy		Volume	
Overflow	Underflow	Overflow	Underflow	Overflow	Underflow
kg	kg	kg	kg	m3	m3
0.0001799	1.32E-02	1.71E-04	5.61E-02	0.000247	1.31E-03
0.0007549	1.08E-02	6.56E-05	4.78E-02	0.0006551	7.98E-04
0.0010499	1.10E-02	7.38E-05	4.25E-02	0.0008093	6.19E-04
0.0014374	1.16E-02	8.29E-05	3.64E-02	0.0007519	4.07E-04
0.0015899	1.03E-02	1.92E-05	3.29E-02	0.000754	2.94E-04
0.00303	9.23E-03	5.76E-05	2.60E-02	0.0007973	1.56E-04
0.0232064	4.62E-03	7.49E-04	5.78E-02	0.0018837	2.22E-04
0.0186315	2.90E-04	8.61E-04	4.05E-02	0.0014057	1.65E-04
0.0198339	9.40E-06	5.73E-04	3.95E-02	0.0014122	1.19E-04

Flow Rate		Split Ratio	Light Recovery	Heavy Recovery	Product Quality
Overflow	Underflow	Underflow	Overflow	Underflow	Overflow
m^3/s	m^3/s	Q_u/Q_f	R_{LO} (%)	R_{hu} (%)	q_o
1.21E-04	6.41E-04	0.84	1.35	99.70	4.43
3.33E-04	4.05E-04	0.53	6.51	99.86	47.51
4.30E-04	3.29E-04	0.43	8.73	99.83	50.42
4.45E-04	2.41E-04	0.32	11.02	99.77	48.53
4.38E-04	1.71E-04	0.22	13.42	99.94	230.32
6.23E-04	1.22E-04	0.16	24.72	99.78	111.77
6.68E-04	7.87E-05	0.10	83.40	98.72	65.21
6.89E-04	8.11E-05	0.11	98.47	97.92	47.26
7.17E-04	6.06E-05	0.08	99.95	98.57	69.86

Note: 1) Table is used in Figure 4.5, 4.6, 4.7, 4.11, 4.12, 4.13,

Table D.5: Effect of Light Particles Size (d_{50}=80μm) on Recovery and Quality of Light and Heavy Particles in Overflow and Underflow Streams (Model A)

Time	Overflow Slurry	Underflow Slurry	Feed Slurry*	Light in Feed*	Heavy in Feed*
s	kg	kg	kg	kg	kg
1.7	2.0E-01	6.5E-01	0.85	2.5E-02	3.9E-02
2.7	6.7E-01	7.1E-01	1.38	4.3E-02	6.2E-02
2.6	8.1E-01	5.7E-01	1.38	4.4E-02	6.8E-02
2.5	8.5E-01	4.6E-01	1.31	4.0E-02	5.5E-02
2.3	8.3E-01	3.2E-01	1.15	3.3E-02	5.5E-02
2.1	8.7E-01	2.5E-01	1.13	3.1E-02	5.0E-02
2.1	8.3E-01	2.1E-01	1.04	2.8E-02	4.5E-02
2.2	9.0E-01	2.0E-01	1.10	2.8E-02	4.1E-02
2.2	9.3E-01	1.7E-01	1.10	2.4E-02	4.3E-02
3.1	1.5E+00	2.3E-01	1.72	5.0E-02	7.0E-02

Light		Heavy		Volume	
Overflow	Underflow	Overflow	Underflow	Overflow	Underflow
kg	kg	kg	kg	m3	m3
5.0E-04	2.5E-02	6.0E-05	3.9E-02	1.9E-04	6.2E-04
2.1E-03	4.0E-02	1.9E-04	6.2E-02	6.7E-04	6.9E-04
2.7E-03	4.2E-02	1.9E-04	6.7E-02	8.2E-04	5.4E-04
3.4E-03	3.6E-02	3.8E-04	5.4E-02	8.5E-04	4.5E-04
4.0E-03	2.9E-02	2.1E-04	5.4E-02	8.2E-04	2.9E-04
6.4E-03	2.4E-02	2.0E-04	5.0E-02	8.6E-04	2.2E-04
1.0E-02	1.8E-02	2.3E-04	4.5E-02	8.5E-04	2.0E-04
1.6E-02	1.2E-02	5.3E-04	4.1E-02	8.9E-04	1.8E-04
2.3E-02	1.1E-03	4.4E-04	4.3E-02	9.3E-04	1.1E-04
4.4E-02	5.6E-03	5.2E-04	7.0E-02	1.6E-03	1.5E-04

Flow Rate		Split Ratio	Light Recovery	Heavy Recovery	Product Quality
Overflow	Underflow	Underflow	Overflow	Underflow	Overflow
m^3/s	m^3/s	Q_u/Q_f	R_{LO} (%)	R_{hu} (%)	q_o
1.1E-04	3.7E-04	0.68	2.0	99.8	12.7
2.5E-04	2.6E-04	0.47	4.9	99.7	16.0
3.1E-04	2.1E-04	0.37	6.0	99.7	21.5
3.4E-04	1.8E-04	0.32	8.6	99.3	12.3
3.6E-04	1.3E-04	0.23	12.3	99.6	31.9
4.0E-04	1.0E-04	0.19	20.9	99.6	52.4
4.1E-04	9.7E-05	0.18	36.5	99.5	71.5
4.1E-04	8.4E-05	0.15	56.2	98.7	44.0
4.2E-04	5.0E-05	0.09	95.5	99.0	94.5
5.1E-04	4.8E-05	0.09	88.7	99.3	120.0

Note: 1) Table is used in Figure 4.8, 4.9, 4.10,

Table D.6: Effect of Light Particles Size (d_{50}=360μm) on Recovery and Quality of Light and Heavy Particles in Overflow and Underflow Streams (Model A)

Time	Overflow Slurry	Underflow Slurry	Feed Slurry*	Light in Feed*	Heavy in Feed*
s	kg	kg	kg	kg	kg
2.0	3.8E-01	6.9E-01	1.07	3.0E-02	6.7E-02
2.4	6.9E-01	7.8E-01	1.47	4.3E-02	9.1E-02
2.9	8.5E-01	6.4E-01	1.49	4.2E-02	9.3E-02
2.9	9.1E-01	5.5E-01	1.46	4.1E-02	9.3E-02
2.4	8.6E-01	3.8E-01	1.25	3.5E-02	8.0E-02
2.4	9.4E-01	3.1E-01	1.25	3.4E-02	8.3E-02
2.5	9.5E-01	2.7E-01	1.21	3.4E-02	7.9E-02
2.3	9.6E-01	2.4E-01	1.20	3.3E-02	8.0E-02
2.3	9.5E-01	2.1E-01	1.16	3.2E-02	7.8E-02
4.2	1.9E+00	3.0E-01	2.22	6.5E-02	1.5E-01
4.1	2.0E+00	2.2E-01	2.19	6.1E-02	1.4E-01

Light		Heavy		Volume	
Overflow	Underflow	Overflow	Underflow	Overflow	Underflow
kg	kg	kg	kg	m3	m3
3.0E-03	2.7E-02	1.0E-03	6.6E-02	3.8E-04	6.6E-04
7.5E-03	3.5E-02	1.4E-03	9.0E-02	6.9E-04	7.4E-04
8.2E-03	3.4E-02	2.1E-03	9.1E-02	8.5E-04	6.0E-04
1.0E-02	3.1E-02	1.7E-03	9.1E-02	9.1E-04	5.1E-04
1.1E-02	2.4E-02	1.6E-03	7.9E-02	8.7E-04	3.4E-04
1.3E-02	2.2E-02	1.5E-03	8.1E-02	9.4E-04	2.7E-04
1.2E-02	2.1E-02	1.3E-03	7.7E-02	9.5E-04	2.3E-04
1.2E-02	2.1E-02	1.9E-03	7.8E-02	9.7E-04	2.0E-04
1.7E-02	1.5E-02	1.7E-03	7.7E-02	9.6E-04	1.7E-04
6.0E-02	5.1E-03	3.4E-03	1.4E-01	1.9E-03	2.2E-04
6.1E-02	4.5E-04	3.0E-03	1.4E-01	2.0E-03	1.4E-04

Flow Rate		Split Ratio	Light Recovery	Heavy Recovery	Product Quality
Overflow	Underflow	Underflow	Overflow	Underflow	Overflow
m^3/s	m^3/s	Q_u/Q_f	R_{LO} (%)	R_{hu} (%)	q_o
1.9E-04	3.3E-04	0.59	10.1	98.4	6.5
2.9E-04	3.2E-04	0.57	17.5	98.5	11.4
2.9E-04	2.1E-04	0.38	19.7	97.8	8.9
3.1E-04	1.8E-04	0.32	24.5	99.5	13.3
3.7E-04	1.5E-04	0.27	30.7	98.0	15.0
4.0E-04	1.1E-04	0.21	36.4	98.2	20.4
3.8E-04	8.9E-05	0.16	36.9	98.4	22.9
4.2E-04	8.8E-05	0.16	37.7	97.7	16.0
4.2E-04	7.4E-05	0.14	52.7	97.8	23.9
4.7E-04	5.2E-05	0.09	92.2	97.7	39.4
4.9E-04	3.4E-05	0.06	99.3	97.9	46.3

Note: 1) Table is used in Figure 4.8, 4.9, 4.10

Table D.7: Effect of Overflow to Underflow Diameter Ratio (D_o/D_u=0.85) on Recovery and Quality of Light and Heavy Particles in Overflow and Underflow Streams (Model A)

Time	Overflow Slurry	Underflow Slurry	Feed Slurry*	Light in Feed*	Heavy in Feed*
s	kg	kg	kg	kg	kg
3.4	5.1E-01	1.8E+00	2.31	2.6E-02	1.4E-01
3.5	5.8E-01	1.8E+00	2.33	2.8E-02	1.5E-01
3.6	6.4E-01	1.7E+00	2.34	3.3E-02	1.5E-01
3.7	6.9E-01	1.6E+00	2.33	3.6E-02	1.5E-01
3.8	7.1E-01	1.4E+00	2.13	4.0E-02	1.4E-01
4.0	7.8E-01	1.4E+00	2.21	4.1E-02	1.4E-01
4.0	7.5E-01	1.4E+00	2.16	5.0E-02	1.4E-01
3.8	7.1E-01	1.3E+00	1.99	3.1E-02	1.2E-01
4.1	7.2E-01	1.4E+00	2.08	2.9E-02	1.3E-01
3.7	7.0E-01	1.2E+00	1.87	3.2E-02	1.1E-01
3.7	6.5E-01	1.1E+00	1.79	3.1E-02	1.1E-01

Light		Heavy		Volume	
Overflow	Underflow	Overflow	Underflow	Overflow	Underflow
kg	kg	kg	kg	m3	m3
1.9E-02	6.4E-03	9.0E-04	1.4E-01	5.1E-04	1.7E-03
2.3E-02	5.5E-03	8.3E-04	1.5E-01	5.8E-04	1.7E-03
2.8E-02	5.1E-03	4.6E-04	1.5E-01	6.5E-04	1.6E-03
3.1E-02	4.9E-03	4.2E-04	1.5E-01	6.9E-04	1.6E-03
3.5E-02	4.1E-03	4.3E-04	1.4E-01	7.1E-04	1.3E-03
3.6E-02	4.8E-03	4.0E-04	1.4E-01	7.8E-04	1.3E-03
4.4E-02	6.2E-03	3.8E-04	1.4E-01	7.5E-04	1.3E-03
2.8E-02	3.6E-03	2.9E-04	1.2E-01	7.1E-04	1.2E-03
2.6E-02	2.7E-03	2.9E-04	1.3E-01	7.3E-04	1.3E-03
2.9E-02	3.4E-03	2.3E-04	1.1E-01	7.0E-04	1.1E-03
2.8E-02	3.5E-03	2.3E-04	1.1E-01	6.5E-04	1.1E-03

Flow Rate		Split Ratio	Light Recovery	Heavy Recovery	Product Quality
Overflow	Underflow	Underflow	Overflow	Underflow	Overflow
m^3/s	m^3/s	Q_u/Q_f	R_{LO} (%)	R_{hu} (%)	q_o
1.5E-04	5.1E-04	0.92	75.2	99.4	116.2
1.7E-04	4.7E-04	0.86	80.6	99.5	148.9
1.8E-04	4.5E-04	0.81	84.4	99.7	269.9
1.9E-04	4.2E-04	0.76	86.3	99.7	300.7
1.9E-04	3.6E-04	0.65	89.7	99.7	298.5
2.0E-04	3.4E-04	0.62	88.3	99.7	314.6
1.9E-04	3.4E-04	0.61	87.6	99.7	323.3
1.9E-04	3.2E-04	0.59	88.4	99.8	374.2
1.8E-04	3.1E-04	0.57	90.5	99.8	410.6
1.9E-04	3.0E-04	0.54	89.5	99.8	445.4
1.7E-04	2.9E-04	0.52	88.8	99.8	421.2

Note: 1) Table is used in Figure 4.11, 4.12, 4.13,

Table D.8: Effect of Vortex Finder Length (L_{vf2}=84mm) on Recovery and Quality of Light and Heavy Particles in Overflow and Underflow Streams (Model A)

Time	Overflow Slurry	Underflow Slurry	Feed Slurry*	Light in Feed*	Heavy in Feed*
s	kg	kg	kg	kg	kg
1.1	7.8E-02	5.1E-01	0.59	4.6E-03	1.7E-02
1.9	4.3E-01	5.8E-01	1.01	7.5E-03	2.8E-02
2.8	8.6E-01	6.4E-01	1.50	1.3E-02	4.2E-02
2.8	1.0E+00	5.3E-01	1.53	1.3E-02	4.3E-02
2.3	9.3E-01	3.4E-01	1.27	1.1E-02	3.5E-02
1.9	8.5E-01	1.8E-01	1.02	9.9E-03	2.8E-02
1.9	9.4E-01	1.2E-01	1.06	1.1E-02	2.9E-02
3.7	2.0E+00	2.3E-01	2.22	2.4E-02	5.8E-02
3.3	1.9E+00	1.8E-01	2.05	2.3E-02	5.5E-02

Light		Heavy		Volume	
Overflow	Underflow	Overflow	Underflow	Overflow	Underflow
kg	kg	kg	kg	m3	m3
1.2E-04	4.4E-03	6.6E-04	1.6E-02	7.8E-05	5.0E-04
9.3E-04	6.5E-03	9.1E-04	2.7E-02	4.3E-04	5.6E-04
2.5E-03	1.0E-02	1.5E-03	4.1E-02	8.6E-04	6.2E-04
3.0E-03	1.0E-02	1.5E-03	4.1E-02	1.0E-03	5.1E-04
4.0E-03	7.4E-03	1.3E-03	3.4E-02	9.3E-04	3.2E-04
5.0E-03	4.9E-03	1.0E-03	2.7E-02	8.5E-04	1.6E-04
8.5E-03	2.5E-03	1.1E-03	2.8E-02	9.5E-04	1.0E-04
2.4E-02	2.7E-04	2.2E-03	5.6E-02	2.0E-03	2.0E-04
2.3E-02	1.0E-04	1.8E-03	5.3E-02	1.9E-03	1.5E-04

Flow Rate		Split Ratio	Light Recovery	Heavy Recovery	Product Quality
Overflow	Underflow	Underflow	Overflow	Underflow	Overflow
m^3/s	m^3/s	Q_u/Q_f	R_{LO} (%)	R_{hu} (%)	q_o
7.3E-05	4.7E-04	0.85	2.6	96.1	0.7
2.3E-04	3.1E-04	0.56	12.4	96.8	3.9
3.1E-04	2.2E-04	0.41	20.1	96.5	5.8
3.6E-04	1.8E-04	0.33	23.3	96.5	6.7
4.1E-04	1.4E-04	0.25	34.8	96.2	9.3
4.5E-04	8.5E-05	0.15	50.2	96.3	13.6
5.0E-04	5.2E-05	0.10	77.1	96.3	20.8
5.4E-04	5.3E-05	0.10	98.9	96.3	26.5
5.6E-04	4.5E-05	0.08	99.6	96.6	29.7

Note: 1) Table is used in Figure 4.14, 4.15, 4.16

Table D.9: Effect of Cylindrical Length (L_2=135mm) on Recovery and Quality of Light and Heavy Particles in Overflow and Underflow Streams (Model A)

Time	Overflow Slurry	Underflow Slurry	Feed Slurry*	Light in Feed*	Heavy in Feed*
s	kg	kg	kg	kg	kg
1.3	6.4E-02	5.1E-01	0.58	4.4E-03	1.5E-02
2.2	5.3E-01	5.8E-01	1.11	7.5E-03	2.9E-02
3.0	8.5E-01	7.1E-01	1.56	1.3E-02	4.1E-02
2.9	9.3E-01	5.4E-01	1.47	1.4E-02	4.1E-02
2.6	9.5E-01	4.0E-01	1.35	1.4E-02	3.6E-02
2.4	9.8E-01	2.5E-01	1.23	1.2E-02	3.4E-02
1.9	8.6E-01	1.5E-01	1.01	1.0E-02	2.9E-02
3.1	1.5E+00	2.2E-01	1.72	2.0E-02	4.5E-02
3.5	1.8E+00	1.9E-01	1.96	2.0E-02	4.9E-02

Light		Heavy		Volume	
Overflow	Underflow	Overflow	Underflow	Overflow	Underflow
kg	kg	kg	kg	m3	m3
3.7E-06	4.4E-03	1.0E-06	1.5E-02	6.5E-05	5.0E-04
8.3E-04	6.7E-03	1.2E-04	2.9E-02	5.3E-04	5.6E-04
1.7E-03	1.2E-02	1.4E-04	4.1E-02	8.5E-04	6.9E-04
1.8E-03	1.2E-02	2.0E-04	4.1E-02	9.3E-04	5.2E-04
2.7E-03	1.1E-02	1.4E-04	3.6E-02	9.5E-04	3.8E-04
3.3E-03	8.5E-03	1.5E-04	3.4E-02	9.8E-04	2.3E-04
7.4E-03	3.0E-03	1.1E-04	2.9E-02	8.6E-04	1.3E-04
1.9E-02	1.0E-04	2.0E-04	4.5E-02	1.5E-03	1.9E-04
2.0E-02	1.3E-05	1.7E-04	4.9E-02	1.8E-03	1.6E-04

Flow Rate		Split Ratio	Light Recovery	Heavy Recovery	Product Quality
Overflow	Underflow	Underflow	Overflow	Underflow	Overflow
m^3/s	m^3/s	Q_u/Q_f	R_{LO} (%)	R_{hu} (%)	q_o
5.2E-05	4.0E-04	0.73	0.1	99.8	12.4
2.4E-04	2.5E-04	0.46	11.1	99.6	25.6
2.8E-04	2.3E-04	0.41	12.4	99.6	35.4
3.2E-04	1.8E-04	0.33	12.7	99.5	26.1
3.7E-04	1.5E-04	0.27	18.8	99.6	48.4
4.1E-04	9.7E-05	0.18	28.0	99.6	62.6
4.5E-04	7.0E-05	0.13	70.9	99.6	193.7
4.8E-04	6.1E-05	0.11	99.5	99.6	223.5
5.1E-04	4.6E-05	0.08	99.9	99.6	289.1

Note: 1) Table is used in Figure 4.17, 4.18, 4.19

Table D.10: Effect of Feed Flowrate (33 L/min) on Recovery and Quality of Light and Heavy Particles in Overflow and Underflow Streams (Model B)

Time	Overflow Slurry	Underflow Slurry	Feed Slurry*	Light in Feed*	Heavy in Feed*
s	kg	kg	kg	kg	kg
1.3	2.6E-01	6.2E-01	0.88	2.4E-02	6.0E-02
2.8	4.7E-01	7.4E-01	1.20	3.1E-02	8.6E-02
3.2	6.9E-01	7.8E-01	1.48	3.9E-02	1.0E-01
3.4	8.4E-01	7.4E-01	1.58	4.1E-02	1.1E-01
3.0	8.5E-01	5.8E-01	1.43	3.8E-02	1.0E-01
3.0	9.0E-01	5.1E-01	1.42	3.7E-02	1.0E-01
2.7	9.1E-01	4.4E-01	1.35	3.5E-02	9.5E-02
2.7	8.9E-01	3.9E-01	1.28	3.3E-02	8.8E-02
2.7	9.2E-01	3.6E-01	1.28	3.4E-02	8.9E-02
4.5	1.7E+00	4.9E-01	2.19	5.6E-02	1.5E-01
4.7	1.8E+00	4.7E-01	2.30	5.9E-02	1.6E-01

Light		Heavy		Volume	
Overflow	Underflow	Overflow	Underflow	Overflow	Underflow
kg	kg	kg	kg	m3	m3
2.8E-03	2.1E-02	8.9E-04	5.9E-02	2.6E-04	5.9E-04
3.7E-03	2.8E-02	1.4E-03	8.4E-02	4.7E-04	6.9E-04
7.5E-03	3.2E-02	1.9E-03	9.8E-02	7.0E-04	7.2E-04
1.0E-02	3.1E-02	2.7E-03	1.1E-01	8.4E-04	6.7E-04
1.2E-02	2.6E-02	1.9E-03	9.8E-02	8.5E-04	5.2E-04
1.3E-02	2.5E-02	2.0E-03	1.0E-01	9.0E-04	4.5E-04
1.3E-02	2.3E-02	1.6E-03	9.3E-02	9.1E-04	3.8E-04
1.3E-02	2.1E-02	1.5E-03	8.6E-02	8.9E-04	3.4E-04
1.4E-02	2.0E-02	1.5E-03	8.7E-02	9.2E-04	3.1E-04
5.5E-02	7.3E-04	2.7E-03	1.5E-01	1.7E-03	4.0E-04
5.9E-02	6.9E-04	2.5E-03	1.5E-01	1.8E-03	3.7E-04

Flow Rate		Split Ratio	Light Recovery	Heavy Recovery	Product Quality
Overflow	Underflow	Underflow	Overflow	Underflow	Overflow
m^3/s	m^3/s	Q_u/Q_f	R_{LO} (%)	R_{hu} (%)	q_o
2.0E-04	4.4E-04	0.80	11.4	98.5	7.7
1.7E-04	2.5E-04	0.45	11.9	98.4	7.3
2.2E-04	2.3E-04	0.41	19.2	98.1	10.0
2.5E-04	2.0E-04	0.36	25.2	97.6	10.6
2.8E-04	1.7E-04	0.31	31.1	98.1	16.4
3.0E-04	1.5E-04	0.27	33.7	98.1	17.6
3.3E-04	1.4E-04	0.26	36.1	98.3	21.5
3.3E-04	1.2E-04	0.23	37.7	98.3	22.0
3.4E-04	1.2E-04	0.21	41.1	98.3	23.7
3.8E-04	8.9E-05	0.16	98.7	99.2	55.2
4.0E-04	8.0E-05	0.13	98.8	98.4	61.0

Note: 1) Table is used in Figure 4.21 – 4.29

Table D.11: Effect of Feed Flowrate (46 L/min) on Recovery and Quality of Light and Heavy Particles in Overflow and Underflow Streams (Model B)

Time	Overflow Slurry	Underflow Slurry	Feed Slurry*	Light in Feed*	Heavy in Feed*
s	kg	kg	kg	kg	kg
1.5	3.0E-01	6.5E-01	0.95	2.4E-02	6.0E-02
1.5	4.2E-01	6.3E-01	1.05	2.5E-02	8.6E-02
1.8	6.4E-01	6.6E-01	1.31	3.2E-02	1.0E-01
2.1	8.4E-01	6.7E-01	1.51	3.8E-02	1.1E-01
2.2	9.0E-01	5.9E-01	1.49	3.6E-02	1.0E-01
1.9	9.1E-01	4.7E-01	1.38	3.5E-02	1.0E-01
1.9	9.1E-01	4.3E-01	1.34	3.3E-02	9.5E-02
2.0	9.3E-01	3.8E-01	1.30	3.2E-02	8.8E-02
1.9	9.8E-01	3.6E-01	1.35	3.7E-02	8.9E-02
3.6	2.0E+00	6.3E-01	2.68	6.8E-02	1.5E-01
3.2	1.8E+00	5.0E-01	2.30	5.8E-02	1.6E-01

Light		Heavy		Volume	
Overflow	Underflow	Overflow	Underflow	Overflow	Underflow
kg	kg	kg	kg	m3	m3
1.4E-03	2.3E-02	8.9E-04	5.9E-02	3.1E-04	6.5E-04
2.1E-03	2.3E-02	1.4E-03	8.4E-02	4.3E-04	6.0E-04
5.1E-03	2.7E-02	1.9E-03	9.8E-02	6.6E-04	6.5E-04
7.3E-03	3.1E-02	2.7E-03	1.1E-01	8.4E-04	6.3E-04
6.1E-03	3.0E-02	1.9E-03	9.8E-02	9.0E-04	5.7E-04
8.6E-03	2.7E-02	2.0E-03	1.0E-01	9.3E-04	4.6E-04
8.9E-03	2.4E-02	1.6E-03	9.3E-02	9.4E-04	4.1E-04
9.0E-03	2.3E-02	1.5E-03	8.6E-02	9.2E-04	3.9E-04
1.7E-02	2.0E-02	1.5E-03	8.7E-02	9.9E-04	3.6E-04
5.6E-02	1.2E-02	3.0E-03	1.5E-01	2.1E-03	5.3E-04
5.6E-02	1.9E-03	2.5E-03	1.5E-01	1.9E-03	4.0E-04

Flow Rate		Split Ratio	Light Recovery	Heavy Recovery	Product Quality
Overflow	Underflow	Underflow	Overflow	Underflow	Overflow
m^3/s	m^3/s	Q_u/Q_f	R_{LO} (%)	R_{hu} (%)	q_o
2.1E-04	4.4E-04	0.79	5.6	98.5	3.8
2.8E-04	3.9E-04	0.72	8.2	98.4	5.0
3.6E-04	3.5E-04	0.64	15.9	98.1	8.3
4.1E-04	3.0E-04	0.55	18.9	97.6	8.0
4.1E-04	2.6E-04	0.47	16.9	98.1	8.9
4.9E-04	2.4E-04	0.44	24.4	98.1	12.7
5.0E-04	2.2E-04	0.39	26.8	98.3	16.0
4.7E-04	2.0E-04	0.36	28.0	98.3	16.3
5.3E-04	1.9E-04	0.35	44.8	98.3	25.8
5.9E-04	1.5E-04	0.27	82.8	98.0	41.9
6.0E-04	1.2E-04	0.22	96.7	98.4	59.7

Note: 1) Table is used in Figure 4.21, 4.22, 4.23

Table D.12: Effect of Light Particles Size (d_{50}=80μm) on Recovery of light particles in Overflow Stream (Model B)

Time	Overflow Slurry	Underflow Slurry	Feed Slurry*	Light in Feed*	Heavy in Feed*
s	kg	kg	kg	kg	kg
1.7	1.4E-01	6.3E-01	0.77	2.0E-02	1.5E-02
1.6	1.7E-01	6.2E-01	0.79	1.7E-02	2.0E-02
1.9	2.1E-01	6.8E-01	0.89	2.1E-02	1.4E-02
1.7	1.5E-01	6.3E-01	0.78	2.0E-02	4.5E-02
1.7	1.8E-01	6.2E-01	0.80	2.1E-02	6.2E-02
1.7	1.6E-01	6.6E-01	0.83	2.2E-02	1.1E-01
1.7	1.9E-01	6.3E-01	0.82	2.3E-02	9.4E-02
1.7	1.8E-01	6.7E-01	0.85	2.8E-02	1.5E-01
1.7	1.5E-01	5.8E-01	0.73	2.6E-02	1.0E-01
3.3	3.5E-01	1.3E+00	1.63	4.7E-02	3.8E-01
3.5	3.7E-01	1.4E+00	1.74	5.2E-02	4.6E-01

Light		Heavy		Volume	
Overflow	Underflow	Overflow	Underflow	Overflow	Underflow
kg	kg	kg	kg	m3	m3
7.9E-03	1.2E-02	6.0E-05	1.5E-02	1.5E-04	6.5E-04
1.3E-02	4.1E-03	1.9E-04	2.0E-02	2.0E-04	5.9E-04
1.7E-02	3.6E-03	1.9E-04	1.4E-02	2.4E-04	6.6E-04
1.6E-02	3.3E-03	3.8E-04	4.5E-02	1.7E-04	5.7E-04
1.8E-02	3.2E-03	2.1E-04	6.2E-02	2.3E-04	5.4E-04
1.8E-02	3.4E-03	2.0E-04	1.1E-01	2.1E-04	5.3E-04
2.0E-02	3.1E-03	2.3E-04	9.3E-02	2.4E-04	5.1E-04
2.5E-02	3.4E-03	5.3E-04	1.5E-01	2.2E-04	5.0E-04
2.4E-02	2.7E-03	1.7E-04	1.0E-01	1.9E-04	4.6E-04
4.1E-02	5.4E-03	5.6E-04	3.8E-01	4.4E-04	8.8E-04
4.6E-02	6.0E-03	6.3E-04	4.6E-01	4.5E-04	9.0E-04

Flow Rate		Split Ratio	Light Recovery	Heavy Recovery	Product Quality
Overflow	Underflow	Underflow	Overflow	Underflow	Overflow
m^3/s	m^3/s	Q_u/Q_f	R_{LO} (%)	R_{hu} (%)	q_o
9.1E-05	3.9E-04	0.72	57.8	99.6	98.2
1.3E-04	3.7E-04	0.67	75.6	99.1	80.6
1.3E-04	3.5E-04	0.63	82.6	98.7	61.2
1.0E-04	3.4E-04	0.61	83.4	99.2	99.1
1.4E-04	3.3E-04	0.59	84.5	99.7	250.5
1.2E-04	3.1E-04	0.57	84.2	99.8	453.9
1.4E-04	3.1E-04	0.56	86.5	99.8	352.4
1.3E-04	2.9E-04	0.53	88.1	99.6	242.1
1.1E-04	2.8E-04	0.50	89.8	99.8	536.7
1.3E-04	2.7E-04	0.48	88.4	99.9	612.3
1.3E-04	2.6E-04	0.47	88.3	99.9	645.2

Note: 1) Table is used in Figure 4.24, 4.25, 4.26, 4.29

Table D.13: Effect of Light Particles Size (d_{50}=360μm) on Recovery of light particles in Overflow Stream (Model B)

Time	Overflow Slurry	Underflow Slurry	Feed Slurry*	Light in Feed*
s	kg	kg	kg	kg
4.4	3.3E-01	2.0E+00	2.31	3.2E-02
3.6	4.5E-01	1.5E+00	1.97	4.1E-02
3.5	4.4E-01	1.4E+00	1.89	4.2E-02
3.4	4.4E-01	1.5E+00	1.90	4.0E-02
3.8	4.8E-01	1.6E+00	2.09	3.3E-02
3.7	4.9E-01	1.6E+00	2.10	1.7E-02
2.6	3.6E-01	1.1E+00	1.43	3.3E-02
2.9	3.5E-01	1.2E+00	1.55	2.9E-02

Light		Heavy	Volume	
Overflow	Underflow	Overflow	Overflow	Underflow
kg	kg	kg	m3	m3
2.5E-02	6.4E-03	6.0E-05	3.4E-04	1.9E-03
3.6E-02	4.1E-03	1.9E-04	4.5E-04	1.4E-03
3.7E-02	4.8E-03	1.9E-04	4.4E-04	1.4E-03
3.3E-02	6.2E-03	3.8E-04	4.4E-04	1.4E-03
2.9E-02	3.6E-03	2.1E-04	4.8E-04	1.5E-03
1.4E-02	2.7E-03	2.0E-04	4.9E-04	1.5E-03
3.0E-02	3.4E-03	2.3E-04	3.7E-04	1.0E-03
2.5E-02	3.5E-03	3.0E-04	3.6E-04	1.1E-03

Flow Rate		Split Ratio	Light Recovery
Overflow	Underflow	Underflow	Overflow
m^3/s	m^3/s	Q_u/Q_f	R_{LO} (%)
7.8E-05	4.3E-04	0.78	79.8
1.2E-04	4.0E-04	0.72	89.9
1.3E-04	3.9E-04	0.70	88.6
1.3E-04	4.0E-04	0.73	84.4
1.3E-04	4.0E-04	0.73	88.8
1.3E-04	4.1E-04	0.75	84.0
1.4E-04	3.8E-04	0.70	89.8
1.2E-04	3.8E-04	0.70	87.9

Note: 1) Table is used in Figure 4.24

Table D.14: Hydrocyclone A and B, Effect of Feed Flowrate (80μm, Cenosphere) on Recovery and Quality of Light Particles in Overflow Stream (Model A)

Time	Overflow Slurry	Underflow Slurry	Feed Slurry*	Light in Feed*	Heavy in Feed*
s	kg	kg	kg	kg	kg
2.3	6.3E-01	1.6E+00	2.19	1.6E-02	7.0E-02
1.7	8.4E-01	9.9E-01	1.83	1.4E-02	6.2E-02
1.9	9.0E-01	7.9E-01	1.70	1.5E-02	5.8E-02
1.3	8.1E-01	4.3E-01	1.25	1.2E-02	4.3E-02
1.3	8.4E-01	3.7E-01	1.21	1.2E-02	4.4E-02
1.2	8.0E-01	1.8E-01	0.98	9.4E-03	3.4E-02
1.1	8.1E-01	1.4E-01	0.95	1.1E-02	3.9E-02
2.9	2.4E+00	3.1E-01	2.73	3.1E-02	9.8E-02
2.6	2.7E+00	2.3E-01	2.89	3.2E-02	9.3E-02

Light		Heavy		Volume	
Overflow	Underflow	Overflow	Underflow	Overflow	Underflow
kg	kg	kg	kg	m3	m3
2.9E-04	1.6E-02	1.7E-04	7.0E-02	6.3E-04	1.5E-03
6.8E-04	1.4E-02	2.8E-04	6.2E-02	8.4E-04	9.6E-04
8.1E-04	1.5E-02	2.6E-04	5.8E-02	9.1E-04	7.6E-04
1.0E-03	1.1E-02	1.9E-04	4.3E-02	8.1E-04	4.1E-04
1.1E-03	1.1E-02	2.4E-04	4.4E-02	8.4E-04	3.4E-04
1.5E-03	7.9E-03	2.1E-04	3.4E-02	8.0E-04	1.6E-04
7.4E-03	3.4E-03	8.0E-04	3.8E-02	8.2E-04	1.2E-04
3.1E-02	3.0E-05	2.4E-03	9.6E-02	2.4E-03	2.5E-04
3.2E-02	3.0E-05	2.0E-03	9.1E-02	2.7E-03	1.7E-04

Flow Rate		Split Ratio	Light Recovery	Heavy Recovery	Product Quality
Overflow	Underflow	Underflow	Overflow	Underflow	Overflow
m^3/s	m^3/s	Q_u/Q_f	R_{LO} (%)	R_{hu} (%)	q_o
2.8E-04	6.6E-04	0.66	1.8	99.8	7.2
4.9E-04	5.6E-04	0.56	4.8	99.5	10.5
4.8E-04	4.0E-04	0.40	5.3	99.6	11.8
6.1E-04	3.1E-04	0.31	8.7	99.6	20.1
6.3E-04	2.6E-04	0.26	9.5	99.5	17.3
6.8E-04	1.4E-04	0.14	15.8	99.4	25.3
7.7E-04	1.1E-04	0.11	69.0	98.0	33.8
8.4E-04	8.6E-05	0.09	99.9	97.6	40.9
1.0E-03	6.7E-05	0.07	99.9	97.9	46.5

Note: 1) Table is used in Figure 4.27, 4.28

Table D.15: Hydrocyclone A and B, Effect of Overflow to Underflow Diameter Ratio (D_o/D_u=0.85, Cenosphere) on Recovery of Light Particles in Overflow Stream (Model A)

Time	Overflow Slurry	Underflow Slurry	Feed Slurry*	Light in Feed*
s	kg	kg	kg	kg
4.7	4.9E-01	1.7E+00	2.14	7.0E-02
4.4	7.9E-01	1.5E+00	2.31	2.7E-02
4.5	8.2E-01	1.5E+00	2.31	5.5E-02
4.1	7.4E-01	1.3E+00	2.07	5.0E-02
4.6	7.6E-01	1.4E+00	2.15	4.9E-02
4.0	7.1E-01	1.2E+00	1.94	4.7E-02
4.2	7.3E-01	1.3E+00	2.00	4.7E-02

Light		Heavy	Volume	
Overflow	Underflow	Overflow	Overflow	Underflow
kg	kg	kg	m3	m3
3.4E-02	3.7E-02	6.0E-05	5.0E-04	1.7E-03
1.9E-02	7.7E-03	1.9E-04	8.1E-04	1.5E-03
4.7E-02	7.7E-03	1.9E-04	8.5E-04	1.5E-03
4.3E-02	7.0E-03	3.8E-04	7.8E-04	1.3E-03
4.4E-02	5.3E-03	2.1E-04	7.9E-04	1.4E-03
4.1E-02	6.1E-03	2.0E-04	7.6E-04	1.2E-03
4.1E-02	6.5E-03	2.3E-04	7.9E-04	1.3E-03

Flow Rate		Split Ratio	Light Recovery
Overflow	Underflow	Underflow	Overflow
m^3/s	m^3/s	Q_u/Q_f	R_{LO} (%)
1.0E-04	3.6E-04	0.65	47.9
1.8E-04	3.5E-04	0.54	64.5
1.9E-04	3.3E-04	0.48	71.4
1.9E-04	3.2E-04	0.47	86.0
1.7E-04	3.1E-04	0.45	85.9
1.9E-04	3.0E-04	0.41	89.1
1.9E-04	3.0E-04	0.38	87.2

Note: 1) Table is used in Figure 4.29